ASSESSMENT OF LOW TEMPERATURE CRACKING IN ASPHALT PAVEMENT MIXES AND RHEOLOGICAL PERFORMANCE OF ASPHALT BINDERS

by

DAVID SOWAH-KUMA

A thesis submitted to the Department of Chemistry

in conformity with the requirements for

the degree of Master of Science

Queen's University

Kingston, Ontario, Canada

(APRIL, 2015)

Abstract

Government spends a lot of money on the reconstruction and rehabilitation of road pavements in any given year due to various distresses and eventual failure. Low temperature (thermal) cracking, one of the main types of pavement distress, contributes partly to this economic loss, and comes about as a result of accumulated tensile strains exceeding the threshold tensile strain capacity of the pavement. This pavement distress leads to a drastic reduction of the pavement's service life and performance. In this study, the severity of low temperature (thermal) cracking on road pavements selected across the Province of Ontario and its predicted time to failure was assessed using the AASTHO Mechanistic-Empirical Pavement Design Guide (MEPDG) and AASHTOWARE™ software, with inputs such as creep compliance and tensile strength from laboratory test. Highway 400, K1, K2, Y1, Sasobit, Rediset LQ, and Rediset WMX were predicted to have a pavement in-service life above 15 years. Additionally, the rheological performance of the recovered asphalt binders was assessed using Superpave™ tests such as the dynamic shear rheometer (DSR) and bending beam rheometer (BBR). Further tests using modified standard protocols such as the extended bending beam rheometer (eBBR) (LS-308) test method and double-edge notched tension (DENT) test (LS-299) were employed to evaluate the failure properties associated with in service performance. The various rheological tests showed K1 to be the least susceptible to low temperature cracking compared to the remaining samples whiles Highway 24 will be highly susceptible to low temperature cracking. X-ray fluorescence (XRF) analysis was performed on the recovered asphalt binders to determine the presence of metals such as zinc (Zn) and molybdenum (Mo) believed to originate from waste engine oil, which is

often added to asphalt binders. Finally, the severity of oxidative aging (hardening) of the recovered asphalt binders was also evaluated using the Fourier transform infrared (FTIR) spectroscopy to determine the abundance of functional groups such as the carbonyl (CO) and sulfoxide (SO). Functional groups such as styrene and butadiene were also evaluated to determine the polymer modifier content in recovered asphalt binders.

Acknowledgement

My earnest gratitude goes to my supervisor, Dr. Simon A. M. Hesp, for his enormous assistance, guidance and supervision throughout my study. I deeply appreciate his personality as welcoming and diligent, of which I am challenged. I humbly express my appreciation to my supervisory committee Dr. Donal Macartney and Dr. Gary Vanloon for their great assistance towards a successful completion of my degree.

I am also grateful to the Ontario Ministry of Transportation (MTO), Imperial Oil Research Centre, and Natural Sciences and Engineering Research Council (NSERC) for their financial support towards this research. My gratitude is again extended to Warren Lee and Seyed Tabib of the Ontario Ministry of Transportation (MTO) for their assistance with the MEPDG software analysis. I further thank Ben Rudson, Graeme Gillespie and Jamie-Lee Freeston, for their help in gathering some of the data for my thesis.

Many more thanks to my colleagues of the asphalt research group: Isaac Obeng Omari, John Omo Ikpugha and Bidur Ghimire for their great support towards the completion of this thesis.

My ultimate thanks go to God Almighty for his grace and mercy in ensuring a successful completion of my thesis. To God alone be all the glory and honour for this great success. I also extend my appreciation to my father, Rev. Dr. George Sowah-Kuma and my entire siblings for their prayers and support throughout my study.

Table of Contents

List of Figures

List of Tables

Abbreviations and Acronyms

AASHTO	American Association of State Highway and Transportation Officials
ASTM	American Society for Testing and Materials
AR	Asphalt Rubber
BBR	Bending Beam Rheometer
BSG	Bulk Specific Gravity
CoV	Coefficient of Variation
CTOD	Critical Crack Tip Opening Displacement
DENT	Double-Edge Notched Tension
DSR	Dynamic Shear Rheometer
eBBR	Extended Bending Beam Rheometer
EVA	Ethylene Vinyl Acetate
EWF	Essential Work of Fracture
FTIR	Fourier Transform Infrared
GL	Gauge Length
Gpa	Giga Pascal
Gmb	Bulk specific gravity

Gmm	Maximum specific gravity
HMA	Hot Mix Asphalt
Hwy	Highway
IDT	Indirect Tension Test
KeV	Kilo Electronvolt
KPa	Kilo Pascal
LDPE	Low Density Polyethylene
MEPDG	Mechanistic-Empirical Pavement Design Guide
MTO	Ministry of Transportation of Ontario
MTS	Material Testing System
mN	Mili Newton
NHCRP	National Cooperative Highway Research Program
PAV	Pressure Aging Vessel
PG	Performance Grade
PE	Polyethylene
PB	Polybutadiene
PMA	Polymer Modified Asphalt

PPA	Polyphosphoric Acid
PI	Penetration Index
RAP	Reclaimed Asphalt Pavement
RTFO	Rolling Thin Film Oven
SBR	Styrene Butadiene Styrene
SIS	Styrene Isoprene Styrene
SHRP	Strategic Highway Research Program
Superpave™	SUperior PERforming PAVEments
VMA	Voids in Mineral Aggregate
VFA	Voids Filled with Asphalt
WMA	Warm Mix Additives
XRF	X-ray fluorescence

Symbols

A	Temperature Susceptibility Parameter
a	Length of a sharp crack, m
b	Beam Width, 12.5mm
B	Specimen Thickness, m

D	Specimen Diameter
G*	Complex shear modulus, Pa
G’	Storage modulus, Pa
G”	Loss modulus, Pa
H	Specimen Height, mm
h	Beam thickness, 6.25 mm
K	Stress Intensity factor, N
L	Ligament length, mm
L	Distance between beam supports, 102 mm (BBR)
N	Number of load repetitions
P	Peak Load
t	Loading time, s
T	Temperature, K
T	Specimen thickness
We	Essential fracture energy, J
Wt	Total energy, J
Π	pi (3.142)
°C	Degrees Celsius

CHAPTER 1

INTRODUCTION

1.1 Overview

Low temperature cracking in asphalt pavements is a major distress in Ontario and across North America. Low temperature cracking in pavements occurs when pavements accumulate tensile strains exceeding the threshold tensile strains the pavement can bear during cold conditions. Repeated cooling and heating during the day with large temperature drops can also contribute to low temperature cracking in pavements [1, 2]. It is however facilitated by reversible aging in asphalt binders where the binder shrinks in size due to cold temperatures, hence reducing the adhesive grip the binder has with the aggregate in the pavement [3]. A low temperature crack in pavements is typically initiated at the centre and sides of the pavement structure with a transverse cracking pattern to traffic route [2, 4]. The penetration of water and air into micro cracks in pavements as a result of low temperature cracking leads to drastic deterioration of the pavement, as the water entering the crack strips the asphalt binder from the aggregate and the air also causes oxidative hardening of the asphalt binder [2].

Road pavement failure due to low temperature cracking in Ontario province causes government to spend lots of money in reconstruction and rehabilitation annually. The cost incurred in reconstruction and rehabilitation of road pavement significantly affects the economy and reduces development.

It is however imperative to investigate the cause of low temperature cracking in asphalt pavement, analyse the pavement performance, analyse the performance of the asphalt binder and to predict the expected life span of the road pavements.

1.2 Factors Contributing to Low Temperature Cracking

Factors that contribute to low temperature cracking can be widely classified into: (1) environmental factors; (2) material factors; and (3) pavement structure geometry.

1.2.1 Environmental Factors

Numerous environmental factors influence low temperature cracking in asphalt pavement. A good number of these factors comprise the following:

- Temperature: Temperature is a major environmental factor that influences low temperature cracking. As the climate temperature drops, the pavement surface temperature also drops causing accumulation of stresses in the pavement due to contraction resistance of pavement layers as friction increases in pavement layers. The pavement surface temperature, which is connected to the ambient air temperature and the speed of the wind, when decreased below the glass transition temperature and allowed to stay for a long period of time, instigates micro cracks in the pavement [2, 5].
- Cooling rate: The rate of pavement cooling is a key contributor to low temperature cracking in pavement. The speed and magnitude of crack in a pavement is due to the cooling rate of the pavement. The faster the cooling rate the greater the susceptibility of the pavement to undergo low temperature (thermal) cracking [2]. Stress-relaxation behavior of asphalt pavement is directly influenced by the rate of cooling. And the cooling rate apart from the lowest temperature reached as a result of cooling determines the extent of induced thermal stress in pavements [6].
- Pavement Age: The incidence of the low temperature (thermal) cracking on Pavements is typically due to the aging of the pavement. As the pavement gets older, the more susceptible

it is to thermal cracking and this phenomenon is largely due to increase in stiffness of aging in asphalt binder [2]. Kriz et al. [7] in a study of the effect of physical aging on the viscoelastic and thermodynamic parameters such as rate of physical aging and glass transition temperature on asphalt binder, concluded that, physical aging takes place when asphalt binder is cooled to the glass state leading to increased difficulty of the asphalt binder to relax stresses and hence affecting the viscoelastic properties of the asphalt binder.

1.2.2 Material Factors

Materials used in the construction of asphalt pavement are of great importance. As it goes a long way to determine the pavement's strength and resistance to low temperature (thermal) cracking. Material factors that influence thermal cracking include the following:

- Asphalt Cement: Asphalt Cement, defined according to the American Society for Testing and Materials (ASTM) as a "dark brown or black cementitious material occurring in nature or obtained by crude oil refining where the predominated material is mainly bitumen," is a major material factor to consider in asphalt pavement construction [8]. Asphalt, which naturally originates from lake asphalt, rock asphalt, tar and gilsonite, gives rise to several types of asphalt cement employed in asphalt pavement construction [9, 10]. The type of asphalt cement must be considered in the selection of asphalt to be used in pavement construction due to the wide variability of the viscoelastic properties of the different types of asphalt. The relationship between the stiffness and temperature of the asphalt type to be used in pavement construction is an important factor affecting the extent of low temperature (thermal) cracking in asphalt pavement and must be considered in pavement construction [2].

The stiffness and performance grade of asphalt binders gives a good assessment of the type of asphalt binder to be used in pavement construction at areas of extremely low temperature climates so as to mitigate the effect of low temperature (thermal) cracking.

- Type of Aggregate and Gradation: Aggregates used in pavements should possess some characteristics such as low freeze-thaw loss, high abrasion resistance and low absorption in order to resist low temperature (thermal) cracking. Aggregates of low absorption decrease the low temperature strength due to the reduced amount of asphalt cement in the mixture than that of a non-absorptive aggregate [2].
- Asphalt Cement Content: The increase of asphalt cement content reduces the stiffness and increases the coefficient of thermal contraction and contributes to the overall low temperature (thermal) cracking performance of the asphalt pavement [2].
- Air Void Content: The air voids content, degree of compaction and permeability, even though important factors to be considered in pavement construction, do not affect the low temperature (thermal) cracking of asphalt pavement significantly but can enhance the effect of low temperature cracking if not properly checked [2].

1.2.3 Pavement Structure Geometry Factors

Good pavement structure geometry can help reduce low temperature (thermal) cracking. Numerous pavement structure geometry factors which can affect low temperature cracking include the following:

- Pavement Width: Narrow pavements usually have thermal cracks closely spaced compared to that of wide pavement [2].

- Pavement Thickness: The thicker the pavement, the less susceptible it is to low temperature (thermal) cracking [2].
- Friction Coefficient between the Asphalt Concrete Layer and Base Course: The granular base, which usually has a lower thermal coefficient of contraction, when bonded perfectly to the asphalt concrete layer, reduces the thermal coefficient of the asphalt concrete layer. This phenomenon is observed when there is a reduction on the rate of low temperature (thermal) cracking due to prime coating of untreated aggregates in the base course layer of the pavement [2].
- Type of Subgrade and Construction Defects: Cracks are initiated upon pavement cooling, after transverse defects are produced at high temperature compaction of asphalt layers. Subgrades typically made of sand are very vulnerable to low temperature (thermal) cracking than cohesive subgrades [2].

1.3 Pavement Design

The designing of pavements involves the structural overlay of finished materials on top of the soil sub-grade. The ultimate aim in pavement design is to achieve a pavement structure with good automobile riding quality, tolerable skid resistance, and bearable light reflection, and to ensure that stresses exerted from wheel loads will not exceed the threshold stress capacity of the sub-grade. Road pavements are generally classified in two types, namely, rigid pavements and flexible pavements [11].

In rigid pavement construction, the surface course is typically built using a fast setting hydraulic cement concrete known as Portland Cement Concrete (PCC). Several types of rigid pavements

such as Jointed Plain Concrete Pavement (JPCP), Jointed Reinforced Concrete Pavement (JRCP), Continuous Reinforced Concrete Pavement (CRCP), Prefabricated/Post-Stressed Concrete Pavement, and Pre-Stressed Concrete Pavement are generally stiffer than flexible pavements due to the high inherent stiffness of Portland Cement Concrete [12-14].

Flexible pavements are typically made off asphalt layers in which transmitted stresses from the applied wheel load to the lower layers is achieved through the granular particles, as shown in Figure 1.1.

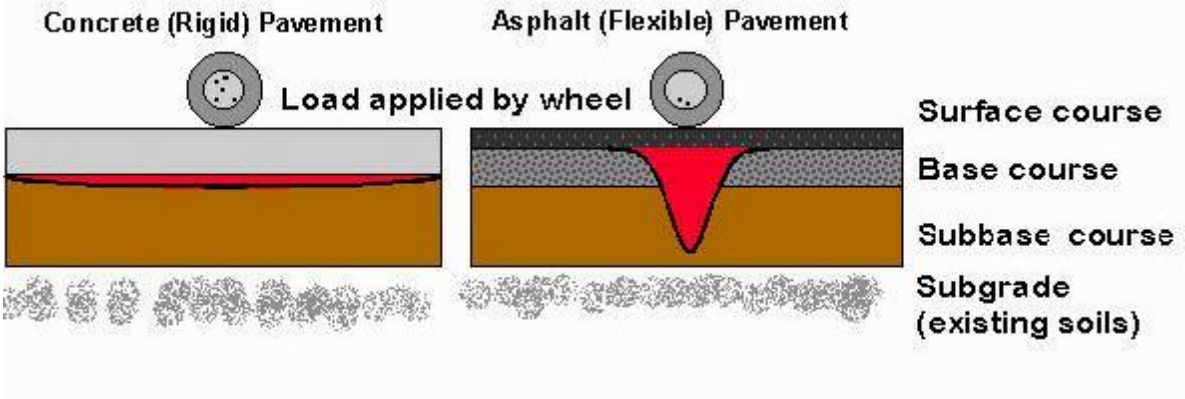

Figure 1.1: Rigid and flexible pavements [16].

In figure 1.1, stress from the load applied by the wheel on flexible pavements is dissipated through granular particles whiles stresses are not dissipated in rigid pavements due to the absence of granular particles. In the designing of flexible pavements the applied stress is taken into consideration so as to not exceed the maximum stress the pavement can contain. Typical examples of flexible pavements include: conventional layered flexible pavement, full-depth asphalt pavement and contained rock asphalt mat (CRAM) [11].

1.4 Pavement Layers

The cross-section of a pavement is usually made up of several layers such as surface course, binder course, base course, sub-base and sub-grade, as shown in Figure 1.2.

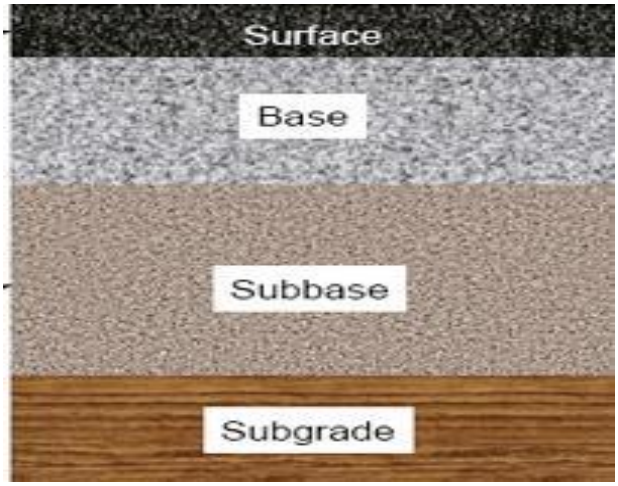

Figure 1.2: Structural layers in an asphalt concrete pavement [9].

1.4.1 Surface Course

The surface course is the topmost layer of the pavement structure which is designed to bear heavy traffic load, prevent skidding and prevent deterioration caused by water and air penetration and also climate changes. The surface layer of flexible pavements is usually made of asphalt concrete, whiles that of rigid pavements is made of Portland Cement Concrete (PCC) [11, 15].

1.4.2 Binder Course

The binder course usually lies between the surface course and the base course and is made up of aggregates with a limiting amount of asphalt binder. Its primary purpose is to evenly channel loads to the base [11, 15].

1.4.3 Base Course

The base course contributes immensely to the structural stability of the pavement by aiding in load distribution. Its constituents are mainly aggregates like gravel, sand and stone [11, 15].

1.4.4 Sub-base

The sub-base becomes a very important layer needed in pavement structure when the sub-grade is of poor quality and stiffness. It is usually located beneath the base course in the pavement structure and generally helps support the base course [11, 15].

1.4.5 Sub-grade

The sub-grade is the initial platform on which the rest of the layers are constructed upon. The ability of the sub-grade to absorb stresses from the layers above, enables it provide good structural stability to the pavement. The sub-grade is generally composed of natural sand and is usually compacted to an adequate density without being overstressed [11, 15].

1.5. Scope and Objectives

The strength of a nation's economy is largely dependent on the accessibility of good transportation. An essential part of a good transportation system stems from quality and durable roads. However the devastating nature of the roads in Ontario due to low temperature cracking in the winter season raises lots of concern to investigate and develop procedures to help mitigate this nuisance. In recent times, the government spends close to $8 billion annually for reconstruction and rehabilitation of worn out roads [17].

To help address this overwhelming occurrence and to reduce cost incurred by government, it is imperative to understand the cause of road pavement failures and to develop procedures to help curb it. The goal of this research study will focus specifically on:

- Predicting the life span of selected highways in Ontario province. The test will require the use of the American Association of State Highway and Transportation Official's (AASHTO) mechanistic-empirical pavement design guide (MEPDG) to predict the life span of the highways.
- Determining the rheological properties and performance of the recovered asphalt binder using Superpave™ tests such as the Dynamic Shear Rheometer (DSR), Bending Beam Rheometer (BBR) and the Double Edge-Notched Tension (DENT) Test.
- Analysing some metals and functional groups in asphalt binder responsible for oxidative hardening with the use of X-Ray Fluorescence (XRF) and Fourier Transform Infrared Spectroscopy (FTIR) respectively.
- Predicting the thermal cracking resistance of some rubberised asphalt samples.

CHAPTER 2

BACKGROUND AND LITERATURE REVIEW

2.1 Deterioration of Asphalt Pavement

Deterioration of asphalt pavement occurs when an asphalt pavement begins to wear and weaken due to the presence of water, air, chemicals and sunlight. The penetration of water into asphalt pavement reduces the adhesive strength of the binder on the aggregates. Also the penetration of air containing oxygen into asphalt pavement brings about oxidative hardening of the asphalt binder in the pavement, leading to binder adhesive failure and gradual wearing of the pavement. The incorporation of chemicals such as grease and waste engine oil to asphalt binder in road pavement construction could as well weaken the strength of the pavement and ultimately lead to pavement deterioration. Excessive exposure of sunlight on asphalt pavements for a long period of time could also bring about ravelling due to the drying of the asphalt binder by the radiant sunlight. In addition to these factors, bad pavement construction practices generally bring about pavement deterioration [18].

2.2 Pavement Distresses

The main aim in pavement design is to achieve a longer performance life span with little maintenance and preservation of the pavement. However, pavements can undergo a number of distresses such as low temperature (thermal) cracking, rutting, fatigue cracking, and moisture damage (stripping) when exposed to chemicals, rain, oxygen, sunlight, thermal stresses, distortions and repetitive traffic loading over a long period of time, which reduces its performance life span [5, 19].

2.2.1 Rutting

The phenomenon of rutting as a pavement distress occurs when repetitive heavy traffic loading on asphalt pavement during high temperature condition causes pavement materials to be permanently dislocated. Rutting often arises when the subgrade layer of a pavement becomes weakened due to inadequate compaction, repeated traffic loading, moisture penetration and air penetration of pavements [20, 21]. The formation of a rut as shown in Figure 2.2 (a), is typically due to heavy traffic loading on asphalt binders with reduced viscosity at high temperature condition. Laboratory evaluation of the rutting behavior of asphalt binders is done using the dynamic shear rheometer (DSR) to measure the rutting resistant factor $G^*/\sin\delta$ (where G^* is the complex modulus and δ is the phase angle).

Figure 2.2: (a) Permanent pavement deformation (rutting) [22].

2.2.2 Fatigue Cracking

Fatigue cracking also known as alligator cracking due to resemblance of an alligator skin is caused by cyclic loading of vehicles under moderate temperature conditions. A characteristic feature of fatigue cracking is the appearance of several micro cracks in all directions of the pavement leading to the formation of potholes as shown in Figure 2.2 (b) [23]. The dynamic shear rheometer is used to measure the fatigue resistance factor G*sinδ (where G* is the complex modulus and δ is the phase angle) of asphalt binders, which predicts the fatigue behavior of the asphalt binder.

Figure 2.2: (b) Fatigue cracking (alligator cracking) [24].

2.2.3 Moisture Damage

Moisture damage is the reduction of the adhesive property of asphalt cement to the aggregate due to water penetration as shown in Figure 2.2 (d). The penetration of water into pavement can occur through several means such as flow of rain, snow, and capillary absorption of ground water into the pavement structure. However, it is virtually impossible to prevent pavement from coming to contact with water. The resistance of a pavement to stripping and moisture damage depends on the pavement's material property, gradation of asphalt mix, additives, pavement structure and good pavement design. The higher the viscosity of the asphalt binder the greater its adhesiveness and hence the more difficult water can interfere with bonding. Nevertheless chemical constituents such as carboxylic acids and sulfoxides in asphalt can be easily displaced by water and affect moisture sensitivity. The chemical composition of aggregate, size and extent of pores in the aggregate surface can enhance water penetration. The type of mix gradation such as open-graded mix is permeable to water and enhances moisture damage whiles dense-graded mix and gap-graded mix has low permeability. Stripping can be prevented by the implementation of good drainage, use of anti-stripping agents and by adhering to proper pavement compaction [25, 26].

Figure 2.2: (c) Moisture damage [27].

2.2.4 Low Temperature Thermal Cracking

Low temperature thermal cracking is one the major pavement distress observed in North America and other colder areas in the world. This kind of pavement distress comes about when stresses that builds up in the pavement strata exceeds the threshold stress the pavement can bear. Once more, temperature fluctuations such as the dropping of temperature during a warm day or the rising of temperature during a cold can lead to continuous expansion and contraction of the pavement which may eventually contribute to the build-up of stress and cracks in the pavement [1, 2]. Cracks on a pavement as a result of low temperature cracking can be facilitated by the penetration of water into the cracks, which reduces the adhesive grip between the aggregate and the binder. The asphalt binder content in the pavement can as well also contribute to low temperature cracking. The lower the asphalt binder content the less effective adhesion between the aggregate and the binder and this can reduce the ability of the pavement to bear stress. However, not only environmental and material factors contribute to low temperature cracking but the pavement geometry as well. The width, thickness and designing of the pavement strata must be done appropriately without defects so as to accommodate stress and resist cracking [5].

Figure 2.2: (d) Thermal cracking [90].

2.3 Thermal Cracking Analysis

2.3.1 Indirect Tensile (IDT) Creep and Strength Test

In the analysis of thermal cracking of asphalt pavement two major properties of the Hot Mix Asphalt (HMA) are considered according to the AASHTO T332-07 Standard test method [88]. The AASHTO T332-07 Standard test method was originally developed by Roque and his co-workers at the Pennsylvania State University and codified as AASHTO provisional method of test TP9 [91]. According to this standard test method, creep compliance is defined as the time-dependent strain divided by the applied stress, whiles the tensile strength is defined as the strength shown by a specimen when subjected to tension which is void of torsion, compression or shear [88]. In the determination of creep compliance according to the AASHTO T332-07 Standard test method, Hot Mix Asphalt (HMA) specimen of diameter 150 ± 9 mm and thickness of 38 to 50 mm are produced from cutting a cylindrical core of the (HMA) sample which has been compacted to a desired air void. The specimen is then subjected to a static load along a diametral axis under a regulated temperature for approximately 100 seconds using an Indirect Tensile Device. However, during the loading process vertical and horizontal displacements are measured by means of extensometers attached to magnetic stubs on the middle section of the two opposite surfaces of the specimen [88, 92]. Furthermore, sufficient load is required to cause horizontal displacement (≥ 0.00125 or 33 micro-strain based on a 38 mm gauge length) to ensure an insignificant noise in the data acquisition [92]. The determination of creep compliance can be calculated from the measured vertical and horizontal displacements according to the equation [88]:

$$D(t) = \frac{\Delta X_t * D_{avg} * b_{avg}}{P_{avg} * GL} * C_{cmpl} \quad (1)$$

Where D(t) is the creep compliance as a function of time (kPa^{-1}) , C_{cmpl} is the creep compliance correction factor, P_{avg} is the average creep load, GL is the gauge length of 0.038 for a 150 mm diameter specimen, ΔX_t is the horizontal trimmed mean displacement, D_{avg} is the average diameter and b_{avg} is the average sample thickness.

The creep compliance factor (C_{cmpl}) is obtained according to the equation [88]:

$$C_{cmpl} = 0.6354\left(\frac{\Delta Y_t}{\Delta X_t}\right) - 0.332 \quad (2)$$

However, prior to the calculation of the creep compliance a trimmed mean approach is used to help reduce the coefficient of variation for the measurements by discarding the highest and lowest displacements in both vertical and horizontal directions. The trimmed mean of the vertical and horizontal displacements is calculated using the following equations [88]:

$$\Delta X_t = \frac{\sum_{j=2}^{N-1} \Delta X_j}{N-2} \quad (3)$$

$$\Delta Y_t = \frac{\sum_{j=2}^{N-1} \Delta Y_j}{N-2} \quad (4)$$

Where ΔX_t is the horizontal trimmed mean displacement (mm) and ΔY_t is the vertical trimmed mean displacement (mm). ΔX_j and ΔY_j are the displacement values sorted in increasing order, and N is the total number of samples.

The tensile strength test is a destructive test carried out on an (HMA) specimen to determine its strength when subjected to tension. The specimen is loaded at a rate of 12.5 mm/min after conditioning at a desired temperature for the specified duration until the specimen fails. The tensile strength of the specimen is calculated based on the maximum load recorded during testing, which is the load at tensile failure of the specimen [88, 92].

Therefore the tensile strength can be obtained according to the equation [88]:

$$S_{t,n} = \frac{2P_{f,n}}{\pi * b_n * D_n} \quad (5)$$

Where $S_{t,n}$ is the tensile strength, $P_{f,n}$ is the load at failure, b_n is the thickness, and D_n is the diameter of sample n.

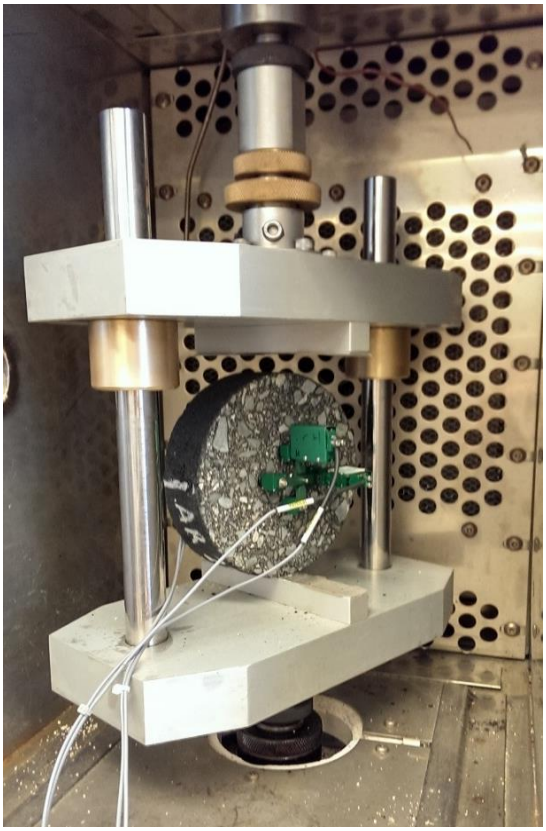

Figure 2.3: Creep compliance test.

2.3.2 Low Temperature Cracking Models

In general, low temperature cracking models can be classified as empirical and mechanistic models. Empirical models are developed based on field data regression analyses but do not comprehensively explain the basis of the cracking occurrence. However, the mechanistic or mechanistic-empirical models on the contrary, employ principles of material mechanics to describe the cracking behaviour observed on pavements [93].

2.3.2.1 Empirical Thermal Cracking Models

Empirically-based thermal cracking models are relatively easy to use when appropriate developed inputs have been established. Examples of empirical model inputs include fracture toughness and the thickness of the pavement. A key example of empirical thermal cracking models is the Fromm and Phang's models [95]. In the models of Fromm and Phang, several regression equations aimed at predicting the cracking index were developed [93, 94]. The cracking index measures the cracking severity on a pavement and can be calculated according to the equation [93, 94]:

$$I = N_m + N_f + 0.5*N_h \quad (6)$$

Where: I = cracking index

N_m = number of multiple cracking occurrences in 150 m of pavement

N_f = number of full cracking occurrences in 150 m of pavement

N_h = number of half cracking occurrences in 150 m of pavement

One major parameter developed by Fromm and Phang was the Critical Temperature Parameter. This parameter accounts for the flow properties of the asphalt pavement. According to Fromm and Phang, "the critical temperature, is the temperature at which viscous flow under creep

loading in one hour equals the temperature shrinkage in one hour" [93, 94]. However, it is believed that the viscous flow of the pavement material is adequately good to get rid of stresses instigated by shrinkage when temperatures go above the critical temperature. On the other hand, the growth of thermal stresses occurs faster than relaxation when temperatures go below the critical temperature which is likely to generate cracks. On the premise of this observation, the elastic nature of the asphalt pavement becomes more conspicuous than the viscous behaviour when temperatures fall below the critical temperature [93]. Another example of the empirical thermal cracking model is the Airport Pavement Model. This model is an empirical study conducted by Haas et al [95], whereby asphalt concrete cores from 26 airport pavements throughout Canada were tested in the laboratory. An empirical model was then proposed after a series of statistical analyses and evaluation [93, 97].

2.3.2.2 Mechanistic Thermal Cracking Models

The mechanistic thermal cracking models, generally considers the asphalt mixture layer in its analysis and are more complex than the empirical thermal cracking models. The surface of the asphalt pavement is off most importance in mechanistic thermal cracking models. However, a few mechanistic thermal cracking models consider the interfacial friction between the surface of the asphalt pavement and the supporting layers in analyses [93]. Among several mechanistic thermal cracking models include, the Hills and Brien-Fracture Temperature Prediction, Christison, Murray and Anderson - Thermal Stress Prediction, Fictitious Crack Model, Frictional Constraint Model, and the Thermal Cracking (TC) Model [93].

2.3.3. AASTHO Mechanistic-Empirical Pavement Design Guide (MEPDG) and Software

The evolution of pavement design from empirical-based methods to mechanistic –based methods can be traced from the late 1950s [96]. The MEPDG is an update of the 1993 AASHTO Guide for pavement design, which was founded on the premise of the AASTO Road Test that began in the 1950s [97]. The MEPDG is characterised by two major sections, which are the mechanistic component that relies on physical causes and the empirical component that depends on the use of observed performance. The main aim of the MEPDG is to detect physical causes of stresses in pavement structures and to standardize them with the observed pavement performance [97]. In the procedures of the MEPDG, factors that directly affect the pavement performance are incorporated. These factors include the following [96]:

- Traffic Loading: The distribution of axle load for an axle type, the duration of load distribution (hourly and monthly), the type and number of truck are factors that constitute the traffic loading.
- Material Properties: The material layers of the pavement structure such as asphalt, concrete, cementitious and loose granular materials and the sub-grade soil with their measured properties is of much importance. Material properties such as dynamic modulus for asphalt layers, elastic modulus for concrete and chemically stabilized layers, and resilient modulus for unbound layers and sub-grade soils are taken into consideration.
- Climatic Effects: The effect of climatic factors such as temperature, moisture, wind speed, cloud shield, and relative humidity on each layer of the pavement is modeled using an Integrated Climatic Model. Aging of asphalt layers, curling and moisture susceptibility of the sub-grade soil are a few examples of the result of the effect of climatic factors on the pavement layers.

These factors are utilised by the AASHTO MEPDG Software to help predict the performance of the asphalt pavement over a period of time. The AASHTO MEPDG Software also considers certain assumptions in its pavement performance prediction such as assuming that each pavement layer has a homogeneous material property; with the exception of the lowest layer of the pavement all other layers have a finite thickness; all layers are boundless in the lateral view of the pavement; each layer shows an isotropic property; shear forces acting on the surface of the pavement are not considered; the elastic modulus and the Poisson's define the stresses and there is considerable amount of friction between successive layers [98, 99].

On the contrary, some criteria's are considered in the AASHTO MEPDG Software computation process. A good example is the summation of the critical stress and strain values over a two week or one month increment calculation. Weather factors, traffic conditions and all moduli are held constant in the confines of each increment. An accurate traffic data with a 1 year minimum weather data is also considered in the processing. The software computational process can be fully described as follows [98, 99]:

- The software requires inputs of creep compliance at -20, -10, and 0°C and tensile strength at -10°C.
- Creep compliance master curves are fitted into the Power law model and the Prony series.
- Conversion of creep compliance to relaxation modulus together with climate data is used to predict the severity of thermal stress at any time.
- The Paris law makes use of the stress intensity and fracture parameters to determine the crack growth.

- The stress intensity characterises the physical cracking with an acceptance criteria of 1000 ft of thermal cracking per mile (190 m per km) and a model calibration of 500 ft extrapolated to a mile on a section.

The maximum cracking distress assumed is 800 m per km but when the crack depth equals the layer thickness, the model cannot predict more than half this value. The standard error is determined by an empirical equation shown below [98, 99]:

$$Standard\ Error = 0.2474 * predicted\ thermal\ cracking + 10.619 \quad (7)$$

2.4 Reversible Aging in Asphalt Pavement

The performance of asphalt binders in connection to premature pavement failures and low temperature cracking has in recent times being traced to the phenomenon of reversible aging in asphalt binders. However, the process of reversible aging in asphalt binder when kept under cold conditions entails relevant structural changes such as free volume collapse, asphaltene aggregation and crystallization [3]. The extent of physical hardening of the asphalt binder as reported by Anderson et al [28] depends on its source, isothermal ageing temperature and time of storage. However, the SHRP [29] describes isothermal physical hardening as:

"As bitumen is cooled within the temperature range for which the molecular processes are relatively rapid (e.g., above the softening-point temperature or in the Newtonian flow region), the change in volume with temperature is relatively instantaneous, and no time-dependent volume change is observed. However, as the temperature is further depressed, the volume change does not occur instantaneously but over a nonzero time. This time-dependent volume change is called isothermal physical hardening because the volume change causes a concomitant time-dependent increase in the stiffness of the asphalt. The temperature at which the

molecular processes is slow enough that the volume change is not instantaneous but time dependent is called the glass transition temperature. The glass transition temperature is, however, not uniquely defined but is dependent on the rate of cooling and other aspects of thermal history. Physical hardening is observed at temperatures typically below 0 °C".

It is however imperative to understand the chemistry of the asphalt binder as related to physical hardening. As asphalt is generally known to be a hydrocarbon with composition of hydrogen and carbon atoms to be 90 and 95 weight percent respectively, with the rest being heteroatoms (nitrogen, oxygen and sulphur) and metals (vanadium, nickel and iron) [30, 31]. The presence of sulfur affects the ageing of asphalt binder due to its high oxidizing potential and reactivity than carbon and hydrogen. Molecules in asphalt binder are generally classified into three broad areas; aliphatic, cyclic and aromatics as shown in Fig 2.4 (a) [30, 31].

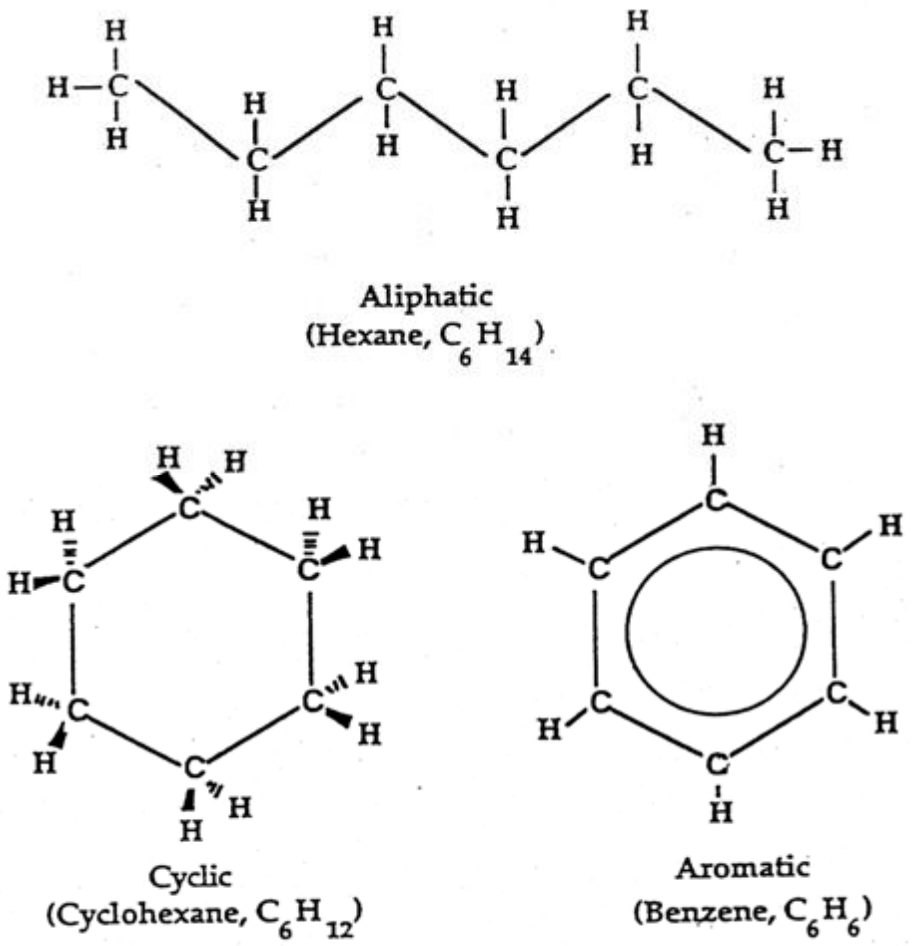

Figure 2.4: (a) Three classes of molecules in asphalt binder [30].

Asphalt binder is generally made up of asphaltenes, resins, saturates and aromatics. Asphaltenes are highly polar with polarised functional groups and a multifaceted aromatic ring system [31]. According to Johanson [32], the composition of resin is due to the presence hydrogen and carbon with a minute quantity of oxygen, sulphur and nitrogen. Naphthenic compounds with paraffinic chains and substituted monocyclic or polycyclic aromatic hydrocarbons make up the aromatic fraction in bitumen whiles straight and branch-chain aliphatic hydrocarbon with alkyl-naphthenes and alkyl aromatics make up saturates [31].

The dispersion of asphaltenes in an oily medium (maltenes) is known to be a colloidal system which results from the adsorption of resins by asphaltenes to form a covering sheath around the asphaltene [33 - 35]. A fully adsorbed amount of resin by the asphaltenes to enhance mobility within the bitumen colloidal system is known as solutions or “sol” type bitumen, whiles an inadequately adsorbed quantity of resin by the asphaltenes will reduce mobility within the bitumen colloidal system and is known as gelatinous or “gel” type bitumen [31]. Figure 2.4 (b) shows a typical representation of “sol” type and “gel” type bitumen.

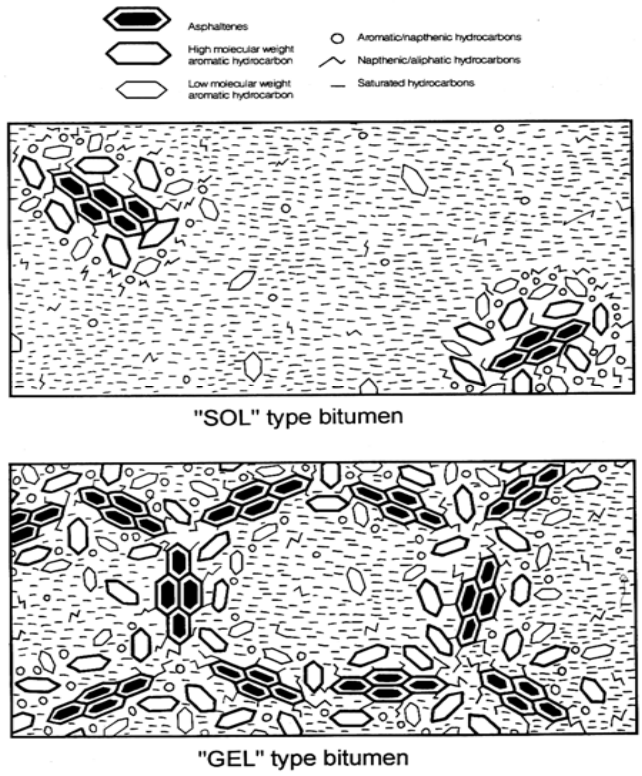

Figure 2.4: (b) Schematic presentation of “sol” and “gel” type bitumen [35].

2.5 Viscoelastic nature of asphalt binders

Asphalt binder is a viscoelastic material because it consists of both viscous and elastic properties and under prevailing conditions can behave as a viscous, elastic or viscoelastic material.

Temperature and loading time are key conditions which affect the viscoelastic behaviour of asphalt binder. Asphalt binders tend to be more elastic under low temperature conditions and more viscous under moderate to high temperatures. The response of asphalt binder to loading determines its viscous or elastic nature under its stress-strain behaviour. The application of stress on asphalt binder results in straining the asphalt binder with a molecular rearrangement in the asphalt binder. According to Barnes et al [37], rheology is defined as: "*the science of deformation and flow (the study of the deformation and flow of matter)".* However, Hooke's law predicts the elastic response of a material. Figure 2.5 (a) shows Hooke's law equation for shear strain given as:

$$\tau = G\gamma \tag{8}$$

where τ is the shear stress in N/m^2, γ is the shear strain and G is the shear modulus in N/m^2.

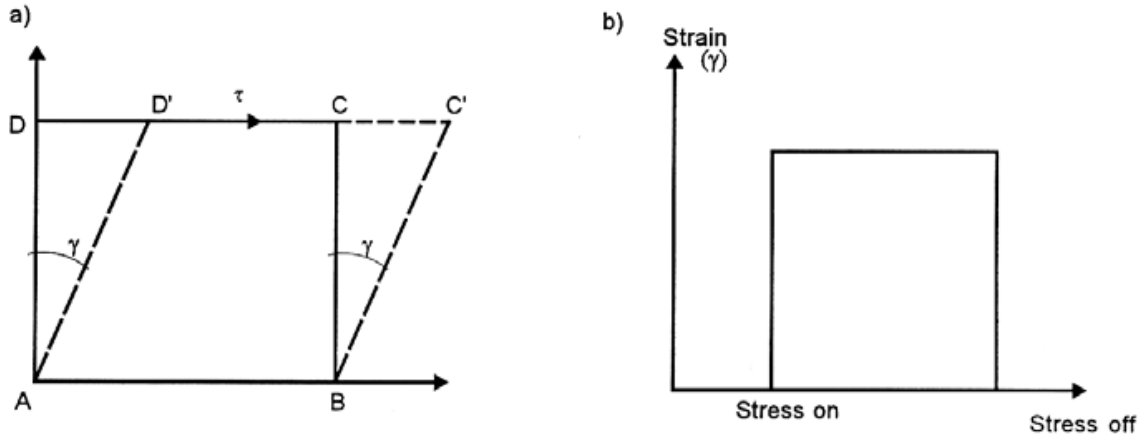

Figure 2.5: (a) Typical solid material response a) applied shear stress b) strain response of applied shear stress [31].

Figure 2.5 (b) shows an ideal response of viscous, elastic and viscoelastic material.

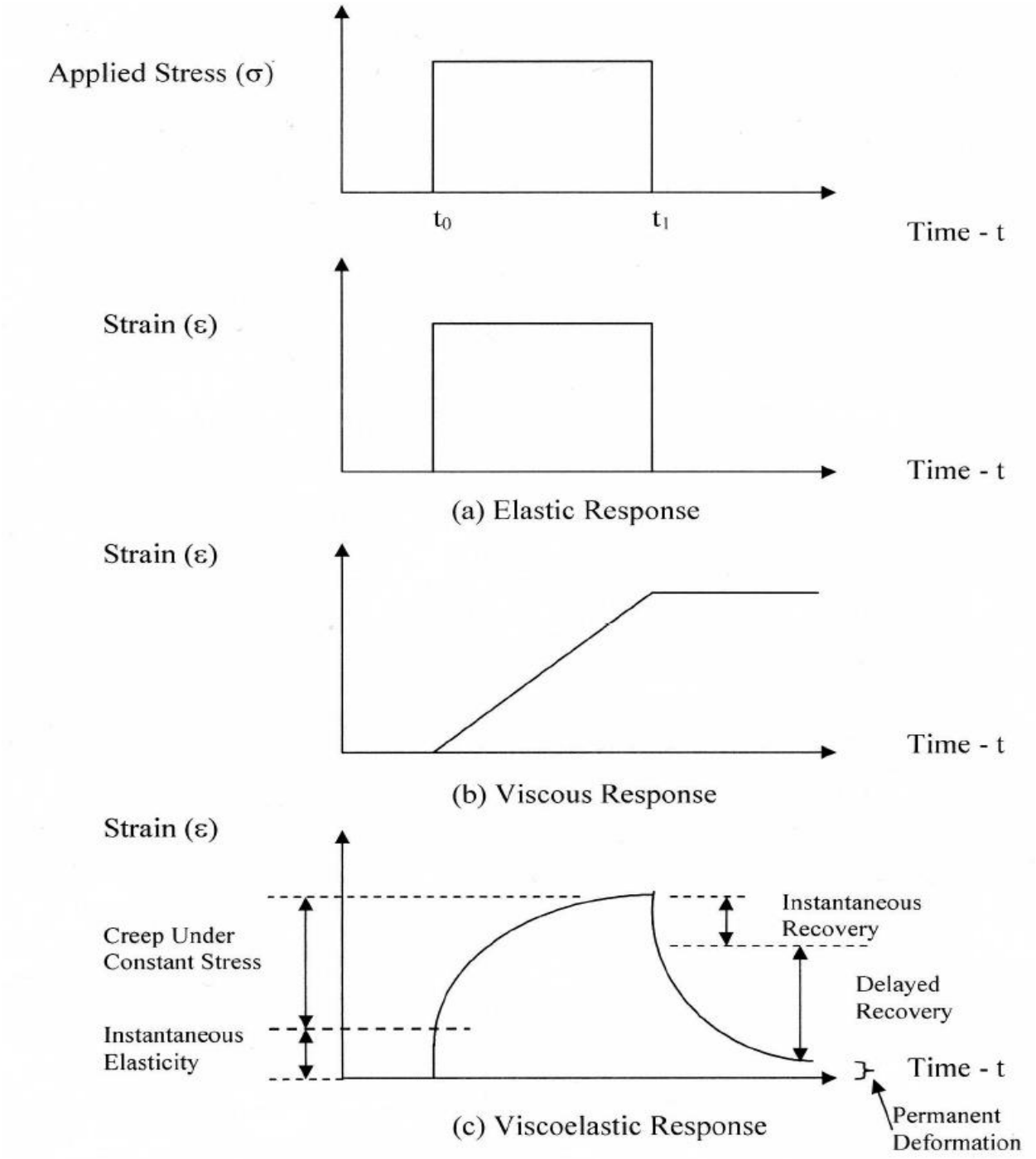

Figure 2.5: (b) An ideal response of elastic, viscous and viscoelastic material under constant stress loading [36].

2.6 Performance Grading of Asphalt Binder

The physical properties of an asphalt binder govern how it would perform as a component in asphalt pavement. Therefore, performance grading of asphalt binder according to Superpave is based on the notion that binder properties should be related to the conditions under which it is used [38, 39]. However, selected Performance Graded (PG) asphalt binder must comply with the expected climatic and aging conditions. Hence, conventional tests such as the penetration and viscosity test were previously used to measure the physical properties of the binder that can be related to its pavement field performance [39]. Due to the failure of the conventional test to give realistic correlation between binder properties and pavement field performance, the Superpave™ (SUperior PERforming PAVEments) testing specifications was developed to correct the failure of the old conventional tests [28, 40].

Table 2.1: Conventional vs. Superpave testing and specification features [38, 42]

Limitations of Penetration, AC and AR Grading Systems	**Superpave Binder Testing and Specification Features that Address Prior Limitations**
Penetration and ductility tests are empirical and not directly related to HMA pavement performance.	The physical properties measured are directly related to field performance by engineering principles.
Tests are conducted at one standard temperature without regard to the climate in which the asphalt binder will be used.	Test criteria remain constant, however, the temperature at which the criteria must be met changes in consideration of the binder grade selected for the prevalent climatic conditions.

The range of pavement temperatures at any one site is not adequately covered. For example, there is no test method for asphalt binder stiffness at low temperatures to control thermal cracking.	The entire range of pavement temperatures experienced at a particular site is covered.
Test methods only consider short-term asphalt binder aging (thin film oven test) although long-term aging is a significant factor in fatigue cracking and low temperature cracking.	Three critical binder ages are simulated and tested: 1. Original asphalt binder prior to mixing with aggregate. 2. Aged asphalt binder after HMA production and construction. 3. Long-term aged binder.
Asphalt binders can have significantly different characteristics within the same grading category.	Grading is more precise and there is less overlap between grades.
Modified asphalt binders are not suited for these grading systems.	Tests and specifications are intended for asphalt "binders" to include both modified and unmodified asphalt cements.

A general nomenclature for grading an asphalt binder can be given as PG 52-28, where the first number 58 represents the average 7 day maximum pavement design temperature and -28 is the minimum pavement design temperature [38, 39]. Depending on grade of an asphalt binder, it can

be modified to suit its application. Asphalt modification is required to improve the grade of an asphalt binder [38, 39].

2.7 Asphalt Modifications

The search to find a solution to pavement distress, so as to increase the life span of asphalt pavement has led to asphalt modification. The modification of asphalt is done to generally improve on its quality and performance grade. In much detail, asphalt binder is modified to [42]:

- Reduce the stiffness or viscosity of the asphalt binder at high temperatures, so as to facilitate mixing and compaction.
- Minimize rutting by increasing stiffness at high service temperatures.
- Minimize low temperature (thermal) cracking by reducing stiffness and increasing relaxation at low service temperatures.
- Enhance the adhesive interaction between the asphalt binder and the aggregate in the presence of moisture, so as to reduce the effect of moisture damage.

Several modifiers such as polyphosphoric acid (PPA), anti-stripping additives and polymers are employed in asphalt modification in order to meet specifications. Polymers are the most widely used modifier because of its numerous advantages.

Table 2.2: Examples of polymer modifiers with their advantages and disadvantages [13]

Polymer Modifier	Advantages	Disadvantages
Styrene Butadiene Copolymer	Very resistant to fatigue and great creep rate.	Highly prone to oxidation
Polyethylene (PE)	Thermal extension is high with low stiffness.	
Styrene Butadiene Rubber (SBR)	Resistant to weather with good aging qualities.	Prone to oxidation, less resistant to ozone and a minimal tear strength.
Polybutadiene (PB)	Very resistant to wear and impact.	Minimal Strength
Ethylene Vinyl Acetate Copolymer (EVA)	Very stable when stored and viscous at high temperatures. Creep resistance is low.	Prone to crosslinking.

Polymers which are prepared before added to the asphalt and then mixed are referred to as "passive" polymers [43]. Passive polymers can be further grouped into elastomers and plastomers depending on their elastic properties. An elastomer, when stretched will quickly return to its original state when the load is released due to the arrangement of its molecules with a typical crosslink molecular conformation. Typical examples of elastomers are styrene butadiene styrene (SBS) and styrene-isoprene-styrene (SIS) [43, 44]. Plastomers on the other hand, when stretched will not quickly return to its original state but will remain in its stretched

state for a period of time before returning to its original state. Typical examples of plastomers include polybutadiene, polyisoprene, natural rubber and styrene butadiene rubber (SBR).

An “active” polymer is defined as one which does not undergo crosslinking and would rather go through specific chemical reactions with specific functional groups in asphalt [5].

Their main goal is to influence the viscosity, penetration and softening point of the bitumen without affecting the elasticity [5]. Key examples of active polymers include ethylene vinyl acetate (EVA), polyethylene (PE) and polystyrene (PS) [43].

Anti-stripping agents comprising of polyamines and fatty amido amines are another class of asphalt modifiers which increase the adhesive interaction between the asphalt binder and the aggregates. Thereby decreasing its vulnerability to moisture damage or stripping [45].

The addition of polyphosphoric acid (PPA) as an asphalt modifier, extends the performance grade range of the asphalt at elevated temperatures and increases its softening point [46].

2.8 Warm Mix Technology and Additives

In order to improve the performance of asphalt, reduce construction cost and increase efficiency in construction, warm mix technology has been exploited by the asphalt paving industry to help achieve these targets [47]. The conventional use of hot-mix asphalt (HMA) technology over the years has been out weighted by the use of warm-mix asphalt (WMA) technology due to the great benefits derived from the application of warm-mix asphalt (WMA) technology [48]. Such of these benefits derived from employing warm-mix additives in the paving industry include, lowering the viscosity of asphalt binders, lowering the compaction temperature, reduction of

energy cost, reduction of carbon dioxide (CO_2) and green-house gas emissions [48]. In addition to the above benefits, warm-mix additives enhance the use of reclaimed asphalt pavement (RAP) [48, 49].

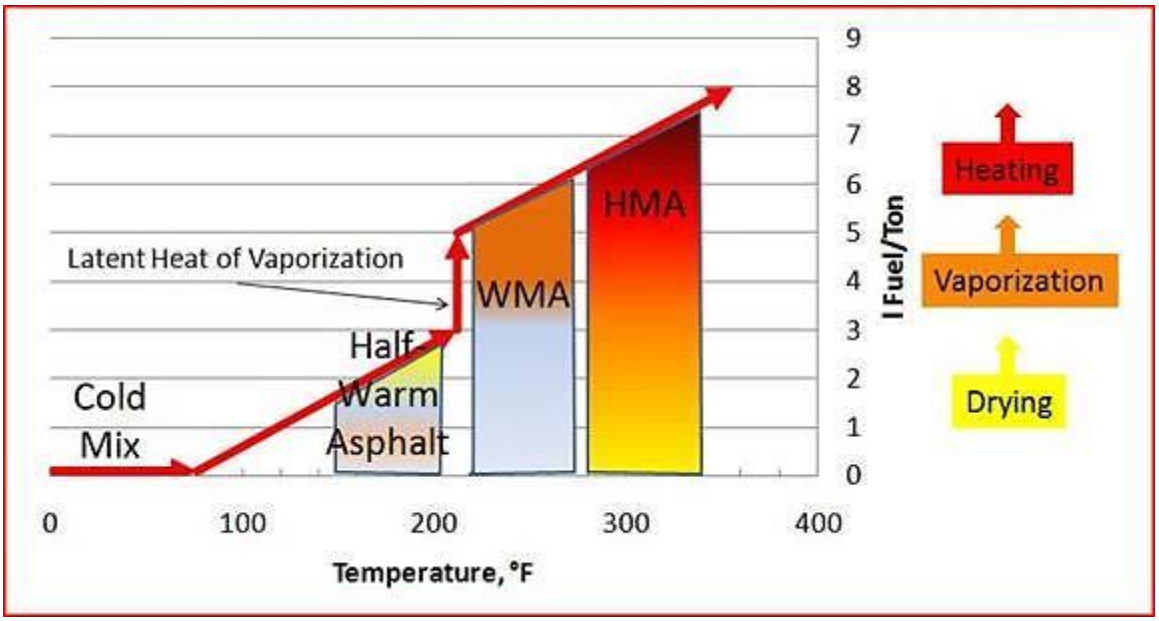

Figure 2.8: (a) Classification of asphalt mixtures by temperature [52]

Warm-mix asphalt (WMA) technology can be categorised into three broad areas. These are the foaming technique, Organic additive and chemical additive technique.

The foaming technique employs the WAM-foam process which is mostly used in Europe in a two phase operation. The first phase deals with the mixing of soft asphalt with aggregate at low temperature. The second phase is aimed at reducing high shear viscosity by mixing foamed hard asphalt to a mixture of soft asphalt and aggregate [50]. The low energy asphalt (LEA) process is another foaming process which incorporates an adhesive additive into the asphalt binder before mixing [49]. Lastly the Double Barrel Green process, which is the prevalent foaming process in

the United States, makes use of a single phase foaming process. The process is carried out by injecting water through a nozzle into the asphalt binder to foam it [49, 51].

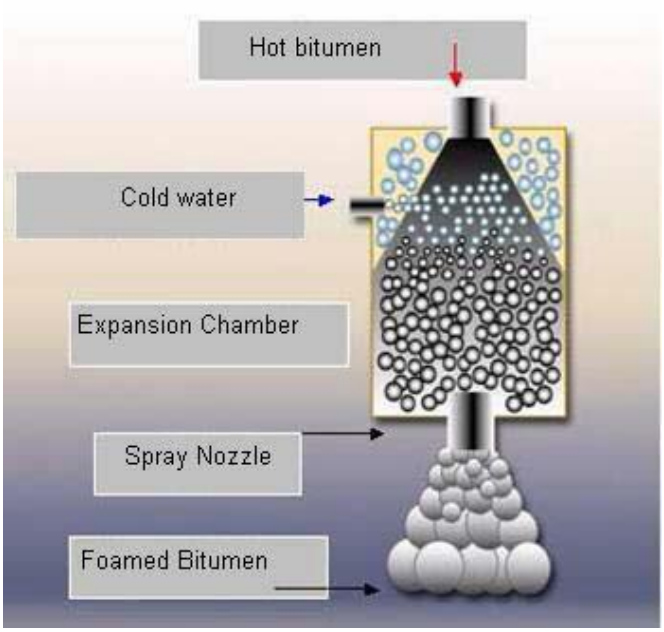

Figure 2.8: (b) Foaming nozzle technique [53]

The organic additive, when mixed with the asphalt binder reduces the viscosity of the binder at temperatures exceeding 90 ºC. Organic additives are noted for a general reduction in temperature between 20 – 30 ºC and also improve the binder's resistance to deformation. Examples of organic additives include fatty amides and waxes but paraffin wax is the most regularly used organic additive [54].

Chemical additives are surfactants which when added to the bitumen; enhance the interface interaction between the bitumen and the aggregate. This interfacial interaction is also regulated together with the frictional force at the interface by the chemical additive. They help to reduce

compaction temperatures between 20 – 30 ºC and a key example of a chemical additive is sodium aluminium silicate (Aspha-Min®) [54, 55].

2.9 Testing Methods

2.9.1 Conventional Test Methods

Asphalt performance grading and property evaluation, in the early 1990s has been successful with the use of conventional test methods such as penetration, viscosity and point test [41, 57]. Grading of asphalt with the use of the conventional test methods were based only on field performance and not on essential engineering properties [56].

There are basically four conventional grades of asphalt binder properties. These include the penetration grade, cut back grade, oxidized grade and the hard grade. The penetration grade is the most important grade among the grades and is obtained through the use of the needle penetration method. The blend of viscosity and softening point methods is ideal in determining the oxidised and hard grades. However, the viscosity test is used to determine the cutback grade [5, 56].

2.9.1.1 Penetration Test

The penetration test is an old method of measuring the hardness of bitumen at standard test conditions [58]. In the standard procedure according to ASTM D5, a needle of 100 g is perforated through the surface of an asphalt binder at 25 ºC for 5 seconds [59]. The depth of

penetration of the needle is reported in units of 0.1 mm. The relation between bitumen hardness to temperature changes can be observed by the equation [60]:

$$\log P = AT + K \quad (9)$$

Where P is the penetration at temperature T, K is a constant and A is the temperature susceptibility, which is also defined as the Penetration Index (PI) and can be obtained using the equation [60]:

$$A = PI = \frac{\log (Pen\ @\ T1) - \log (Pen\ @\ T2)}{T1 - T2} \quad (10)$$

The PI characterises bitumen with a change in value over a range of temperatures [61].

Figure 2.9.1.1: Penetration Test Equipment [62]

2.9.1.2 Softening Point Test

Figure 2.9.1.2 (a) shows the ring and ball softening point test apparatus, which is used to deter mine the softening point (consistency) of the asphalt binder. The softening point test is carried out at a temperature range of 30-157 ºC, when the ring and ball is submerged in ethylene or water. The softening point is then measured at the temperature when the asphalt binder can no longer hold the ball. The flow ability of the asphalt binder is known from this test as well as its consistency [61].

Figure 2.9.1.2: Ring and Ball Softening Point Apparatus [63]

2.9.1.3 Viscosity Test

Viscosity is referred to as the deficiency of slipperiness and can be qualitatively defined as the property of a material that is measured by ratio of the applied shear stress to its induced shear strain [31]. This test employs the unaged and RTFO aged asphalt binders. However, the property characterisation of asphalt binder before HMA processing is achieved through AC grading test. On the other hand AR grading test is carried out on asphalt binders after HMA processing to kindle the property of the asphalt binder. Hence the performance of asphalt binder in HMA pavements is characterised [64]. With the aid of Brookfield and capillary viscometers, the viscosity of an asphalt binder can be easily determined according to the required specifications as shown in Figure 2.9.1.3 [65].

Figure 2.9.1.3: Capillary Viscometer and Brookfield Viscometer [66]

2.9.2 Superpave® Specification Test

The commencement of the Superpave® specification tests was as a result of the failures of the conventional tests to predict a good correlation of the performance of asphalt pavement in-service. Superpave® measures the physical properties of asphalt binder that can be directly related to the pavement in-service performance. The aim of this test is to effectively reduce the various pavement distresses such as fatigue cracking, thermal cracking and permanent deformation [5].

2.9.2.1 Dynamic Shear Rheometer (DSR) Method

The Dynamic Shear Rheometer (DSR) method measures the rheological properties of the asphalt binder like complex shear modulus, G*, G' (elastic component), G'' (viscous component) and phase angle (δ), which helps determine the intermediate and high temperature grade of the asphalt binder [67]. The complex shear modulus (G*) is defined as the measure of a material's resistance to deformation when sheared repeatedly. The phase angle (δ), on the other hand shows the relative amount of recoverable and non-recoverable deformation [68]. In performing this test, the asphalt binder is heated and poured into a thin disc-like silicon mould to take that shape when it cools down. This disc-like shaped asphalt binder is then placed between two parallel plates for oscillation. The disc-like asphalt binder is usually in diameters of 8 mm and 25 mm and is used for low and high temperature respectively. A gap of 2 mm is set between an 8 mm diameter disc-like sample and the parallel plate. However, for a 25 mm diameter disc-like sample, a gap of 1 mm is required. When torsion force at a frequency of 10 rad/s and

temperature of 25 ºC is applied to the sample between the parallel plates, shear modulus can be measured. Complex shear modulus (G*) can be calculated according to the equation [58]:

$$G^* = \tau_o / \gamma_o \quad (11)$$

Where complex shear modulus (G*), characterises the resistance of the material to deformation under an applied shear stress. τ_o is the peak shear stress, which helps to determine the shear stress (τ) according to the equation [58]:

$$\tau = \tau_o \sin (wt + \delta) \quad (12)$$

Where, δ is the phase angle which relates the time lag between the applied stress and the resulting strain. It can also be calculated from the ratio of G'' (viscous or loss modulus) to G' (storage or elastic modulus). According to equation 11, γ_o is the peak shear strain and helps to determine the oscillatory strain (γ) according to the equation [58]:

$$\gamma = \gamma_o \sin wt \quad (13)$$

Where, w is the angular velocity in radian/seconds and t is the time.

Relating the complex shear modulus (G*) to the phase angle (δ) for an unaged asphalt binder, the high temperature grade of the asphalt binder can be obtained from G*/sin δ being greater than 1.00 kPa and greater than 2.20 kPa for RTFO-aged asphalt binder [69].

G*sin δ, is used according to AASHTO specification to determine the intermediate temperature grade of the asphalt binder and must not exceed 5000 kPa [69]. G*sin δ, helps to measure the extent of fatigue cracking an asphalt binder can undergo. G*/sin δ, addresses the extent of permanent deformation (rutting), which an asphalt binder can experience.

Figure 2.9.2.1: (a) Dynamic Shear Rheometer AR 2000 Instrument [13].

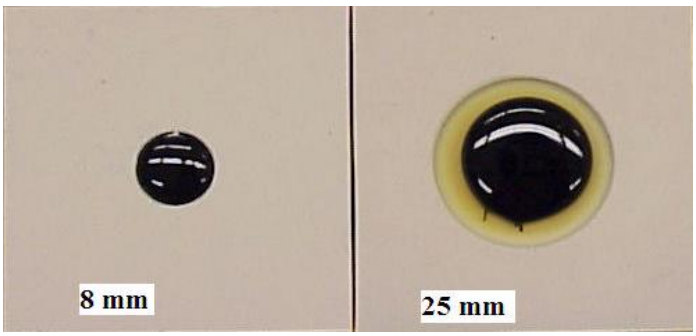

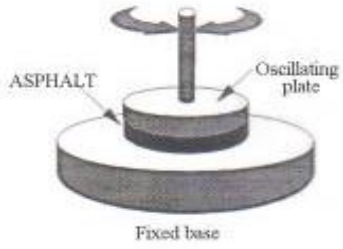

Figure 2.9.2.1: (b) Silicon mold [13, 70]. Figure 2.9.2.1: (c) Parallel plate [13, 71].

2.9.2.2 Bending Beam Rheometer (BBR) Method

The Bending Beam Rheometer (BBR) method is employed to measure the stiffness of the binder when a constant load is applied on the binder which gives a measured deflection (creep). It was developed by the Strategic Highway Research Program (SHRP) to address low temperature cracking distress and has now being accepted in the AASHTO M320 standard protocol [28, 41]. The AASHTO M320 standard protocol gives the specifications required for passing or failing an asphalt binder using the BBR test [72]. With these specifications in place, the idea behind the BBR test is to measure two major parameters. These parameters are the m-value, defined as the slope of the creep stiffness master curve and the creep stiffness S(t). The effect of low temperature cracking is addressed on the basis of these two parameters (S(t) and m-value).

Figure 2.9.2.2: (a) Bending Beam Rheometer (BBR) [73].

In performing this test the asphalt binder sample is heated, poured into a silicon mold to form beams and then trimmed when cooled. The beams are then conditioned in an ethanol bath for one hour at a preferred temperature. The test is then performed at a temperature above the designed pavement temperature by mounting the specimen (the beam) on a support to apply a three-point

load. The load is applied at loading times of 8, 15, 30, 60, 120 and 240 seconds. A graph of load and deflection versus time is obtained with the instrument automatically measuring the m-value and creep stiffness S(t).

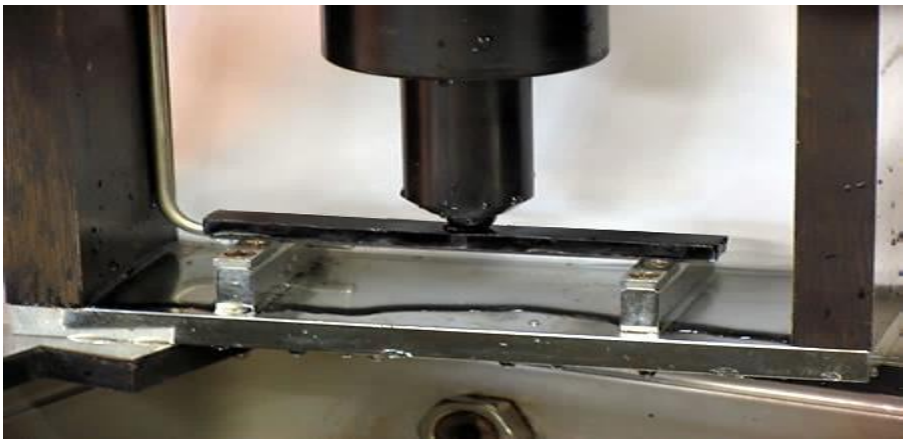

Figure 2.9.2.2: (b) Close-up of the BBR beam on its support [73].

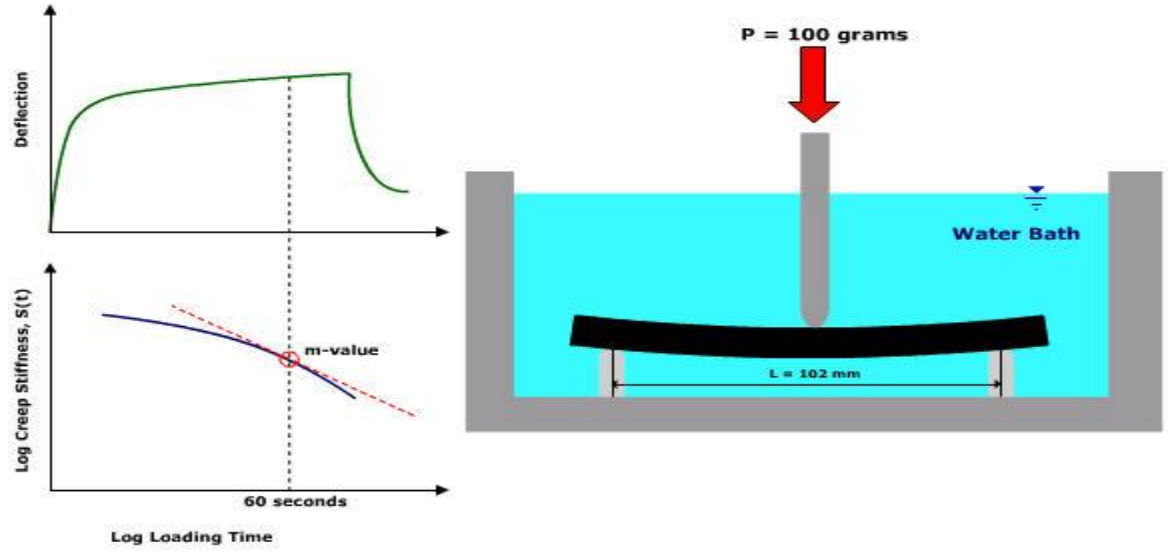

Figure 2.9.2.2: (c) Schematic diagram of the Bending Beam Rheometer (BBR) [74].

According to the given specifications, the asphalt binder fails when the measured m-value is less than 0.3 and the creep stiffness S(t) is greater than 300 MPa. The sample passes when the m-value is greater than o.3 with creep stiffness S(t) less than 300 MPa.

Creep stiffness of the asphalt binder can then be calculated according to the equation:

$$S(t) = PL^3 / 4bh3\delta(t) \quad (14)$$

Where:

S(t) = creep stiffness at time, t;

P = applied load, 100 grams;

L = distance between beam supports, 102 mm b = beam width, 12.5 mm; and

h = beam height, 6.25 mm; and δ(t) = deflection at time, t.

2.9.3 Improved Ministry of Transportation of Ontario (MTO) Test Methods

The AASHTO M320 specification is used in the measurement of the rheological properties such as creep and stress relaxation of an asphalt binder, but the physical aging (hardening) of the asphalt binder is not taken into consideration properly [75-78]. Insufficient aging and conditioning time of the asphalt binder does not give a good representation of its rheological properties which is related to the pavement in service performance. In view of this flaw, the Ontario Ministry of Transportation in alliance with Queen's University has developed new testing methods to help address this challenge. These tests include:

- Extended Bending Beam Rheometer (eBBR) test (LS-308) [79] ; and
- Double-Edge-Notched Tension (DENT) test (LS-299) [80].

2.9.3.1 Extended Bending Beam Rheometer (eBBR) Method LS-308

The conditioning time and temperature of an asphalt binder, goes a long way to predict the extent of physical hardening of the asphalt binder. The regular BBR conditions asphalt binder specimens for only 1 hour but this short conditioning time does not give a good measurement of the hardening in asphalt binders. This defect in the regular BBR has resulted in the development of the extended BBR, which conditions asphalt binder samples for not only 1 hour but at 24 and 72 hours, which accounts efficiently for the physical hardening effect and the low temperature cracking in pavements [77]. In the application of the extended BBR two conditioning temperatures are considered, which are:

- $T_1 = T_{design} + 10^oC$; and
- $T_2 = T_{design} + 20^oC$, where T_{design} is the lowest temperature designed for the pavement, prior to testing.

The AASHTO M320 is used to determine the precise grade of the asphalt binder by using a pass and a fail temperature value through interpolation. The grade temperature and subsequent grade loss can be evaluated after a temperature conditioning period. The best grade lost can be evaluated by taking the difference between the least warm and least cold limiting temperature (where S (60s) reaches 300MPa and m-value (60s) reaches 0.3) [21]. The worst grade on the other hand can be evaluated by taking the difference of the warmest and coldest limiting temperature (where S (60s) reaches 300MPa and m-value (60s) reaches 0.3) [21]. Thus, this method gives a good evaluation of the performance of the asphalt binder in low temperature cracking [57].

2.9.3.2 Double-Edge Notched Tension (DENT) Test LS-299

Asphalt binder has ductile and brittle properties which can be evaluated using the double edge notch tension test and on the wheels of the theory of essential work of fracture, which was first instigated by Cotterell and Reddel [81]. The double edge notched tension test does not only seek to measure the essential work of failure in asphalt binders but also the plastic work of failure and the critical crack tip opening displacement (CTOD) [80]. To carry out this test, the asphalt binder after being heated is poured into special molds to form notched specimens with the distance between the opposite notches ranging as 5 mm, 10 mm and 15 mm. The prepared specimens are then conditioned in a water bath at a specified temperature. The test is then carried out by stretching the specimens until a failure as observed in figure 2.9.3.2 (a).

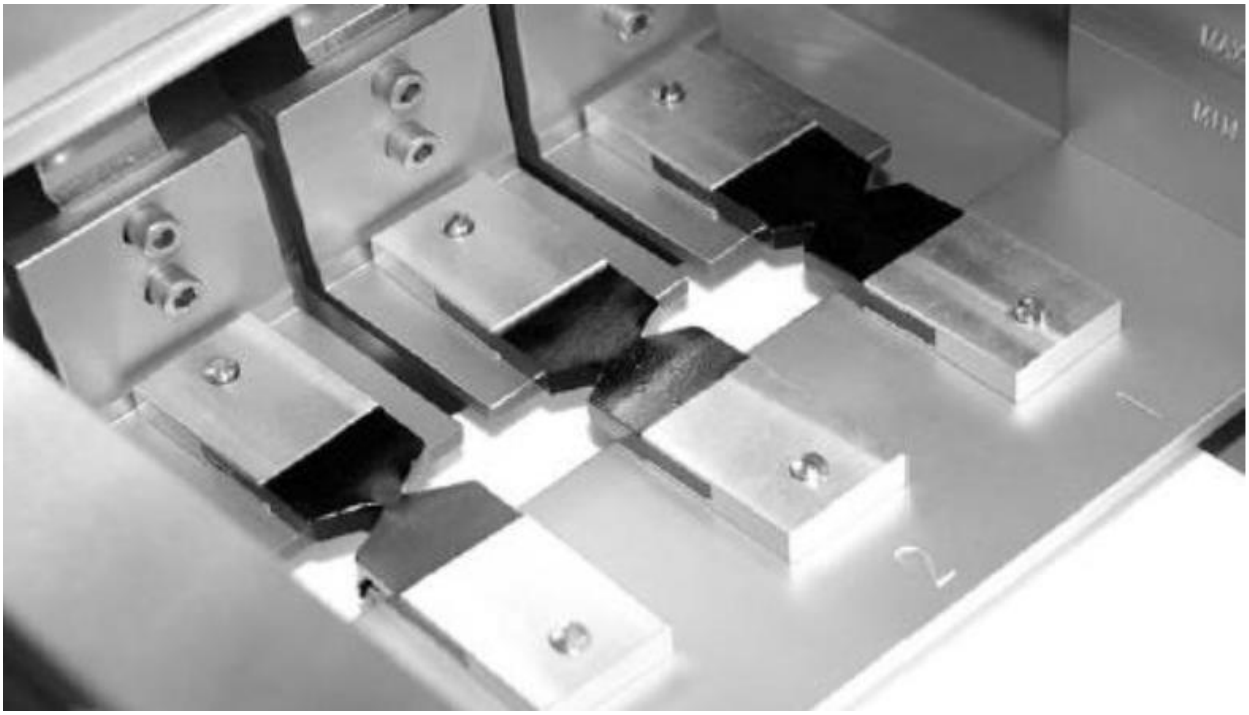

Figure 2.9.3.2: (a) Double Edge Notched Tension (DENT) Test set up [84].

The total work of fracture is made up of the sum of the essential work of fracture energy and the plastic work of fracture energy, as shown in figure 2.9.3.2 (b).

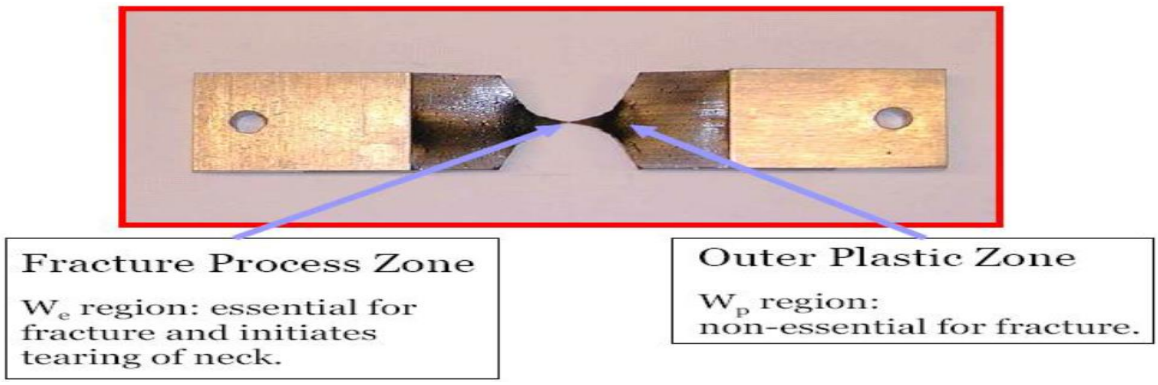

Figure 2.9.3.2: (b) Fracture and plastic zone of asphalt binder [82].

The total work fracture (Wt) can be evaluated from the total area under the force-displacement curve according to the equation:

$$W_t = W_e + W_p \quad (15)$$

Where, W_e is the essential work of failure and W_p is the plastic work of failure, and can be determined according to the following equations:

$$W_e = w_e \times LB \quad (16)$$

$$W_p = w_p \times \beta L^2 B \quad (17)$$

Where, w_e = specific essential work of fracture (J/ m^2);

w_p = specific plastic work of fracture (J/ m^2);

L = the ligament length in the DENT specimen (m);

B = the thickness of the sample (m); and

β = the shape factor of the plastic zone, which is dependent on the geometry.

By substituting equations 16 and 17 into 15 gives,

$$W_t = (w_e \times LB) + (w_p \times \beta L^2 B) \quad (18)$$

By dividing equation (18) by the cross-sectional area of the plastic zone (LB),

$$\frac{Wt}{LB} = w_t = w_e + w_p \beta LB \quad (19)$$

Where, w_t = specific total work of fracture (J/ m^2).

A plot of the specific total work of failure, w_t, against the ligament length, L, in equation (19) gives a straight line with slope and intercept on the w_t axis. CTOD, which predicts the fatigue cracking resistance of an asphalt binder, can be determined using w_e according to the equation [83]:

$$\delta_t = \frac{We}{\sigma n} \quad (20)$$

Where, δ_t is the crack tip opening displacement parameter (m); and

σ_n is the net section stress or yield stress (N/m^2), determined from the 5 mm ligament length of the DENT mould.

CHAPTER THREE

MATERIALS AND EXPERIMENTAL METHODS

3.1 Materials

The sample materials used in this study were obtained from the Ontario Ministry of Transportation (MTO), City of Kingston and the York Region. These sample materials are Hot Mix Asphalt (HMA) designed according to the Ontario Ministry of Transportation (MTO) specifications with the exception of K1 and K2 designed in conformity to City of Kingston specification and Y1 designed in conformity to the York Region specification. Additionally, already prepared stone mastic asphalt rubber samples were also tested in this study. The various Hot Mix Asphalt (HMA) samples were made up of a mixture of sand and aggregate bound together by the asphalt binder. The nature of the samples depends on the type of aggregate, sand, additives, modifiers and Performance Grade (PG) of the asphalt binder, which are clearly stated in the mix design of the various samples. The mix design describes the manner in which the components in the sample have been mixed to achieve good pavement performance. It also contains information about conditions to be adhered to when using the sample and also the source of the sample. The desired volumetric parameters such as voids filled with asphalt (VFA), voids in mineral aggregate (VMA) and air voids of the samples were achieved by the use of the mix design. The mix design gives parameters such as the bulk specific gravity (Gmb) and maximum specific gravity (Gmm) upon which the desired air voids of the samples can be determined. Further details about the mix properties of the respective Highway samples used in this study are shown in Table 3.1.

Table 3.1: HMA Mix Properties Used in this Study.

Sample	Aggregate Type		Additive/ Modifier/ RAP	Performance Grade (PG)
	Coarse	Fine		
HIGHWAY 1	HL-1 STONE	DFC FINES	N/A	64-28 MD
HIGHWAY 6	DFC COARSE	DFC FINES	CELLULOSE FIBRE	70-28 MD
HIGHWAY 7A	HL-1 STONE	UNWASHED SAND	N/A	58-28
HIGHWAY 7B	HL-1 STONE	WASHED FINES	N/A	58-34 P
HIGHWAY 11	12.5 (HL-1) STONE	CHIP, WASHED SCREENINGS	AD-here LOF 65.00 & RAP	58-34 D
HIGHWAY 17	DYMENT Q	CHIPS	PVB LITE	58-34 P
HIGHWAY 24	HL-1 STONE	ASPHALT SAND	RAP	64-28
HIGHWAY 65	12.5mm STONE	1/4 CHIP	PVB LITE & RAP	52-34
HIGHWAY 400	HL-1 STONE	WASHED & UNWASHED FINES	HYDRATED LIME	64-28 P
HIGHWAY 402	QUARTZITE FC2 STONE	UNWASHED QUARTZITE FC2 FINES	HYDRATED LIME	64-28 MD
HIGHWAY 631	12.5mm STONE	ASPHALT SAND	PVB LITE	52-40 PMA
K2	HL-1 STONE	ASPHALT SAND	N/A	64-28 XD

K1	HL-1 STONE	ASPHALT SAND	N/A	64-28 XD
Y1	12.5mm STONE	ASPHALT SAND	N/A	58-28

3.2 Preparation of Asphalt Mix Samples for IDT Test

3.2.1 Ageing of Samples

The hot mix asphalt (HMA) samples contained in labelled boxes are aged in an oven at 120 ºC for about 18 hours prior to mixing. The aging of the samples is done one at a time for a particular hot mix asphalt (HMA) sample, where two boxes of the sample is first of all weighed to know how much of it will be distributed into six molds before placed in the oven.

3.2.2 Mixing of Samples

The sample in the boxes was gently poured into a hot bucket after ageing, with the temperature of the bucket approximately at 120 ºC so as to ensure a temperature balance in the mixing of the sample. The bucket was then placed in an electric stirrer and with the aid of a stirring rod placed in the bucket; the sample was gently mixed homogeneously for approximately 3 minutes when the switch on the stirrer was turned on.

3.2.3 Compaction of Samples

A calculated amount of the sample was then fed into each of the six moulds with the aid of a scooper and the moulds placed back into the oven at an elevated temperature of 145 ºC for 2 hours prior to compaction. Compaction of the sample in the moulds was then carried out after 2 hours in the oven by means of the Superpave^{TM} gyratory compactor. Parameters such as the

desired height of the sample, maximum number of gyrations, compaction pressure, speed and angle were set on the instrument prior to compaction. The samples were then compacted into briquettes to the desired height and then the moulds containing the compacted samples allowed to cool down to 70 ºC when taken out of the instrument. The aim of cooling the moulds to 70 ºC was to allow easy extrusion of the compacted sample out of the mould. Finally, samples were extruded out of the moulds at 70 ºC to avoid deforming the samples and were then placed on working bench for a day in preparation for cutting.

Figure 3.2.3: Pine Gyratory Compactor [85].

3.2.4 Cutting of Samples

The briquette samples were mounted on a clamp fixed on the cutting surface of the cutting instrument. The desired thickness of the specimens was set on the cutting instrument and the briquette samples sliced into 50 mm disk specimens.

Figure 3.2.4: Exotom-150 Cut-off Machine [86].

3.2.5 Air Void Determination

The air void content of the 50 mm disk specimens was determined after taking the weight in water, surface dry weight and the dry weight of the specimens respectively. The air void content of the specimens was then calculated according to the equation [87]:

$$\% \text{ Air Voids} = (G_{mm}\text{-}G_{mb}/G_{mm}) \times 100 \quad (14)$$

Where, G_{mm} is the Maximum specific gravity; and G_{mb} is the Bulk specific gravity.

However, the bulk specific gravity (G_{mb}) can be obtained from the equation [87]:

$$G_{mb} = (\text{Dry weight} / \text{Weight of saturated surface dry-Weight in water}). \quad (15)$$

The air void content for the specimens produced from all samples tested in this study was between 4 to 6%.

3.3 Indirect Tensile (IDT) Creep and Strength Test

3.3.1 Indirect Tensile (IDT) Creep Test

The Indirect Tensile (IDT) Creep test was carried according to the procedure detailed in AASHTO standard test T322-07 using the Material Test System (MTS) loading frame and software [88]. Prior to the test, the middle section of the two opposite surfaces of the specimens were glued with magnetic stubs and allowed to dry properly for a day. Three replicate specimens were conditioned in the chamber of the Material Test System (MTS) loading frame at a desired temperature for two hours and the test was carried out immediately after conditioning at the conditioning temperature. The test was carried out by attaching strain measuring devises known as extensometers to the magnetic stubs on each side of the specimen and then mounted on the loading frame of the instrument. Constant loads of 8000, 6000, 4000 and 2000 N were applied on the specimens at -30, -20, -10, and 0 °C respectively, with the corresponding strain (displacement values) measured by the extensometers. The raw displacement data was then processed into creep compliance. Three replicate specimens were tested for each load applied at its respective testing temperature for reproducibility.

Figure 3.2.5: Loading Frame and Chamber of Material Testing System (MTS).

3.3.2 Indirect Tensile (IDT) Strength Test

The strength of the specimens was carried out by applying load on the specimen without any attached extensometers till fracture (failure) occurs. Two replicate specimens were failed at -20 and -10 °C after 2 hours of conditioning at the same testing temperatures respectively. The raw data of the maximum load of failure was used to process the strength of the specimen at -20 and -10 °C respectively.

3.4 Recovery of Asphalt Binder from Asphalt Mix

Sample specimens which were failed during the strength test were further broken down into pieces, and about 5 to 6 kg of the pieces of specimen filled in a can. However, only Highway 1, 6, 7A, 24, 400, 402 and K1 samples were recovered for binder performance analysis. The can was then filled with toluene till the entire broken specimen was completely submerged in the toluene. The can containing the broken specimen together with toluene was covered with a lid and allowed to stand overnight to enhance dissolution of the broken specimens. The toluene dissolved the asphalt binder in the mix and was then decanted into an empty labelled bottle. Toluene was however used repeatedly between 6 to 8 times to wash out any remaining asphalt binder and then decanted leaving the sediment sand and aggregate. 85% of toluene and 15% of ethanol (425 ml of toluene and 75 ml of ethanol) was finally used to wash any polar group remaining in the can. The solvent together with the asphalt binder which has been recovered was then fed into a rotary evaporator to extract the solvent leaving the asphalt binder. The extraction of the solvent by means of the rotary evaporator was done by a condensation process. The solvent was condensed between 70 to 80 °C and an aspirator pressure set at 180 mbar. The

aspirator pressure was decreased gently as the extraction process was being carried out until a point where no solvent could be extracted again. Shortly after this process, the temperature was set to 200 °C under a pressure of10 mbar for 2 hours to ensure no trace of the solvent in the asphalt binder. The recovered asphalt binder was then weighed and poured into an empty labelled beaker which was the stored in a drawer. The percentage of asphalt binder content (% A.C) of the mix was calculated according to the equation:

% A.C = (weight of recovered asphalt binder / Total weight of pieces of mix) x100 (16)

Figure 3.4: Rotary Evaporator [89].

3.5 Dynamic Shear Rheometer (DSR) Method

In order to evaluate the rutting (permanent deformation) resistance and fatigue cracking resistance of the recovered asphalt binder at high and intermediate temperatures respectively, the dynamic shear rheometer (DSR) was used to carry out this evaluation. In this test, the DSR test specimens were prepared by heating the various recovered Highway asphalt binder samples in an oven until they became less viscous and easy to pour into silicon moulds with a definite dimension as shown below in Figure 3.5.

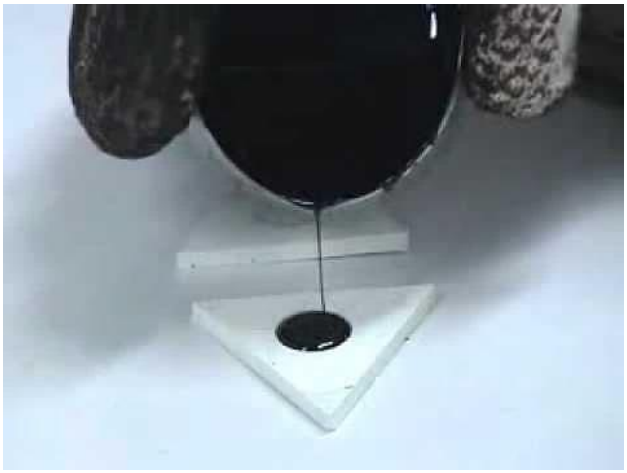

Figure 3.5: DSR Sample Preparation [100].

The DRS test specimen was the allowed to cool and solidify in the silicon mould before it could be tested. Once the specimen has properly cooled and taken shape in the silicon mould, the parallel plates of the DSR instrument was heated at 46 °C to enable the test specimen to be attached to the plate prior to testing. A gap zero procedure was performed on the DSR instrument before mounting the test specimen on the plate and the plate was then adjusted until the upper plate barely touches the surface of the test specimen. With the aid of a trimming tool, a trimming procedure was carried out on the test specimen by removing the excess test specimen adhered to the sides of the parallel plate due to the compression of the plates. The desired test temperature

was then set and when the temperature of the test specimen had gotten to the test temperature, the test carried out at a frequency of 1.59 Hz (10 rad/sec) for 10 cycles. The complex shear modulus (G*) and the phase angle (δ) were measured by the DSR instrument over the 10 cycle. The measured complex shear modulus (G*) and phase angle (δ), were then used to determine the high and intermediate temperature grading of the test specimen.

3.6 Bending Beam Rheometer (BBR) Method

The Bending Beam Rheometer (BBR) method was used to determine the low temperature grades of the various recovered asphalt binders, which characterises the extent of physical hardening and thermal cracking severity of the asphalt binder. The BBR test specimen were prepared by heating the various recovered Highway asphalt binder samples in an oven until they became less viscous and easy to pour into silicon moulds with a definite dimension as shown below in Figure 3.6.

Figure 3.6: BBR Sample Preparation [101].

Likewise, the BBR test specimen which are popularly referred to as BBR beams were trimmed immediately after the specimen were properly cooled and had taken the shape of the mould. Then after trimming the BBR test specimen (beams), they were then conditioned in an ethanol bath for 1 hour at -10 °C prior to testing. The BBR test specimen (beams), were then tested at 0, -10, -20 and -30 °C when mounted on a support frame of the BBR instrument at a varying load responsible in generating sufficient deflection as shown in Figure 2.9.2.2 (b). A graph of load and deflection versus time was obtained, with the instrument automatically measuring the creep stiffness (S) and the creep rate (m). The creep stiffness (S) and the creep rate (m) are then used in determining the low temperature grades of the test specimens.

3.7 Extended Bending Beam Rheometer (eBBR) Method

The extended BBR test was developed with aim of evaluating the extent to which an asphalt binder can undergo physical hardening (reversible aging) when kept for longer periods at low temperatures. Unlike the regular BBR test where the test specimen were kept in an ethanol bath for 1 hour; the extended BBR test specimen were conditioned in an ethanol bath at -10 °C for 72 hours prior to testing. The test was then carried after conditioning using the regular BBR testing procedure at temperatures of 0, -10, -20 and -30 °C to determine creep stiffness (S) and the creep rate (m) of the specimen. An interpolation procedure was then carried out using a pass/fail temperature usually -10 and -20 °C according to AASHTO M320 to determine the grade of the asphalt binder [72].

3.8 Double-Edge Notched Tension (DENT) Test LS-299

The DENT test was developed to address the fatigue cracking distress observed on asphalt pavements. This test also seeks to evaluate the ductile failure resistance of asphalt binder when it is pulled apart at a constant loading rate of 50 mm/min at a temperature of 15 °C. The DENT test specimen were prepared by heating the recovered asphalt binder in an oven until it becomes less viscous and then poured into a brass mould of opposite notches with different notch length of 5 mm, 10 mm and 15 mm. The specimens were then allowed to cool, solidify and to take the shape of the mould as shown in Figure 3.8. The specimens were then taken out of the moulds and conditioned in a water bath at a temperature of 15 °C for 3 hours before testing.

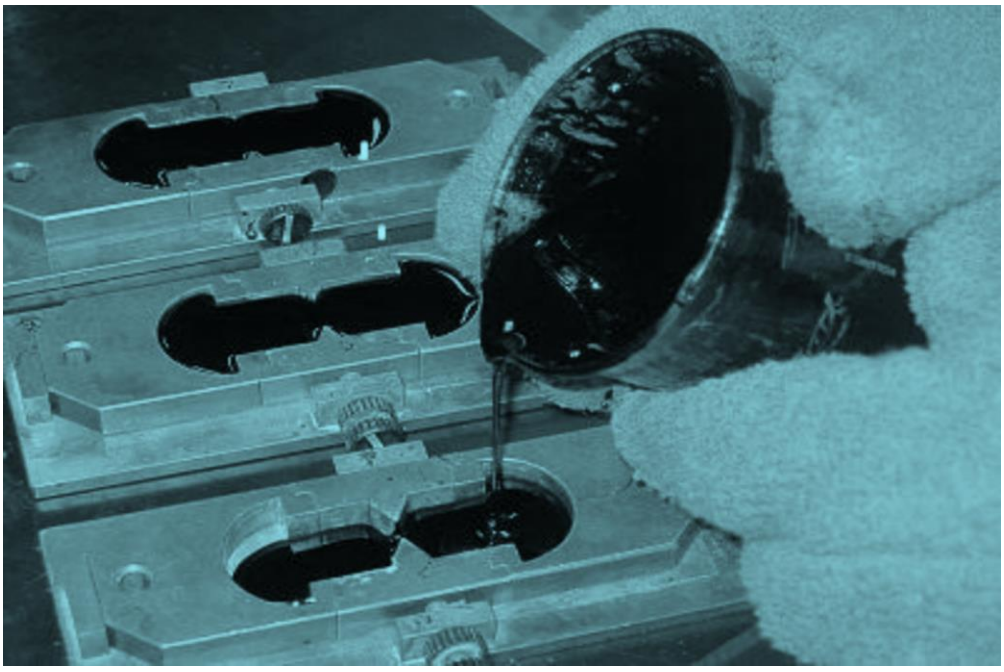

Figure 3.8: DENT Specimen Preparation [5].

The test was then carried out by pulling apart the specimen at a constant loading rate of 50 mm/min in a water bath of 15 °C temperature until failure occurred. The test was repeated for each different notch length to obtain reproducibility of data. The Critical Tip Opening

Displacement (CTOD), Essential Work of Fracture (EWF) and Plastic Work of Fracture (PWF) were determined using an excel sheet to process the data obtained from the test.

3.9 X-Ray Fluorescence (XRF) and Infrared (IR) Spectroscopic Analysis

3.9.1 X-Ray Fluorescence (XRF) Analysis

An X-Ray Fluorescence Analysis was performed on all the recovered asphalt binders and two straight waste engine oils (WEO) samples. The aim of this analysis was to determine the presence and quantity of zinc (Zn) and molybdenum (Mo) in the samples. Zinc occurs in engine oils in the form of zinc dialkyldithiophosphate (ZDDTP) as a universal antioxidant and anti-wear additive [5, 102]. Waste engine oils (WEO) has been found to contain large amounts of metals such as zinc and molybdenum, which aids as catalyst to enhance chemical oxidation in asphalt binders leading to poor in service performance [102, 103]. A hand-held Bruker Tracer XRF Analyser was used to irradiate the surface of the samples. The irradiation of high energy x-rays by the instrument on the surface of the samples causes electrons in the inner K-shell of the heavy metal present to be removed, creating available holes in the K-shell [5, 104]. Electrons from the outer L and M-shells then jump to occupy the holes in the inner K-shell [5, 104]. The process of occupying the holes in the K-shell by electrons from the outer L and M-shells results in an emission of lower energy x-rays which is characteristic of a heavy metal present in the sample. The XRF analyser then detects the emitted radiations and hence a quantitative amount of the heavy metal present was determined. The presence of zinc was determined at 8.64 keV after the thirty second scan whiles molybdenum was determined at 17.48 keV after the thirty second scan.

3.9.2 Fourier Transform Infrared (FTIR) Analysis

Infrared spectroscopy was carried out on all the recovered asphalt binder samples by using a Perkin-Elmer spectrum 400 FT-IR spectrometer. A minute quantity of each sample was smeared on a KBr disc, which was initially heated at 140 °C for about 3 minutes. The IR spectrometer was then calibrated by performing a background scan and the KBr disc placed in the spectrometer. A sixteen scan was carried out on the test specimen over a wavenumber range of 4000 cm^{-1} to 400 cm^{-1} using the IR software. Data obtained from the scan was used in determining the peak areas of the functional groups of interest present in the specimen. The integral boundaries used for determining the peak areas of the functional groups were as follows; 1760 cm^{-1} to 1655 cm^{-1} for carbonyl, 1070 cm^{-1} to 985 cm^{-1} for sulfoxide, 1650 cm^{-1} to 1535 cm^{-1} for aromatic, 983 cm^{-1} to 955 cm^{-1} for butadiene, 710 cm^{-1} to 690 cm^{-1} for styrene, 1400 cm^{-1} to 1330 cm^{-1} for CH_3 and 3121 cm^{-1} to 2746 cm^{-1} for CH_2. The CH_2 was taken as the internal standard because it is relatively inert to oxidative changes, and was however used to determine the functional group indices by taking the ratio of a specific functional group peak area to that of the CH_2 peak area. The functional groups analysed are contained in asphalt and are prone to undergo oxidation in the presence of air containing oxygen and sunlight. Chemical changes that evolve as a result of oxidation can facilitate pavement distress [5].

CHAPTER FOUR

RESULTS AND DISCUSSIONS

4.1 Indirect Tensile Test (IDT) Analysis

4.1.1 Creep Compliance Data Analysis

Creep is defined according to AASHTO T322 as the "*time-dependent part of strain resulting from stress*" [88]. Additionally, creep compliance is defined as "*the time-dependent strain divided by the applied stress*" [88]. In this study, creep compliance data was obtained from a non-destructible test and used to predict the thermal cracking performance of asphalt mixes. A plot of creep compliance at different temperatures against time, generated creep compliance curves which explains the viscoelastic behaviour of asphalt mixes when subjected to loading under a specified temperature condition. Figures 4.1.1 (a) and (b) gives a representation of creep compliance curves at different temperatures.

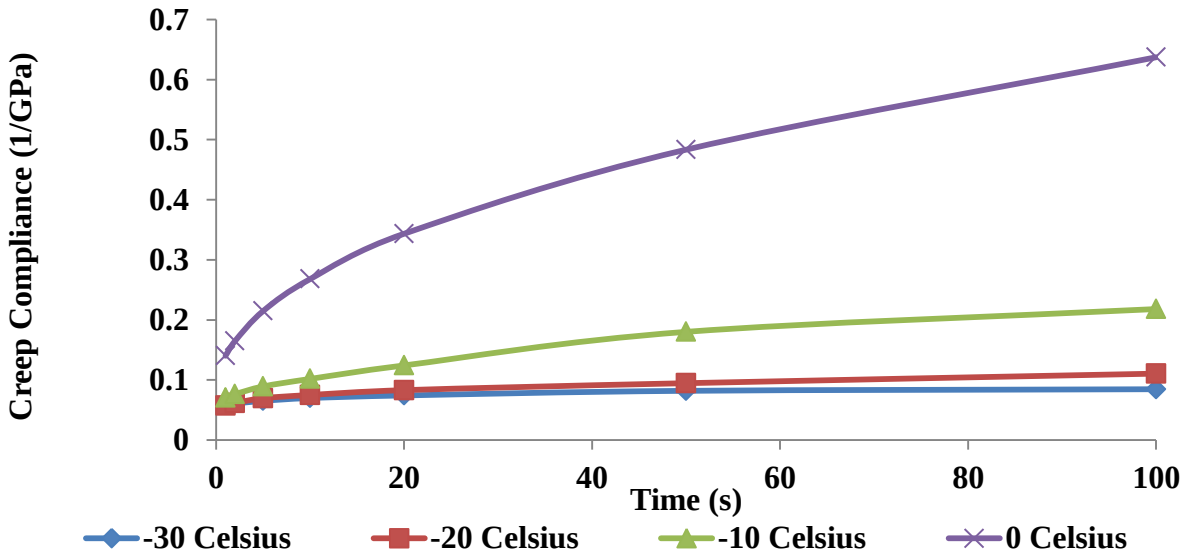

Figure 4.1.1: (a) Creep compliance curves for K1.

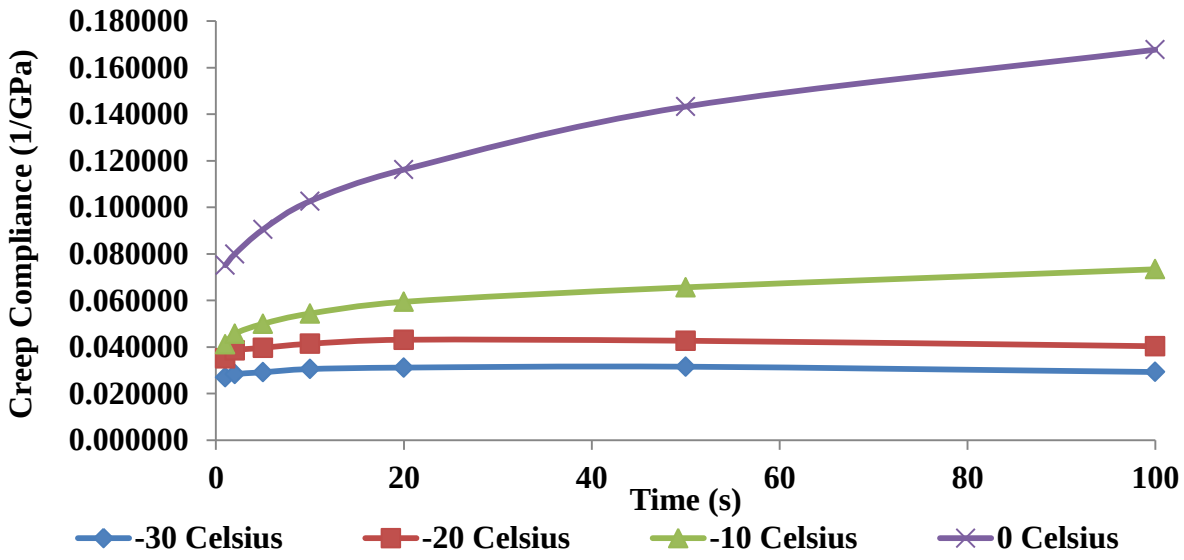

Figure 4.1.1: (b) Creep compliance curves for Highway 24.

From Figures 4.1.1 (a) and (b) the viscoelastic nature of asphalt mixes is clearly observed. At lower temperatures, creep compliance reduces due to decrease in strain response with applied stress as a result of increased stiffness. The sample then becomes more elastic in nature at lower temperatures and creep compliance is reduced. However, at warmer temperatures such as 0 ^{o}C creep compliance increases as a result of reduced stiffness and elasticity. Therefore, the sample responds to higher strain values from an applied stress and is said to be creep compliant. Comparing the creep compliance curves of K1 to that of Highway 24, curves obtained in K1 at -10 ^{o}C,-20 ^{o}C and -30 ^{o}C were at higher creep compliance above 0.8 GPa^{-1} while Highway 24 had curves below 0.8 GPa^{-1}. This suggests that K1is more creep compliant at lower temperatures than Highway 24 and will be able to relax stresses to resist low temperature cracking distress. However, both samples had curves at 0 ^{o}C recording higher creep compliance values. Figures 4.1.1 (c) gives a summary of the average creep compliance at 50 s for all the recovered asphalt samples.

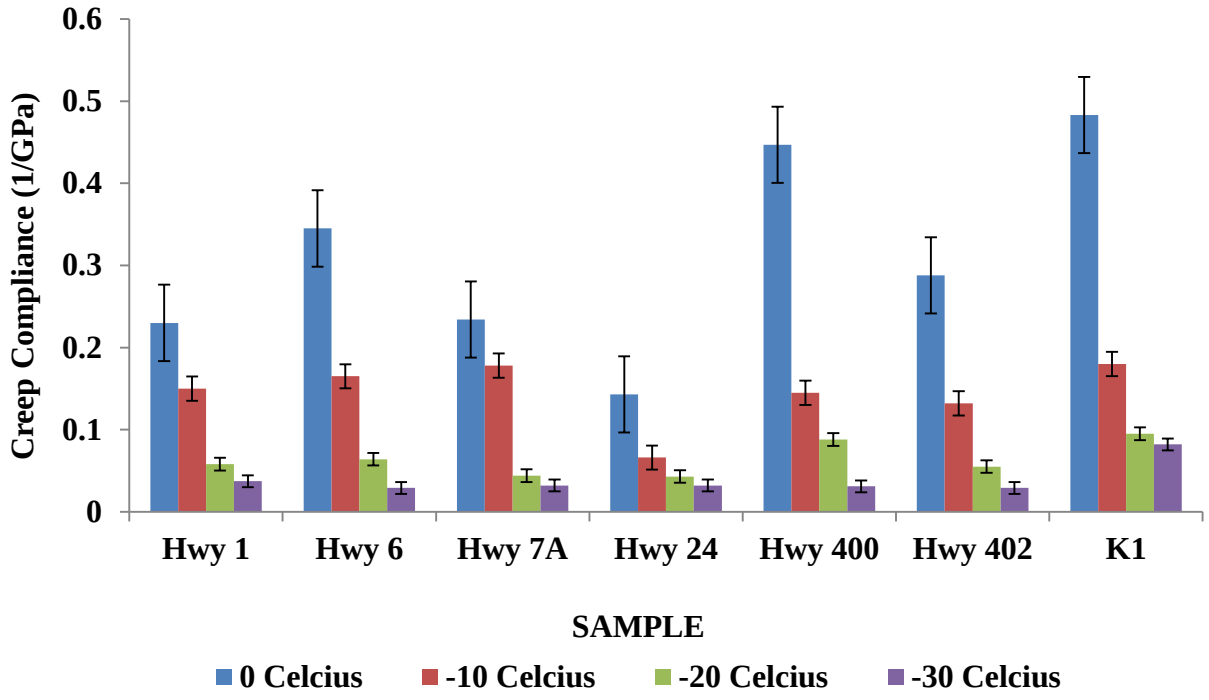

Figure 4.1.1: (c) Average creep compliance at 50 s for the recovered samples.

K1from figures 4.1.1 (c) obtained the highest average creep compliance at 50 s for all temperatures at 0 ^{o}C,-10 ^{o}C,-20 ^{o}C and -30 ^{o}C compared to the remaining samples. This observation suggests the asphalt binder of K1 would be less stiff and less elastic but more creep compliant at lower temperatures. However, the coarse aggregate and fine aggregate used for making the K1 mix samples play a role in the creep performance of the sample. HL-1 stone, a coarse aggregate which is known to be granite stone and asphalt sand, a fine aggregate, were used for making the K1 mix samples. HL-1 stone, which is a granite stone, is known to possess a high load bearing capacity [107]. The asphalt sand is good abrasive sand that works for skid resistance [108]. These mix properties of the K1 mix samples, ultimately enhances the stress relaxation ability of the mix samples, leading to high resistance to low temperature thermal cracking. Although Highway 24 is made up of HL-1 stone and asphalt sand, the addition of

reclaimed asphalt pavement (RAP) to the mix might have caused increased stiffness and elasticity at lower temperatures. Hence Highway 24 had the least average creep compliance at 50 s for all temperatures at 0 ^{o}C,-10 ^{o}C,-20 ^{o}C and -30 ^{o}C compared to the remaining samples. Results obtained from studies conducted with the addition of RAP binder to virgin binders' showed an increase in creep stiffness which would be interpreted as a decrease in creep compliance at low temperatures [109]. This might explain the low measure of creep compliance observed in Highway 24. The remaining samples obtained an appreciable creep compliant value for all temperatures at 0 ^{o}C,-10 ^{o}C,-20 ^{o}C and -30 ^{o}C. Figures 4.1.1 (d) gives a summary of the creep compliance master curve for all the recovered asphalt samples

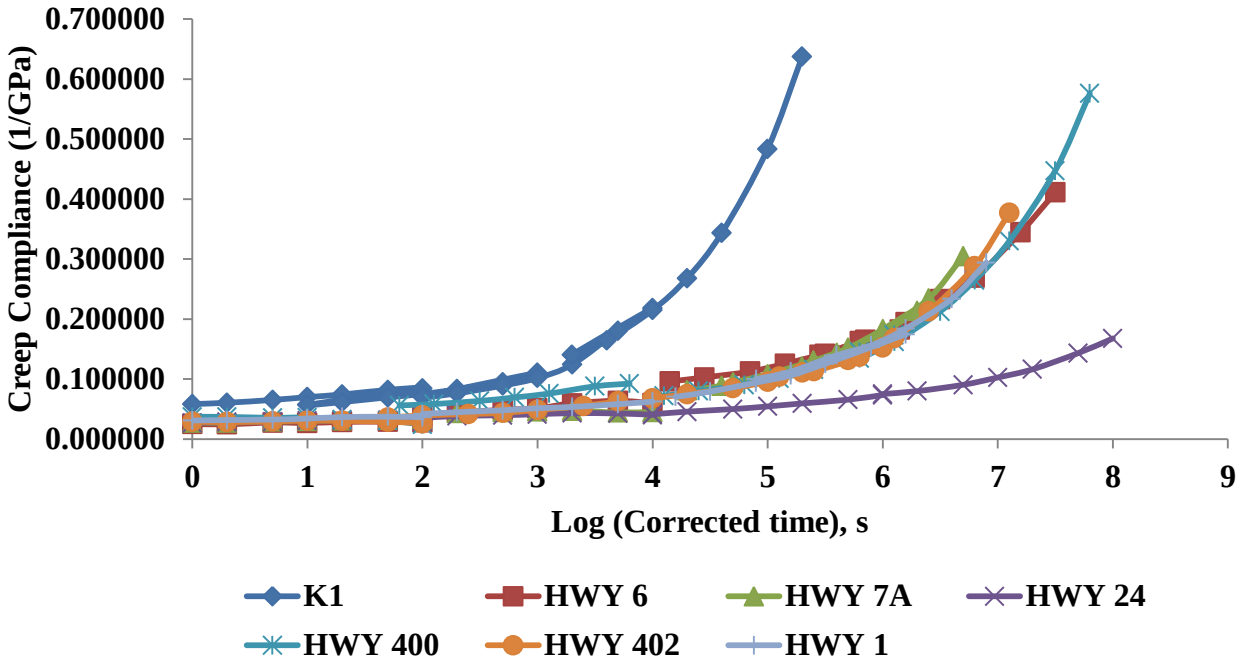

Figures 4.1.1: (d) Creep compliance master curves for all the recovered asphalt samples

The average creep compliance at 50 s for all the unrecovered samples is given in figure 4.1.1 (e) below.

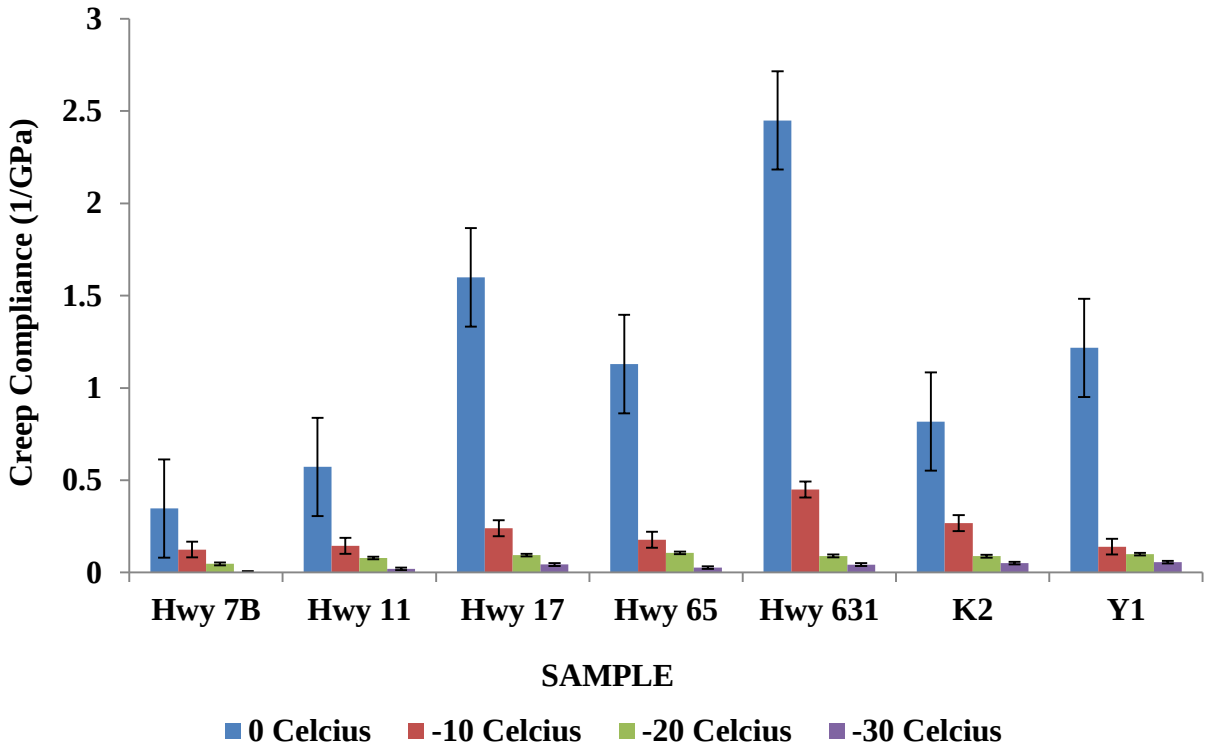

Figure 4.1.1: (e) Average creep compliance at 50 s for the unrecovered samples.

Highway 631 obtained the highest average creep compliance at all temperatures, whiles Highway 7B obtained the least average creep compliance compared to the remaining samples. However, K2, Y1 and Highway 17 all performed very well in terms of creep compliance at temperatures of -10 ^{o}C,-20 ^{o}C and -30 ^{o}C. Figures 4.1.1 (f) also gives a summary of the creep compliance master curves for all the non-recovered asphalt samples.

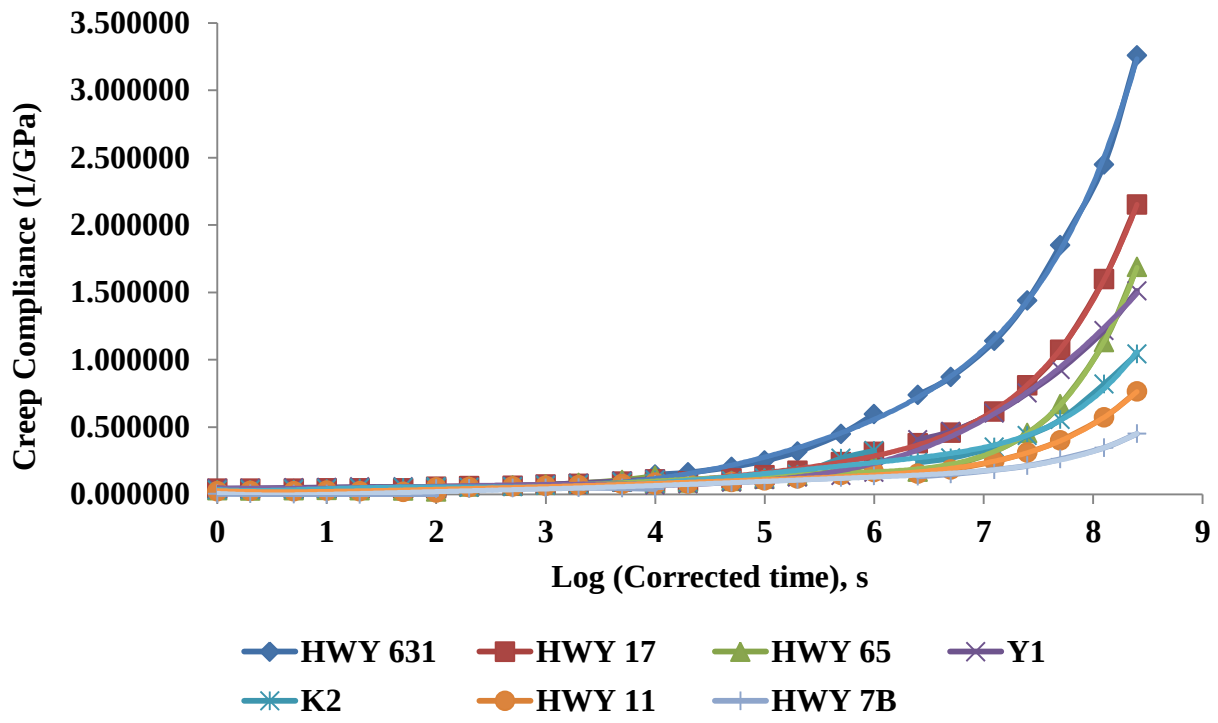

Figures 4.1.1: (f) Creep compliance master curves for all the recovered asphalt samples

Stone mastic asphalt rubber samples were also tested to investigate their creep performance at low temperatures and their resistance to low (thermal) temperature cracking.

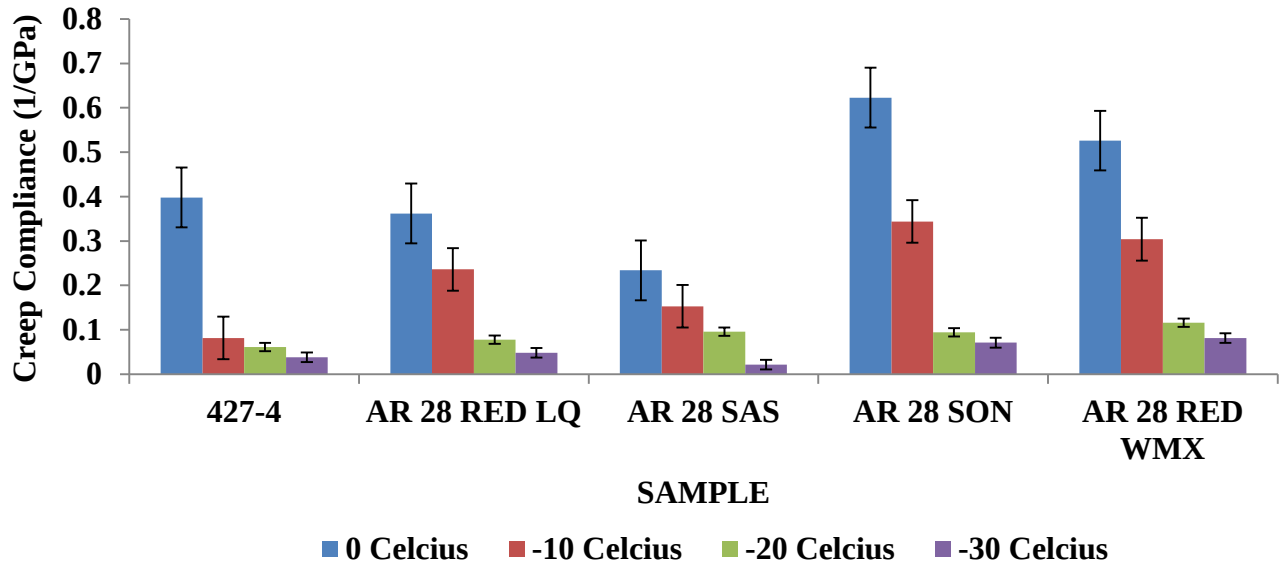

Figure 4.1.1: (g) Average creep compliance at 50 s for stone mastic asphalt rubber samples.

The average creep compliance results for the stone mastic asphalt samples shows Sonnewarm to have obtained the highest average creep compliance at 0 ^{o}C and -10 ^{o}C, whiles Rediset WMX obtained the highest average creep compliance at -20 ^{o}C and -30 ^{o}C compared to the remaining samples. At temperatures of 0 ^{o}C and -30 ^{o}C, Sasobit performed poorly, whiles 427-4 performed woefully at -10 ^{o}C and -20 ^{o}C, in terms of creep compliance.

4.1.2 Indirect Tensile Strength Data Analysis

According to AASHTO T322, strength of a sample determine from an IDT test is defined as "*the strength shown by a specimen subjected to tension, as distinct from torsion, compression, or shear*" [88]. Shown in figure 4.1.2 (a) below is the summary of the strength data for all the recovered asphalt samples.

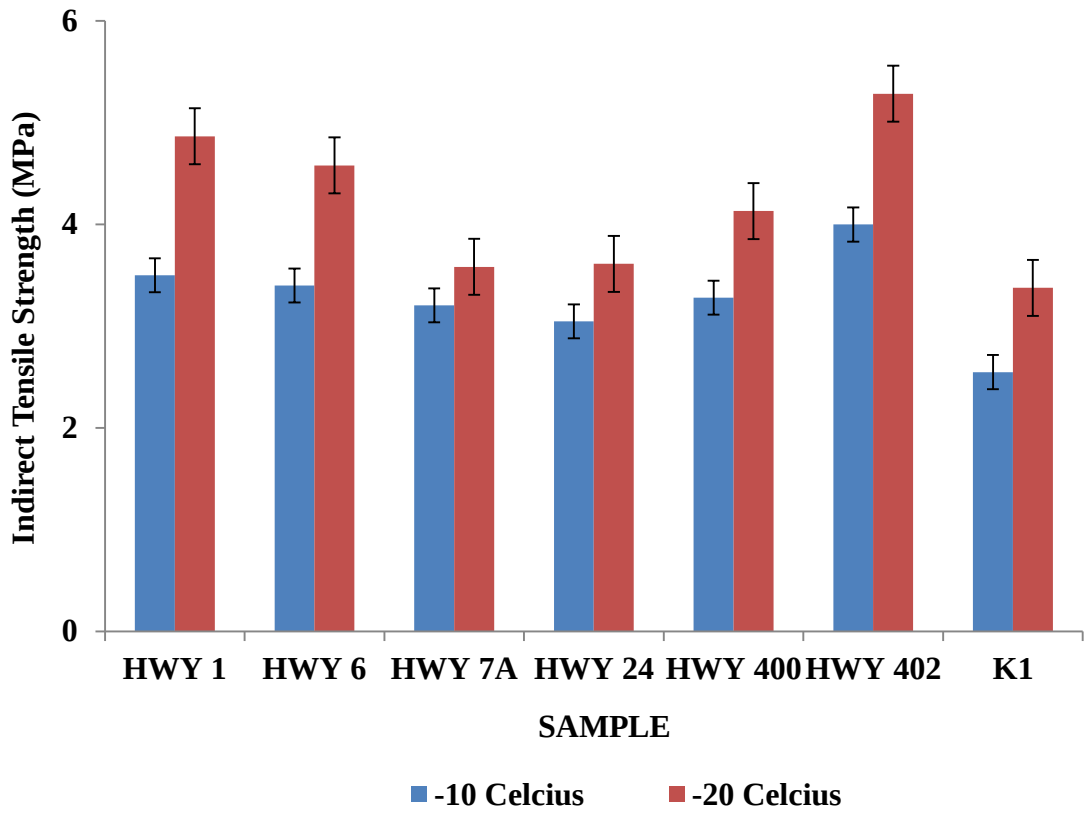

Figure 4.1.2: (a) Average indirect tensile strength for all recovered samples.

The indirect strength data above displays Highway 402 to have obtained the highest strength value at temperatures of -10 ^{o}C and -20 ^{o}C and will be suggested to be more durable to withstand fatigue and low temperature cracking. On the contrary, K1 recorded the least strength value compared to the rest of the samples. However, the strength values obtained by each sample are somewhat acceptable to be able to bear high loads and to resist pavement distress. The strength value cannot be used only in justifying the performance of a sample but is does contribute to the general performance. Coefficient of variation for indirect tensile strength at temperatures of -10 ^{o}C and -20 ^{o}C ranged between 1 % to 32 % and 0.29 % to 20 % respectively. Figure 4.1.2 (b) shows the strength data for all the unrecovered samples.

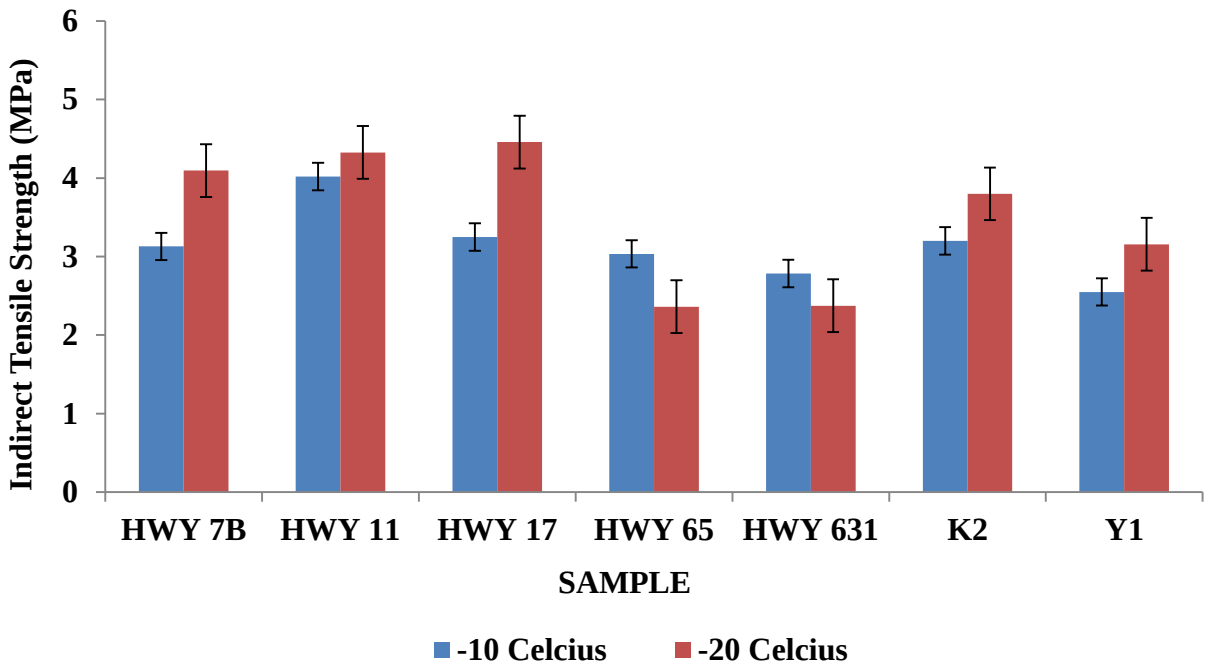

Figure 4.1.2: (b) Average indirect tensile strength for all unrecovered samples.

Highway 11 and 17 obtained higher average strength values at temperatures of -10 ^{o}C and -20 ^{o}C compared to the remaining samples and will likely show high resistance to fatigue and thermal cracking. On the contrary, Highway 65 and 631 recorded the least average strength values at temperatures of -10 ^{o}C and -20 ^{o}C and will most likely show minimum resistance to fatigue and thermal cracking distress compared to the remaining samples. Coefficient of variation for indirect tensile strength at temperatures of -10 ^{o}C and -20 ^{o}C ranged between 0.16 % to 9 % and 1 % to 25 % respectively.

Figure 4.1.2 (c) shows the strength data for stone mastic asphalt rubber samples.

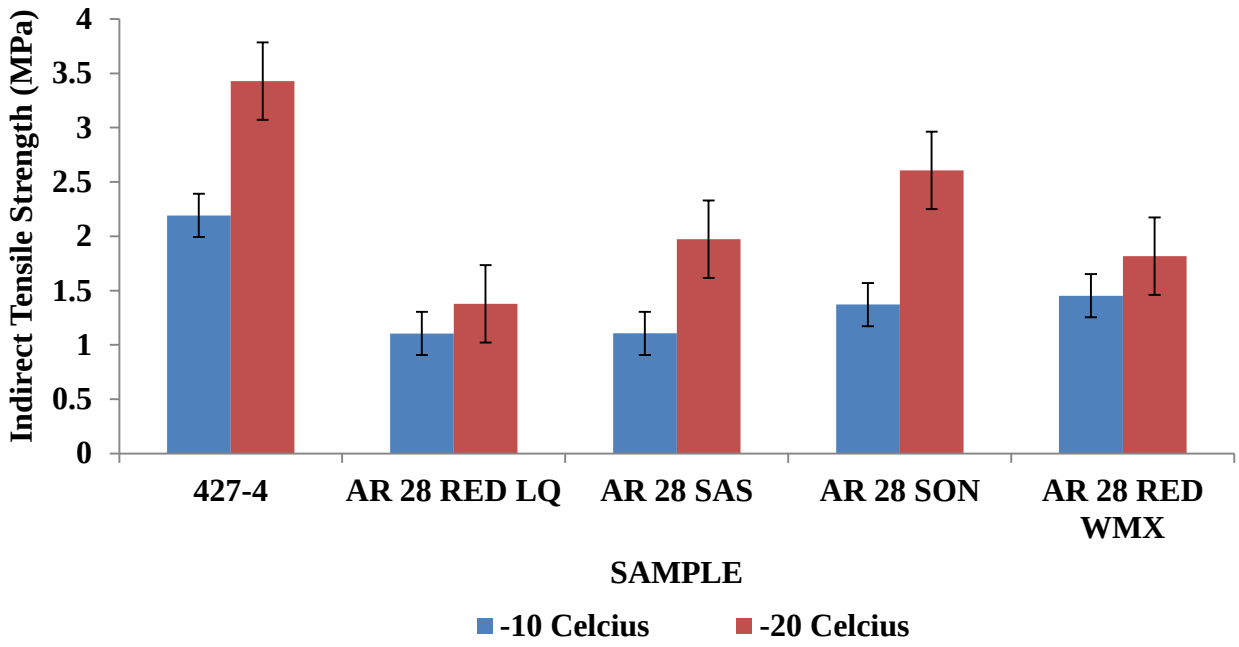

Figure 4.1.2: (c) Average indirect tensile strength for stone mastic asphalt rubber samples.

The strength values at temperatures of -10 ^{o}C and -20 ^{o}C for 427-4 were the highest compared to the remaining samples. Durability and resistance to fatigue and low temperature cracking can be projected to show in this sample. However, strength values cannot conclude the performance of samples. With the remaining samples recording appreciable strength values, Rediset LQ showed the least strength value comparatively. The coefficient of variation for indirect tensile strength at temperatures of -10 ^{o}C and -20 ^{o}C ranged between 9 % to 19 % and 2.3 % to 24 % respectively.

4.1.3 AASHTO MEPDG-Software Crack Prediction Results

The severity of thermal cracking distress on pavements can be evaluated using the AASHTO MEPDG-Software and can as well predict an estimated life span of the pavement. However, the software makes use of laboratory test results such as creep compliance and strength, as well as material and climate inputs in assessing the life span performance of a pavement. Figure 4.1.3 (a) to (c) shows the thermal cracking distress over a time span for all samples.

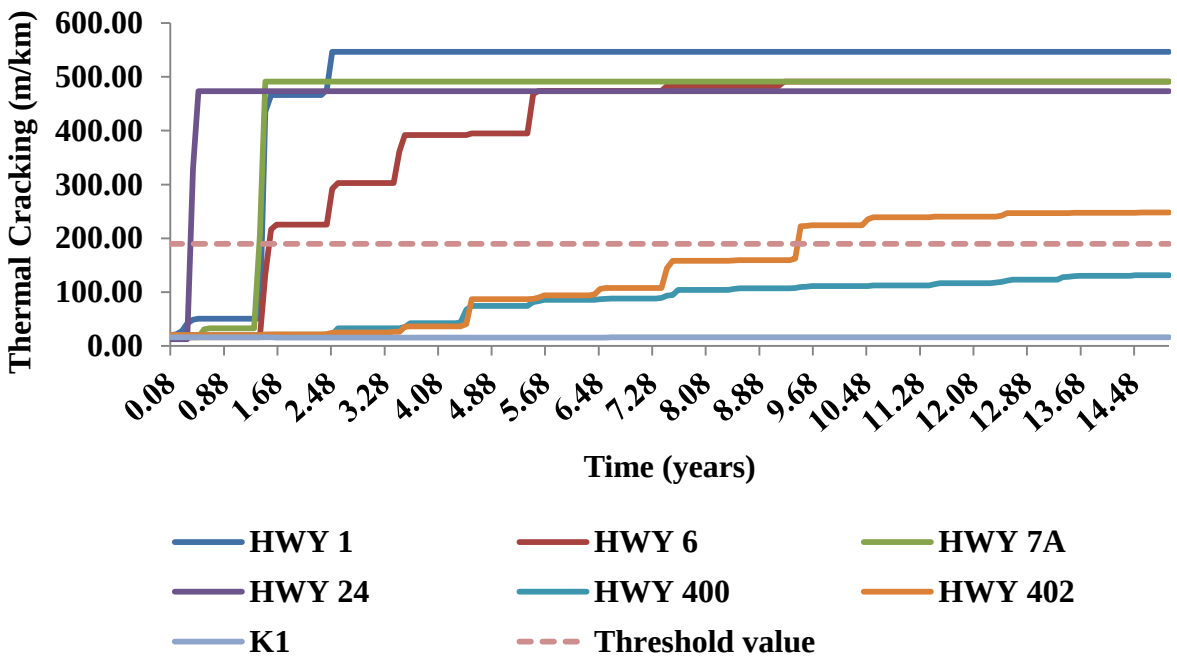

Figure 4.1.3: (a) Thermal cracking severity with predicted time to failure for all the recovered samples.

With a minimum thermal cracking threshold of 190 m/km, K1 and Highway 400 were the only recovered samples to show the least thermal cracking value below the threshold value with a predicted time to failure above 15 years. Highways 1, 6, 7A and 24 all showed very high values of thermal cracking with a predicted time to failure ranging between 1 to 2 years. However, Highway 402 recorded a time to failure of 9 years with a fairly tolerable thermal cracking severity.

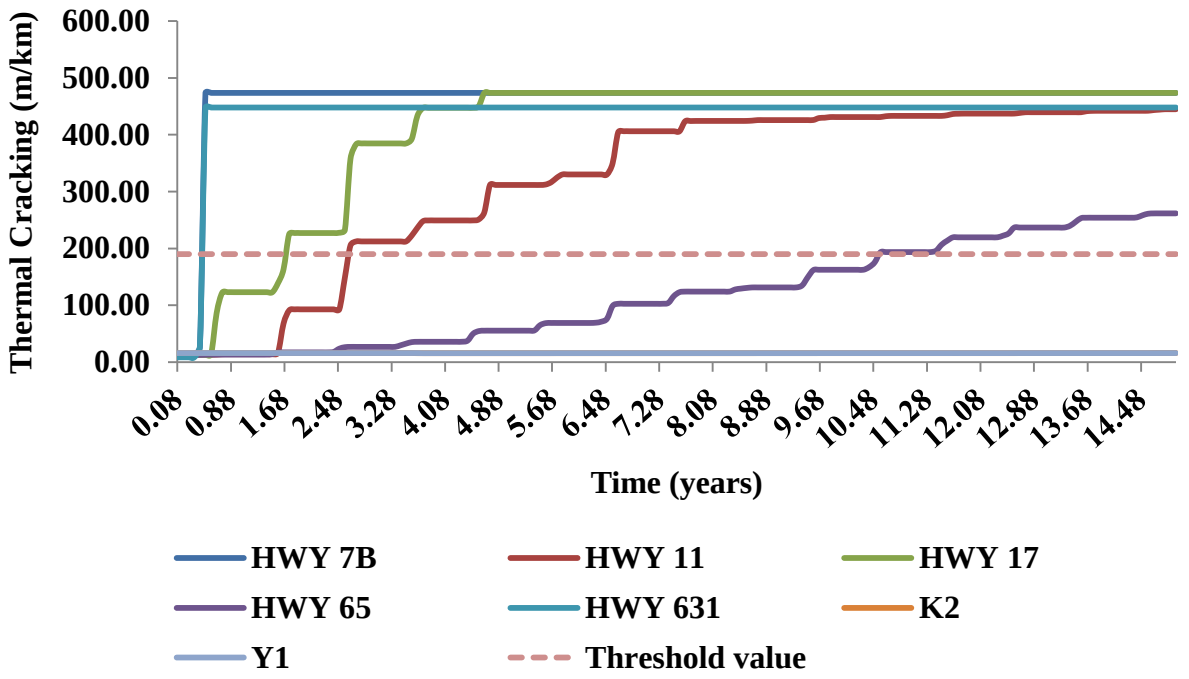

Figure 4.1.3: (b) Thermal cracking severity with predicted time to failure for all the unrecovered samples.

K2 and Y1 were the only unrecovered samples to show very low thermal cracking values far below the threshold value with a predicted time to failure above 15 years. However, Highway 65 recorded a fairly tolerable thermal cracking value with a predicted time to failure of 11 years. On the contrary, the remaining samples recorded very high values of thermal cracking with a predicted time to failure ranging between 1 to 3 years.

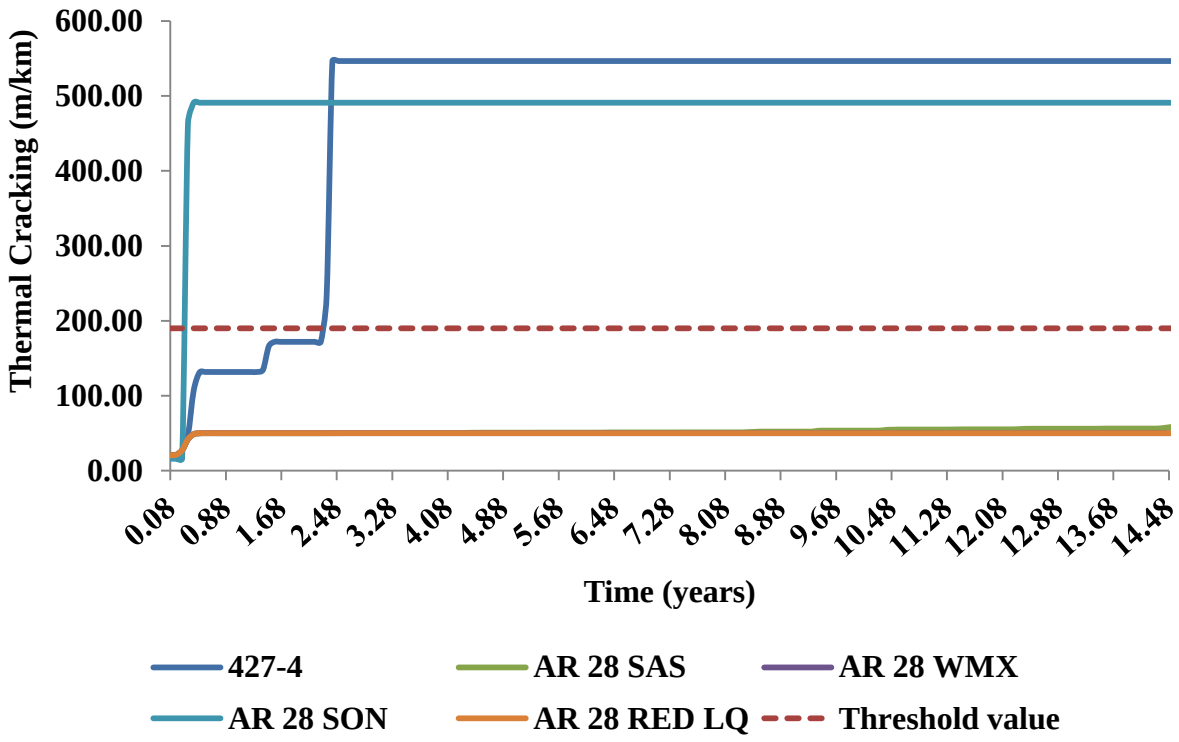

Figure 4.1.3: (c) Thermal cracking severity with predicted time to failure for stone mastic asphalt rubber samples.

Sasobit, Rediset LQ and Rediset WMX, recorded very low values of thermal cacking below that of the threshold value with a predicted time to failure above 15 years. On the other hand, sonnewarm and 427-4 showed very high values of thermal cracking over the time span with a predicted time to failure of 1 and 2 years respectively.

4.2 Dynamic Shear Rheometer Analysis

4.2.1 High Temperature Grading

The high temperature grades (properties) of the recovered asphalt binders of Highway 1, 6, 7A, 24, 400, and 402 from Ontario Ministry of Transportation as well as the recovered binder of K1 from City of Kingston were determined using a TA Instruments AR2000ex DSR. The high temperature grades (properties) show the ability of the samples to resist permanent deformation (rutting) at high temperature climatic conditions. The rutting resistance factor G*/sin δ was used to evaluate the limiting maximum temperature performance grade (PG) of the samples. Figure 4.2.1 shows the high temperature performance grades (PG) for all the samples.

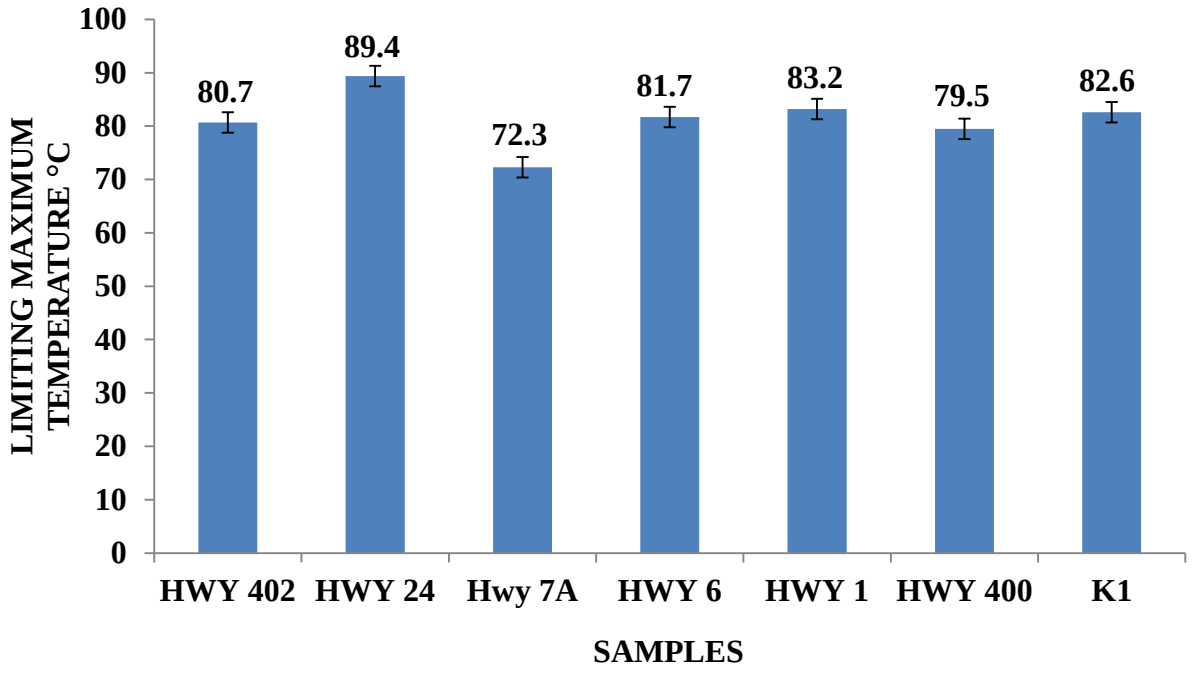

Figure 4.2.1: High Temperature Grades for recovered asphalt binder samples.

From figure 4.2.1, Highway 24 recorded the highest value of limiting maximum temperature grade amongst the samples. This indicates that Highway 24 will show better resistance to rutting

at high temperature conditions and perform much better at high temperature climatic areas as compared to the other samples. Hence Highway 24 will be much more durable and stiff at higher temperature. The high rutting resistance ability of Highway 24 can be attributed to the presence of high amounts of elastic nature and low amounts of viscous nature. However, the presence of asphalt cement from reclaimed asphalt pavement (RAP) could have as well increased the rutting resistance and limiting maximum temperature grade. Results obtained from a study conducted to determine the rheological effect of RAP binder on virgin binders showed significant increase of $G^*/\sin \delta$ upon addition of RAP binder to the virgin binder [109]. This observation ultimately increased the limiting maximum temperature grade of the virgin binder since the $G^*/\sin \delta$ increased [109]. Highway 1, 6, 400, 402 and K1 all showed an appreciable value of limiting maximum temperature grades and can as well also resist rutting at high temperatures not exceeding the its limiting maximum temperature grade. Highway 7 recorded the least value of limiting maximum temperature grade compared to the rest of the samples. This can be attributed to the presence of low amounts of elastic nature compared to its viscous nature. Nevertheless, the limiting maximum temperature grade of Highway 7 is satisfactorily good to perform well in areas and regions where high temperature climatic conditions do not exceed its limiting maximum temperature grade.

4.2.2 Intermediate Temperature Grading

The intermediate temperature grades were determined in conformity to standard procedures using the DSR instrument. The intermediate Superpave® grades are intended to provide an assessment of the fatigue cracking resistance ability of asphalt binders. However, the intermediate Superpave® grades do not satisfactorily give precise assessment of the fatigue cracking resistance of asphalt binders as compared to the Double-Edge Notched Tension

(DENT) Test, which provides a good correlation with fatigue cracking in asphalt binders by measuring its Critical Crack Opening Displacement (CTOD). Figure 4.2.2 shows the intermediate temperature performance grades (PG) for all the samples.

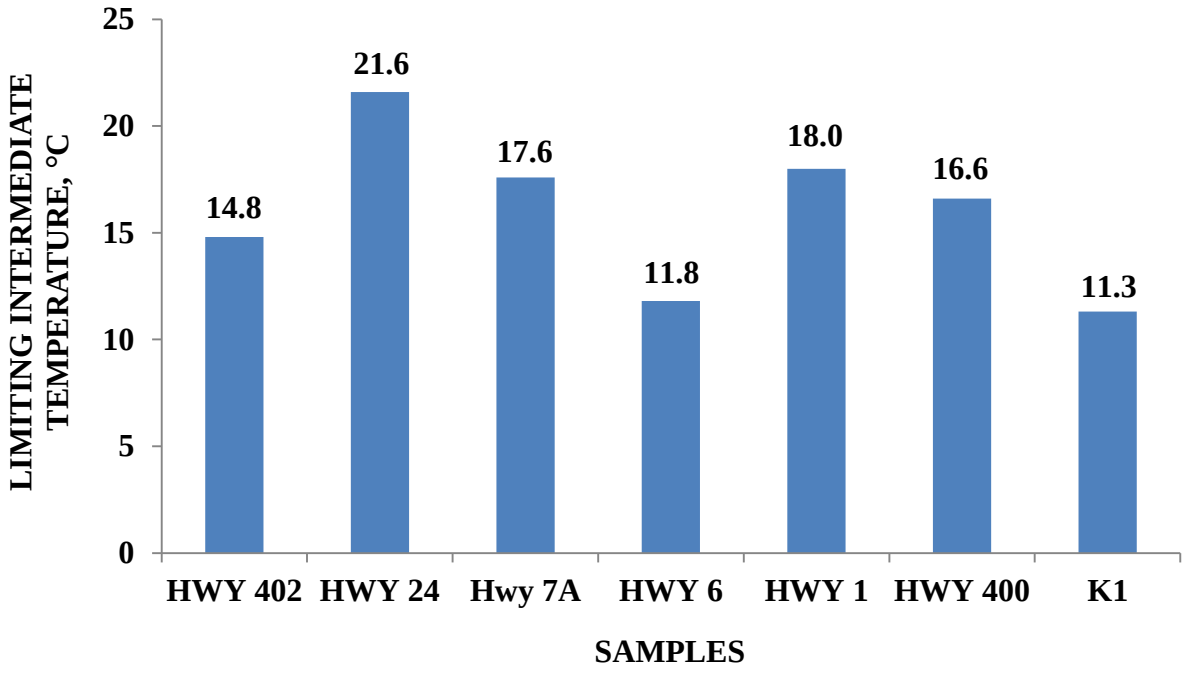

Figure 4.2.2: Intermediate Temperature Grades for recovered asphalt binder samples.

From the results shown in figure 4.2.2 above, Highway 24 recorded the highest value of limiting intermediate temperature grade as compared to the rest of the samples. K1 on the contrary recorded the least value of limiting intermediate temperature grade compared to the rest of the other samples. This observation depicts Highway 24 as a better fatigue cracking resistant sample compared to K1 and the rest of the samples. However, the CTOD value for K1 from the DENT test depicts it as a better fatigue cracking resistant sample compared to Highway 24 and the rest of the samples. Hence the intermediate Superpave® grades do not give good correlation with the fatigue cracking resistance of asphalt binders as compared to the DENT test.

4.2.3 Grade Spans

The grade span is a measure of the difference between the high temperature grade and low temperature grade of an asphalt binder. In asphalt paving, an asphalt binder with a high grade span is usually considered for paving in areas of wide temperature range, whiles that of a low grade span is considered for paving in areas of narrow temperature range.

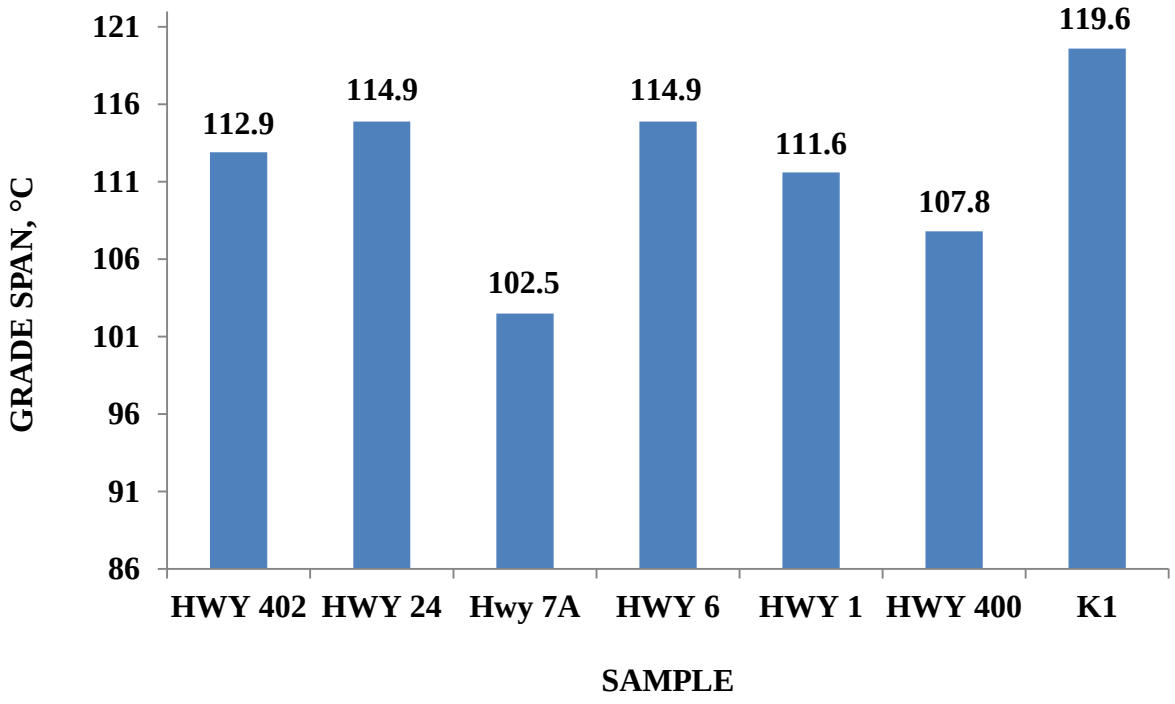

Figure 4.2.3: Grade span for recovered asphalt binder samples.

K1 recorded the highest grade span followed by Highway 6 and 24 obtaining the same value of grade span whiles Highway 7A recorded the least grade span compared to the rest of the samples. This suggests that K1 will be more preferred in paving areas with wide temperature range compared to the other samples. However, the rest of the samples also recorded an appreciable value of grade span and will be preferred in paving areas within the limits of its grade span.

4.2.4 Black Space Diagrams

The Black space diagram is a good approach in characterising the rheological properties of an asphalt binder. The black space diagram helps to distinguish a rheological simple asphalt binder from a rheological complex one, by graphically displaying the correlation between the phase angle and the complex modulus at different temperatures from the DSR test. An asphalt binder with a homogeneous composition and a single phase is believed to be a rheological simple asphalt binder, owing to the fact that an ordered continuous progressing of curves at different temperature is observed from the black space diagram. On the other hand, an asphalt binder with a heterogeneous composition and a multiple phase system is deemed to be a rheological complex asphalt binder, due to a scattered discontinuous progression of curves observed from the black space diagram. A phase separation is the end result of a rheological complex asphalt binder and is usually difficult to be predicted due to its abnormal behaviour as a viscoelastic material. A rheological simple asphalt binder shows a good behavioural trend as a viscoelastic material with no phase separation [5]. The figures below shows the black space diagrams at high and low temperatures for all the recovered asphalt binder samples.

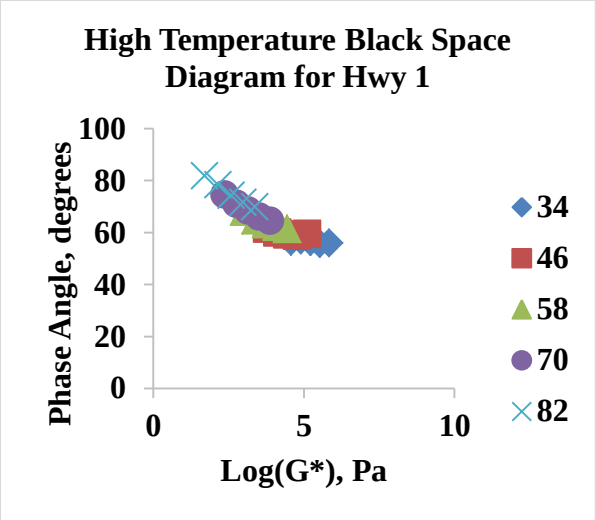

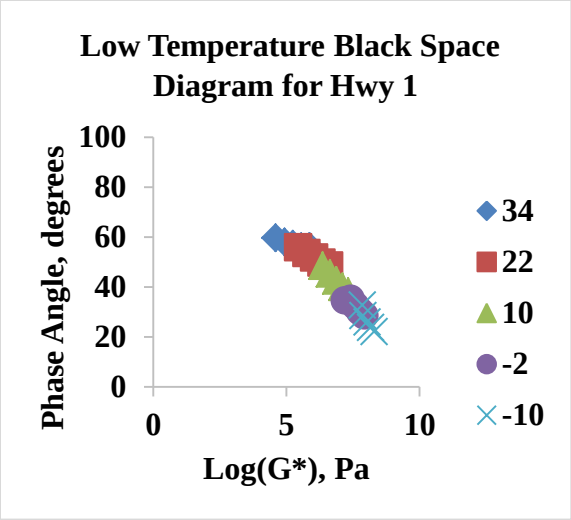

Figure 4.2.4: (a) Black Space Diagrams at High and Low Temperatures for Highway 1.

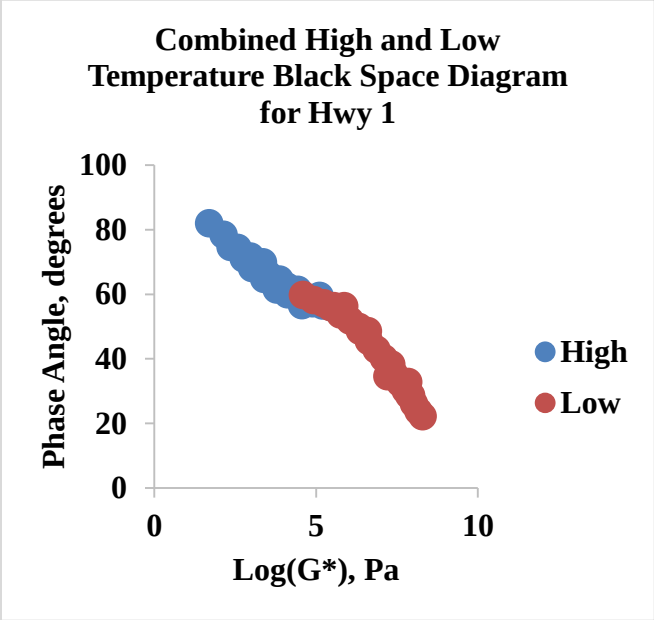

Figure 4.2.4: (b) Combined Black Space Diagram at High and Low Temperatures for Highway 1.

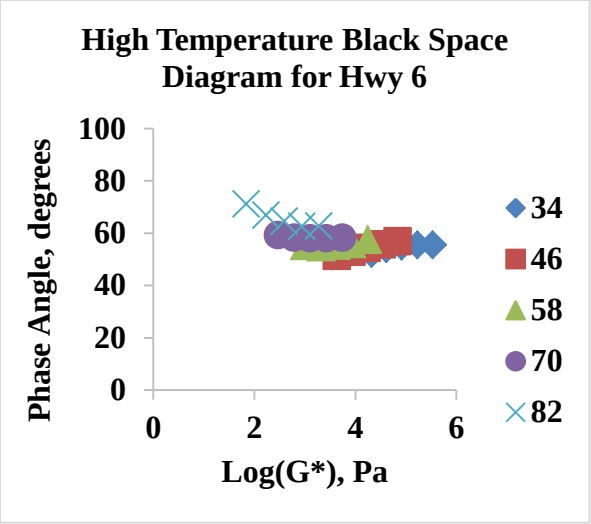

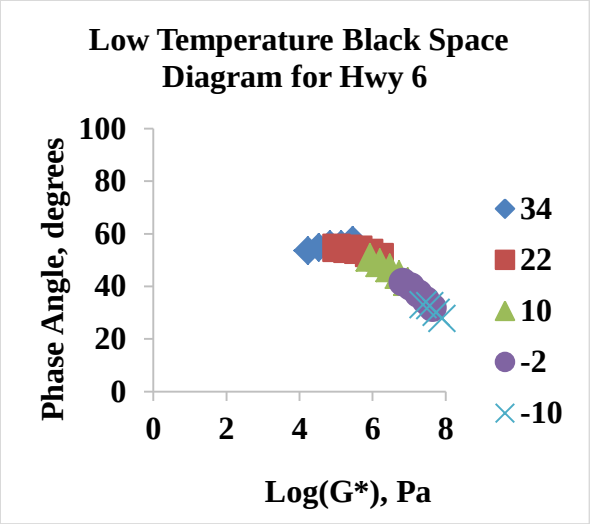

Figure 4.2.4: (c) Black Space Diagrams at High and Low Temperatures for Highway 6.

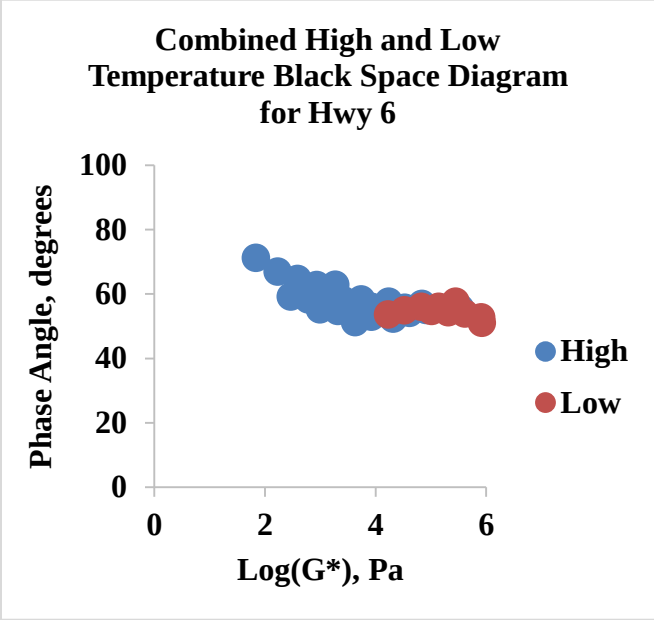

Figure 4.2.4: (d) Combined Black Space Diagram at High and Low Temperatures for Highway 6.

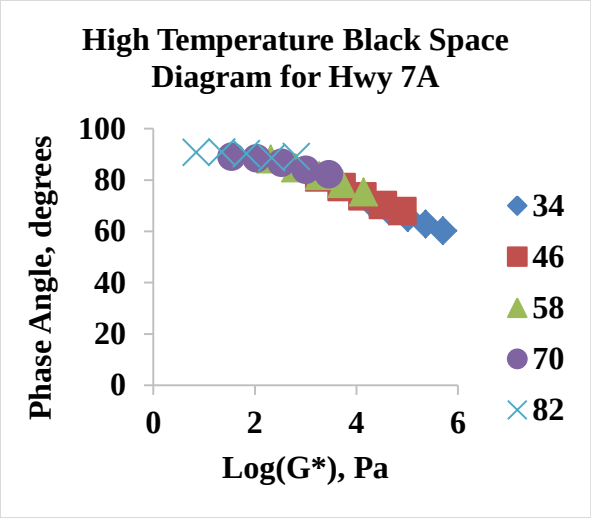

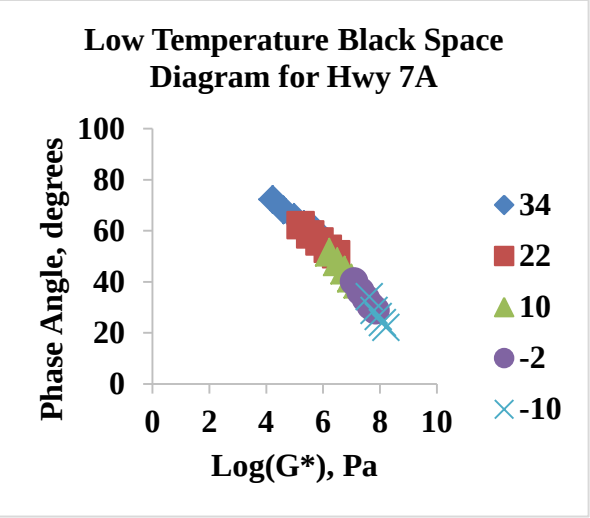

Figure 4.2.4: (e) Black Space Diagrams at High and Low Temperatures for Highway 7A.

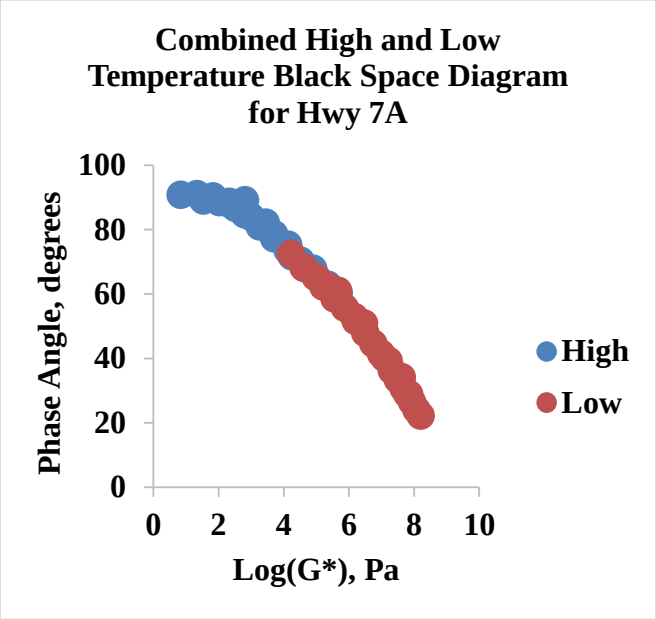

Figure 4.2.4: (f) Combined Black Space Diagram at High and Low Temperatures for Highway 7A.

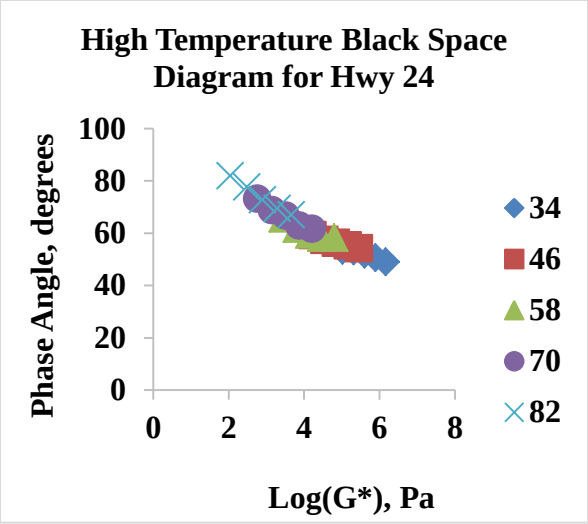

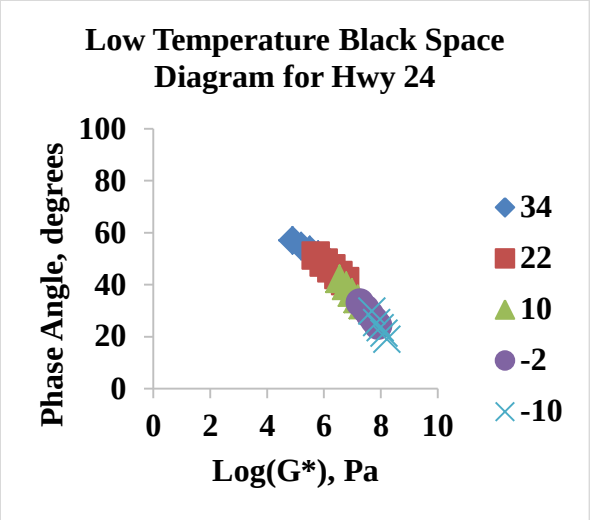

Figure 4.2.4: (g) Black Space Diagrams at High and Low Temperatures for Highway 24.

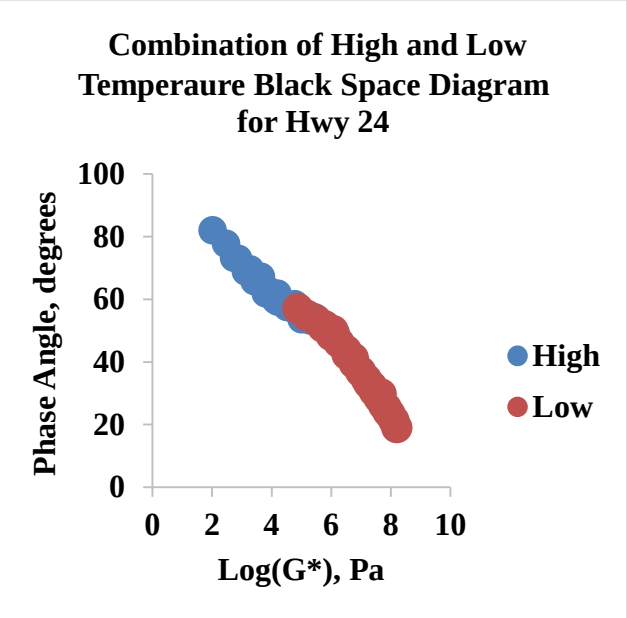

Figure 4.2.4: (h) Combined Black Space Diagram at High and Low Temperatures for Highway 24.

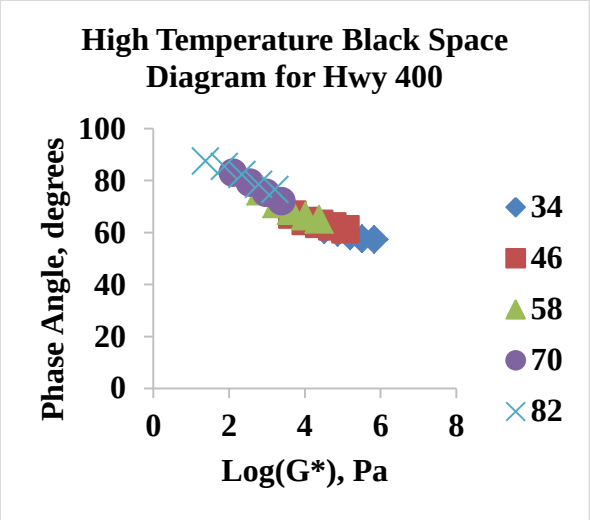

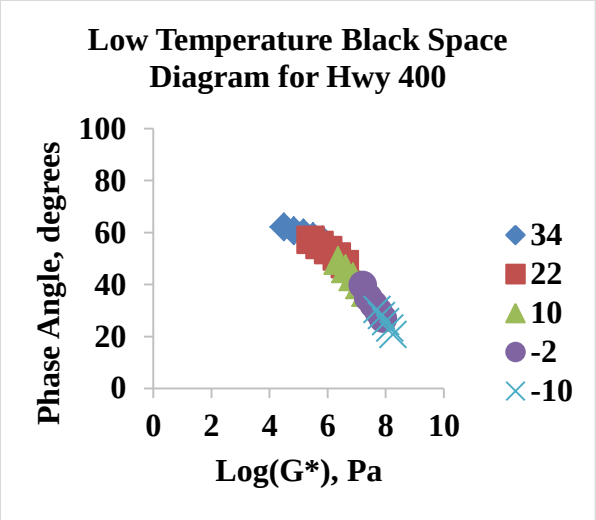

Figure 4.2.4: (i) Black Space Diagrams at High and Low Temperatures for Highway 400.

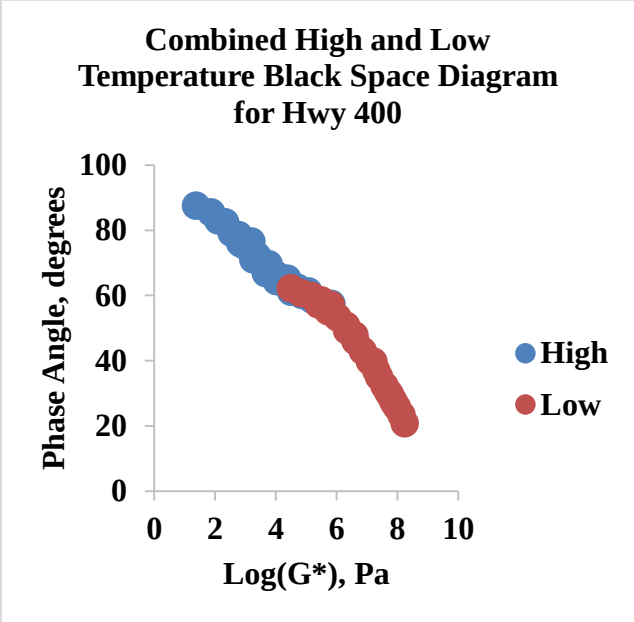

Figure 4.2.4: (j) Combined Black Space Diagram at High and Low Temperatures for Highway 400.

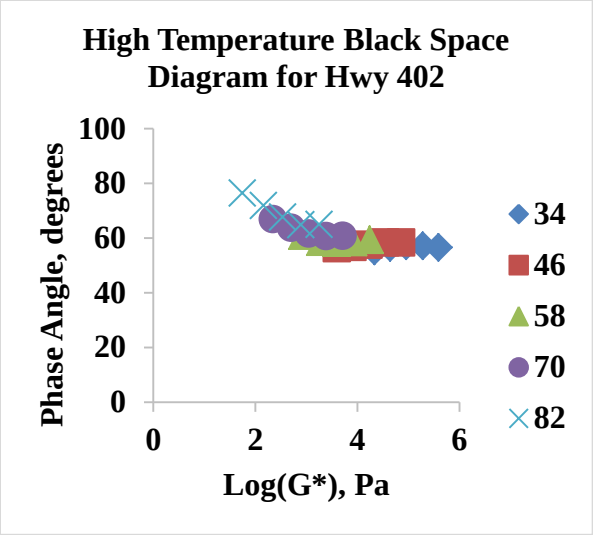

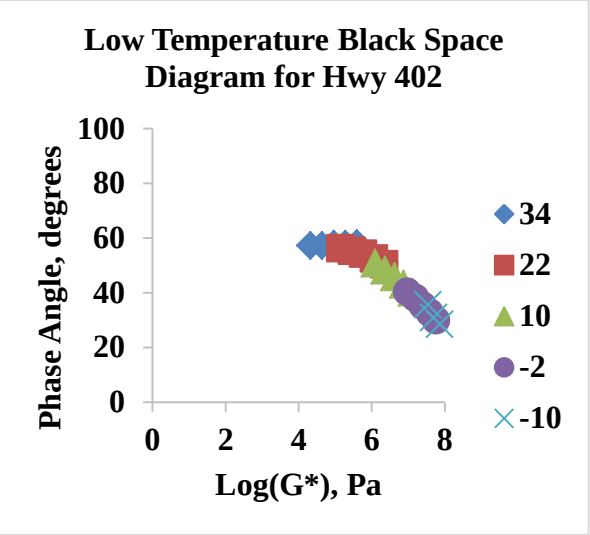

Figure 4.2.4: (k) Black Space Diagrams at High and Low Temperatures for Highway 402.

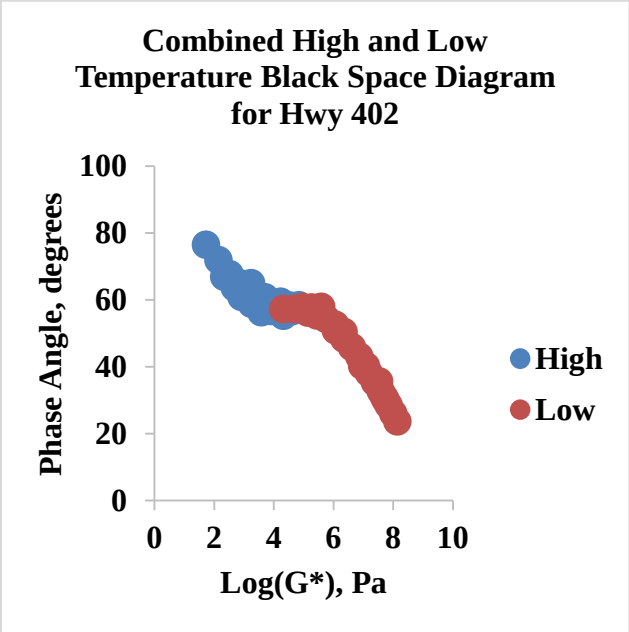

Figure 4.2.4: (l) Combined Black Space Diagram at High and Low Temperatures for Highway 402.

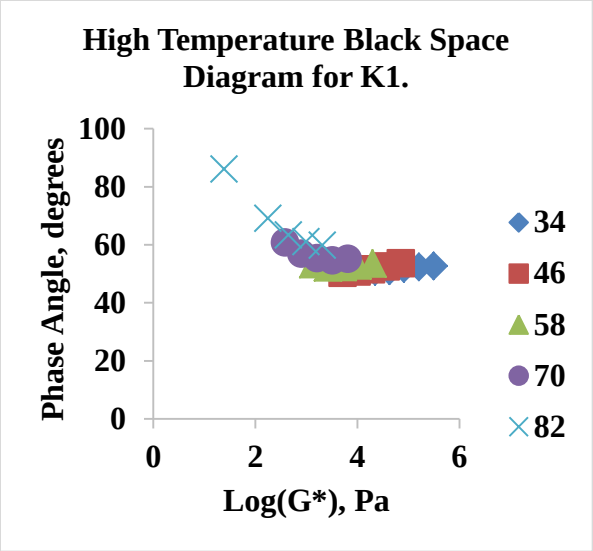

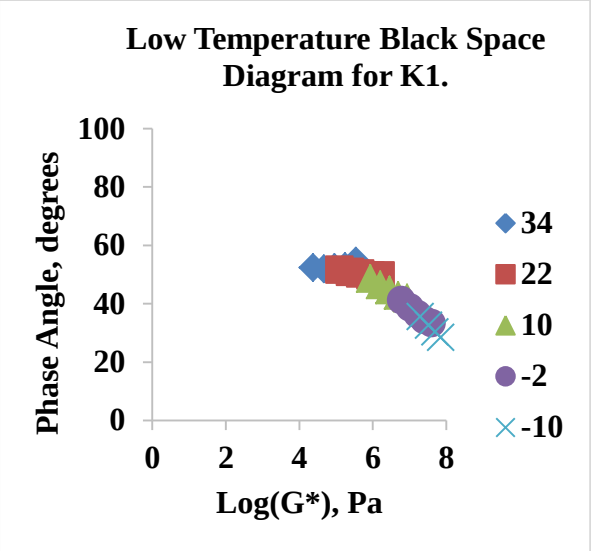

Figure 4.2.4: (m) Black Space Diagrams at High and Low Temperatures for K1.

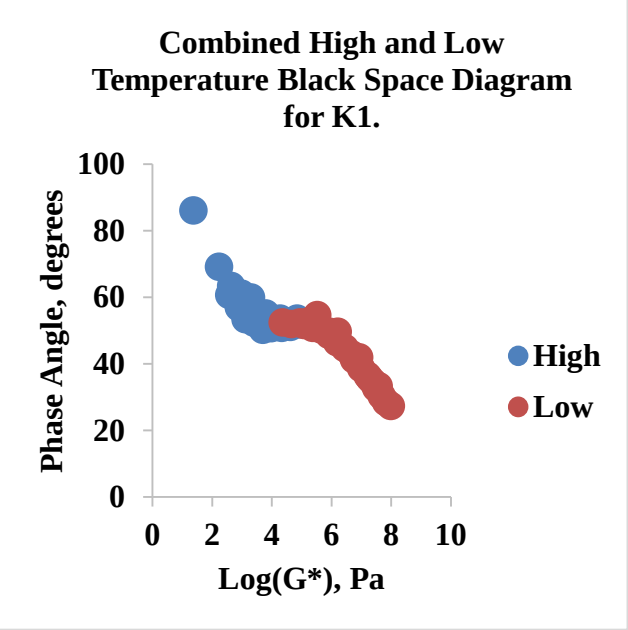

Figure 4.2.4: (n) Combined Black Space Diagram at High and Low Temperatures for K1.

The Black space diagrams above reveals highways 1 and 6 to have showed a great deviation from rheologically simple behaviour at both high and low temperatures. This observation might be due to a high level of phase separation occurring in these samples at high and low temperatures. However, the remaining samples had deviation from rheologically simple behaviour at only high temperatures. This again might be due to an inherent nature of these samples to show some amount of phase separation at high temperatures compared to low temperatures.

4.3 Traditional Bending Beam Rheometer (BBR) Data Analysis

The traditional Bending Beam Rheometer (BBR) test was performed on all the recovered asphalt binder samples and the limiting minimum temperature grades obtained according to the standard procedures outlined in AASHTO M320. The prepared specimens from the various samples were conditioned for 1 hr at -10 °C prior to testing and the test carried out at 0 °C, -10 °C, -20 °C and -30 °C. The creep stiffness (S) and the slope of the creep stiffness master curve (m-value) were obtained from the test and used in accordance to standard protocols to generate the limiting minimum temperature grades.

4.3.1 Low Temperature Grades

In order to determine the low temperature grades of the samples using the traditional BBR method, the limiting temperature where stiffness (S) = 300 MPa and the limiting temperature where m-value = 0.3 were determined through an interpolation process and the warmest temperature between the two temperatures was set to be the limiting minimum temperature

grade. The results summary for low temperature grades using the regular BBR method is shown below in Figure 4.3.1

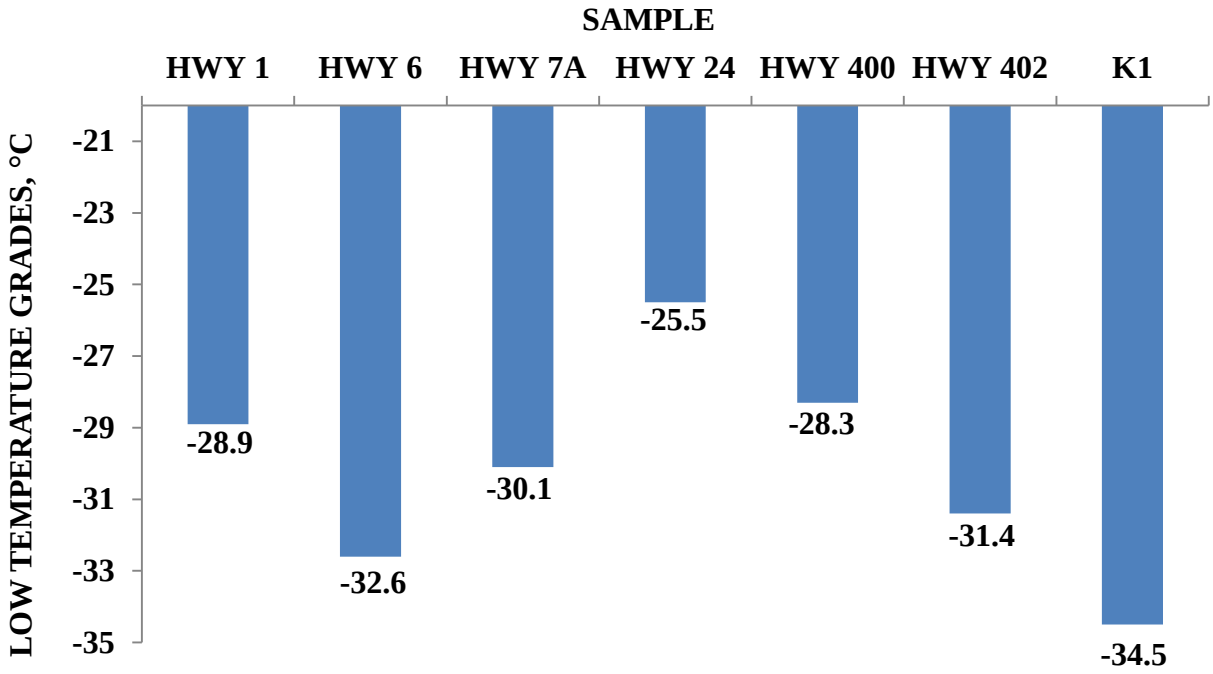

Figure 4.3.1: Low Temperature Grades for recovered asphalt binder samples after 1 hr Conditioning.

The minimum PG grade temperature as given in the mix design specification for each recovered asphalt binder sample was PG-28. However Highway 1 and 400 did not show any significant change in grade but Highway 6, 7 and 402 showed grades of about 4 °C, 2 °C and 2 °C lower than the minimum PG grade temperature respectively. This observation depicts these samples to show a good resistance to thermal cracking at areas with temperatures warmer or equal to the minimum PG grade temperature. K1 showed the lowest grade of about 6 °C lower than minimum PG grade temperature. This observation suggests that K1 will perform much better in terms of thermal cracking resistance as compared to the rest of the samples in areas with temperatures warmer than the minimum PG grade temperature. Highway 24 on the other hand

recorded about 3 °C greater than the minimum PG grade temperature and will be expected to perform poorly in terms of thermal cracking resistance as compared to the rest of the samples.

4.3.2 Extended Bending Beam Rheometer (eBBR) Data Analysis

The inception of the MTO standard method (LS-308) known as the extended BBR method, has greatly accounted for the extent to which physical hardening occurs in asphalt binders when stored in low temperature conditions for longer period of time compared to the regular BBR method. Recovered asphalt binder samples were conditioned for 72 hrs at -10 °C prior to testing and the test conducted at temperatures of 0 °C, -10 °C, -20 °C and -30 °C.

4.3.3 Low Temperature Grades

The low temperature grades of the samples according to the extended BBR method were determined by obtaining the limiting temperature where stiffness (S) = 300 MPa and the limiting temperature where (m-value) = 0.3 through an interpolation process. The warmest temperature between the two temperatures was set to be the limiting minimum temperature grade. The results summary is shown in Figure 4.3.3

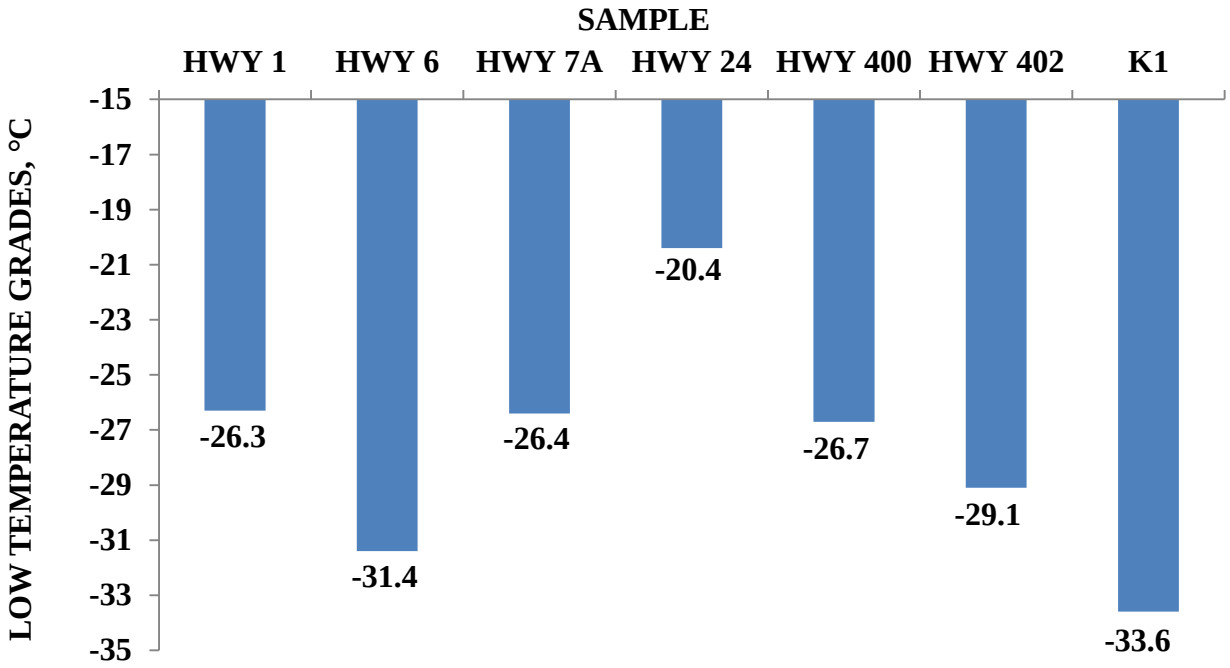

Figure 4.3.3: (a) Low temperature grades for recovered asphalt binder samples after 72 hrs conditioning.

The extended BBR method reveals the degree of physical hardening occurrence in asphalt binders, and the true low temperature grades of the asphalt binder samples. This observation is clearly shown in figure 4.3.3 (a) as Highway 1 and 400 which in the earlier grades obtained from the regular BBR did not change much but recorded a significant change in grade of about 2 °C greater than the minimum PG grade temperature using the extended BBR method. This observation now reverses the earlier suggestion of Highway 1 and 400 to show good resistance to thermal cracking to perform poorly in terms of thermal cracking resistance. Highway 7 also recorded a change in grade of about 2 °C greater than the minimum PG grade temperature. This again suggest Highway 7 to perform poorly in terms of thermal cracking resistance in areas with temperatures lower than the minimum PG grade temperature. However, Highway 24 had the greatest change in grade of about 8 °C greater than the minimum PG grade temperature which

suggests it to be the worst performer in terms of thermal cracking resistance in areas with temperatures lower than the minimum PG grade temperature compared to the rest of the samples. Highway 6, though recorded a grade of about 4 °C lower than the minimum PG grade temperature in regular BBR did not change much in terms of grade in the extended BBR. Highway 6, however recorded a grade of about 3 °C lower than the minimum PG grade temperature which still makes it a good thermal cracking resistant sample compared to the rest of the samples with the exception of K1 which in the earlier suggestion was the best performer still maintained a considerable good grade of about 5 °C lower than the minimum PG grade temperature and hence maintains its proposition as the best performer in terms of thermal cracking resistance in areas of temperatures equal to the minimum PG grade.

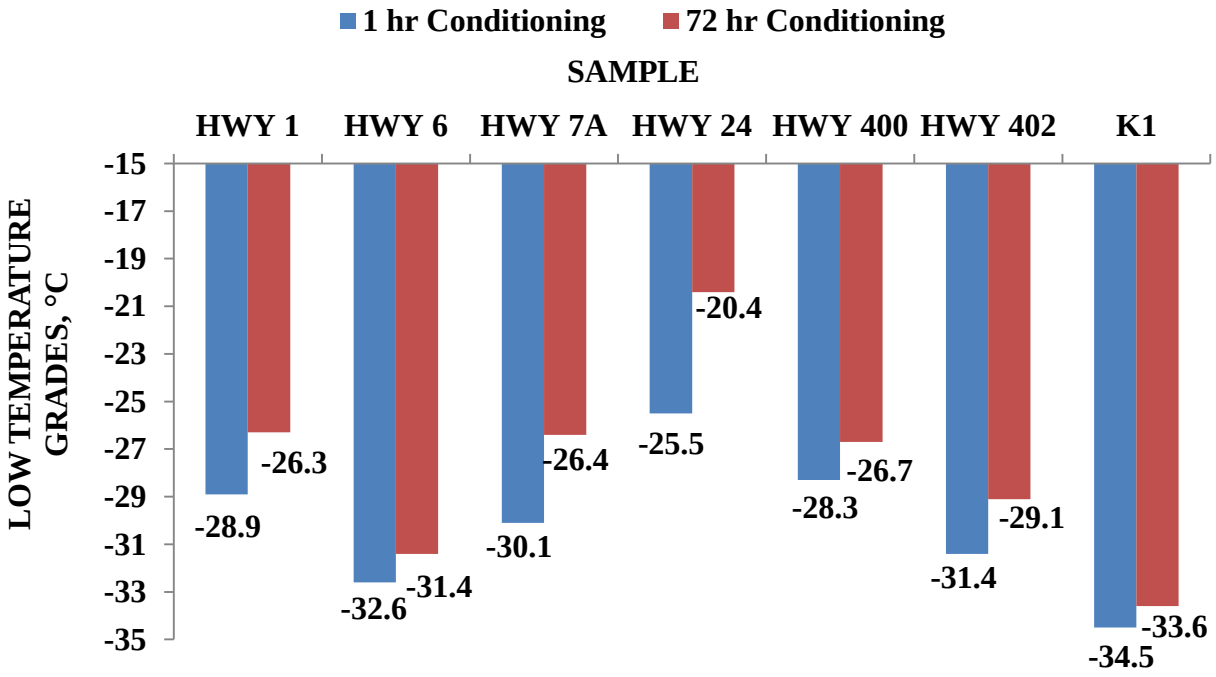

Figure 4.3.3: (b) Low temperature grades for recovered asphalt binder samples after 1 hr and 72 hrs conditioning.

Figure 4.3.3 (b) clearly shows the comparison between grades obtained using the regular BBR after 1 hr conditioning and that of the extended BBR after 72 hrs conditioning. The grades observed justifies the extended BBR method to effectively reveal the true grade of the asphalt binder and hence give a good justification on how the samples will perform on the field.

4.3.4 Grade Losses

The grade loss gives a good representation of the performance of the samples in service and the degree to which it can undergo physical hardening. Figure 4.3.4 shows the grade losses for all the recovered asphalt binder samples.

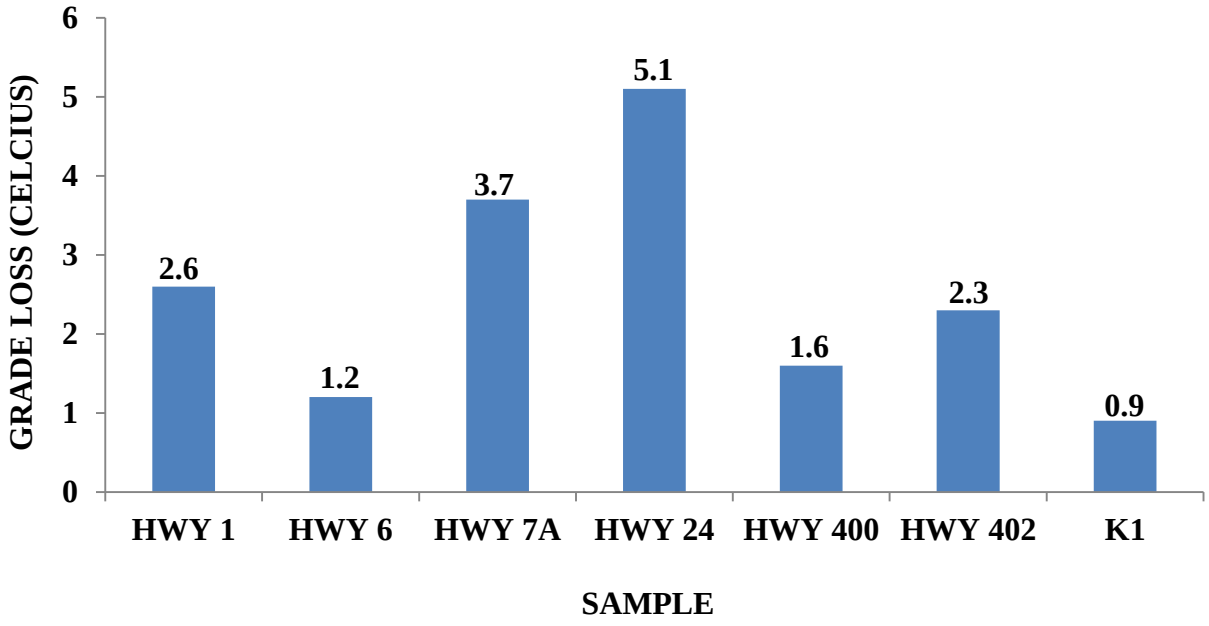

Figure 4.3.4: Grade Loss for all recovered asphalt binder samples.

K1 obtained the least grade loss compared the rest of the samples. This observation indicates that it will show good relaxation to thermal stresses and lower tendency to physical hardening in service. A good pavement performance at lower temperature conditions is then expected of K1 as it will be able to relax thermal stresses before the pavement achieves spring thaw. Thaws and

movements will be expected to occur in the base of the pavement to bring about thermal stress relaxation [5, 105]. Highway 24 on the contrary obtained the highest grade loss and will be expected to be more prone to severe thermal cracking as a result of difficulty in stress relaxation compared to the rest of the samples. However, all the samples obtained an acceptable grade loss according to the LS-308 protocol. Table 4.3 shows a summary of the low temperature grades and grade loss for all the recovered asphalt binders.

Table 4.3: Low temperature grades and grade loss for all recovered asphalt binder samples.

Sample	**Low Temperature Grades (°C) @ 1 Hr Conditioning**	**Low Temperature Grades (°C) @ 72 Hr Conditioning**	**Grade Loss (°C)**
HIGHWAY 1	-28.9	-26.3	2.6
HIGHWAY 6	-32.6	-31.4	1.2
HIGHWAY 7A	-30.1	-26.4	3.7
HIGHWAY 24	-25.5	-20.4	5.1
HIGHWAY 400	-28.3	-26.7	1.6
HIGHWAY 402	-31.4	-29.1	2.3
K1	-34.5	-33.6	0.9

The grade loss is obtained by taking the difference between the low temperature grades at 72 hr conditioning and that at 1 hr conditioning.

4.4 Double Edge Notched Tension (DENT) Test Analysis

The double edge notched tension (DENT) test was carried out on all the recovered asphalt binder samples to evaluate the ductile properties of the samples. The strain tolerance and failure properties were determined on the essential work of fracture (EWF) concept using the DENT test [2]. The ductility test was carried out on the samples by stretching them in an isothermal bath of 15 °C and at a constant loading rate of 50 mm/min until failure occurs according to the Ministry of Ontario LS-299 standard protocol [80]. Figure 4.4 (a) displays the raw force-displacement graph for a duplicate DENT test on K1 and figure 4.4 (b) displays the raw force-displacement graph for a duplicate DENT test on Highway 24.

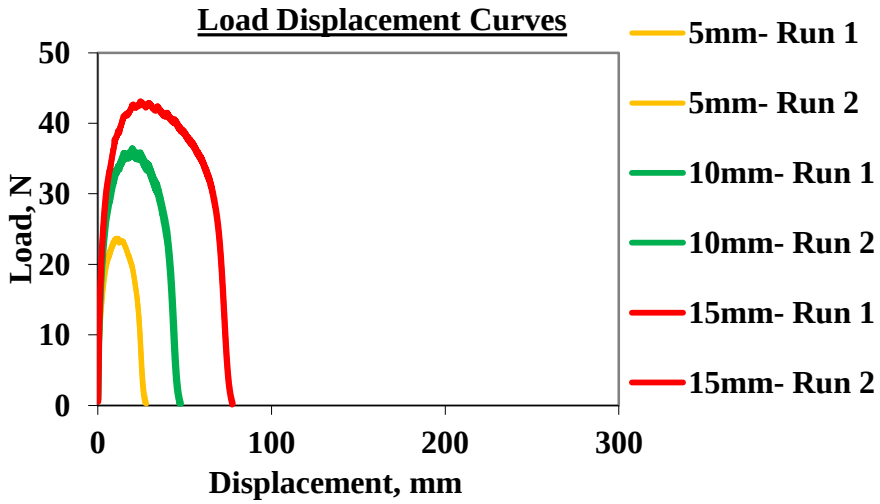

Figure 4.4: (a) Typical Force-Displacement graphs for DENT test on K1

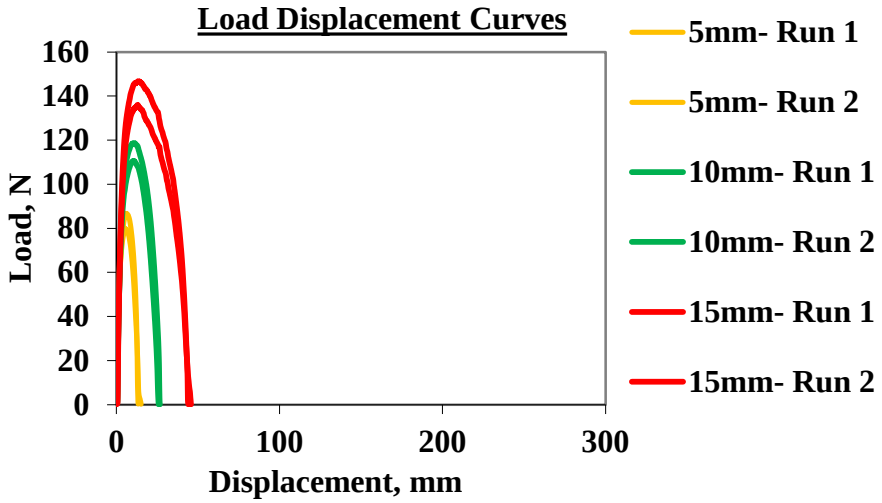

Figure 4.4: (b) Typical Force-Displacement graphs for DENT test on Highway 24.

The force-displacement curve for a duplicate DENT test on K1 from figure 4.4 (a) suggests it to be more ductile compared to Highway 24 shown in figure 4.4 (b). This observation can be attributed to a high content of elastic nature inherent in the K1 sample compared to Highway 24. The test was however observed to be reproducible and similar for various ligament lengths but different for each recovered asphalt binder sample. The DENT test is able to differentiate poor quality asphalt from a superior one based on its ductile performance. Therefore, K1 will be deemed to be a good quality binder compared to Highway 24 from the ductility test.

4.4.1 Essential Work of Failure (W_e)

The concept of essential work of failure (EWF) is often applied in accounting for the fatigue cracking resistance and low temperature cracking distresses of the asphalt pavement. The evaluation of essential work of failure is considered not dependent on the geometry of the material but it is however accepted as material property. A high essential work of failure value

will suggest the asphalt binder as a good fatigue resistant material [5]. Figure 4.4.1 shows the essential work of failure for all the recovered asphalt binder samples.

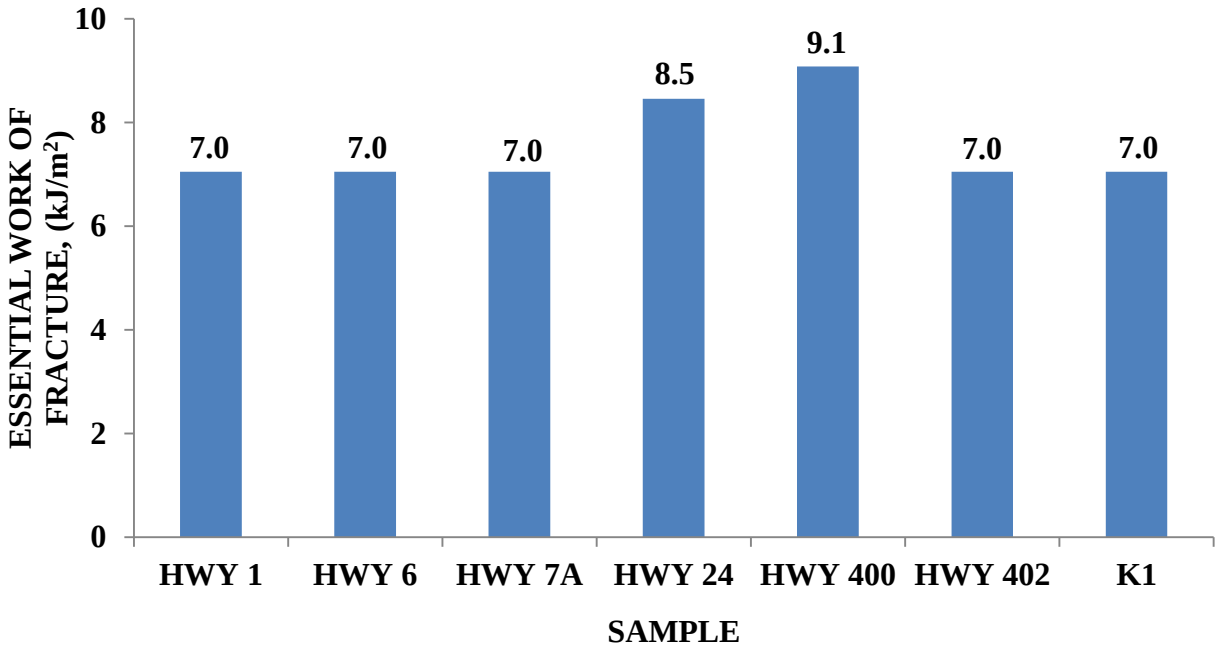

Figure 4.4.1: Essential work of failure for all recovered asphalt binder samples.

Highway 400 and 24 from figure 4.4.1 above, obtained higher values of essential work of failure compared to the rest of the samples. This observation suggests these samples to be more tolerant to strain and to show good resistance to fatigue cracking. Also, the remaining samples recorded the same value of essential work of failure which is reasonably good to resist fatigue cracking. However, the critical crack opening displacement (CTOD) gives a more precise correlation with fatigue cracking resistance as compared to the essential work of failure.

4.4.2 Plastic Work of Failure (βw_p)

The plastic work of failure is the energy associated in bringing about non-essential deformation outside the fracture zone of the material and is not considered to be a material property. However, the plastic work of failure can account for some level of fatigue cracking resistance in asphalt pavement. A high plastic work of failure observed in an asphalt binder sample might suggest it to be a good fatigue cracking resistance sample. However, it has been observed that asphalt cement mixtures with high asphalt binder content (% A.C) will show high plastic work of failure values and hence be attributed as a good fatigue cracking resistant sample [82]. Nevertheless, the plastic work of failure does not give a precise account of fatigue cracking resistance in asphalt binders compared to the critical crack tip opening displacement (CTOD). Figure 4.4.2 shows the plastic work of failure for all the recovered asphalt binder samples.

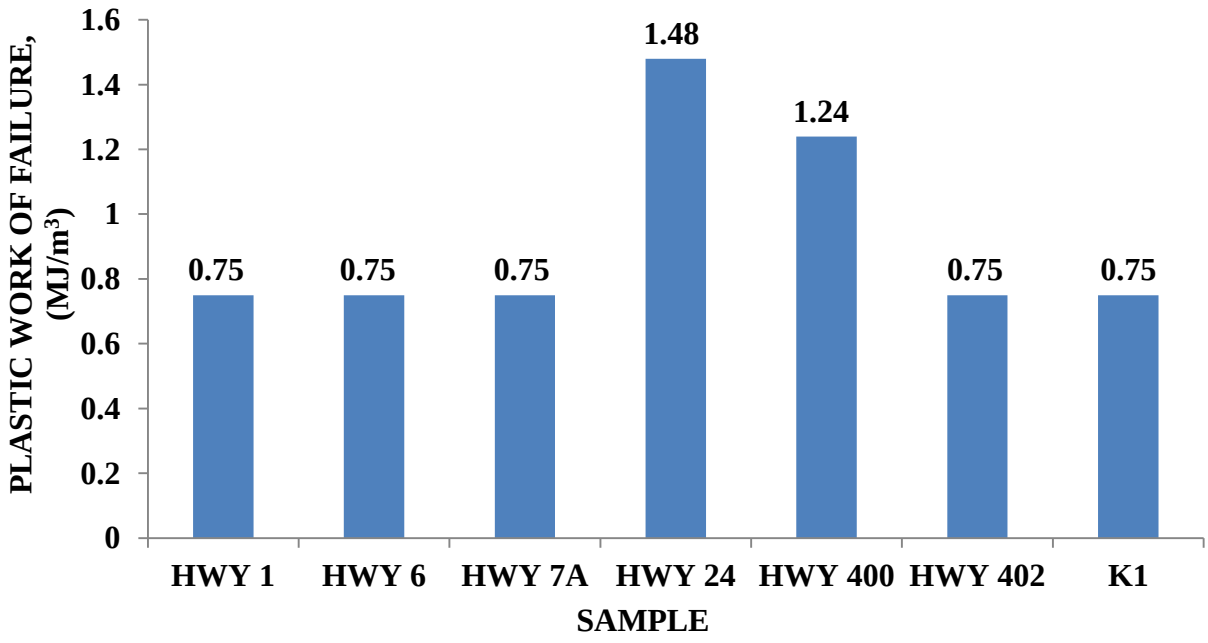

Figure 4.4.2: Plastic work of failure for all recovered asphalt binder samples.

The plastic work of failure values for Highway 24 and 400 was higher than the remaining samples, which might indicate these samples to be good fatigue cracking resistant samples and to have high asphalt binder content (% A.C). However, the % A.C obtained from the lab was much lower than that given in the mix design. This observation might rule out these samples as being good fatigue cracking resistant samples and to justify the CTOD's evaluation of fatigue cracking resistance better than that of the plastic work of failure. Table 4.4 shows the asphalt binder content (% A.C) as given in the mix design specification compared to that measured in the lab.

Table 4.4: Percentage asphalt binder content (% A.C) of all recovered samples.

Samples	**% Asphalt Binder Content (% A.C) By Mix Design**	**% Asphalt Binder Content (% A.C) Determined In Lab**
HIGHWAY 1	5.00	4.90
HIGHWAY 6	5.90	N/A
HIGHWAY 7A	4.90	5.40
HIGHWAY 24	5.00	4.34
HIGHWAY 400	5.00	4.20
HIGHWAY 402	4.80	4.10
K1	5.30	4.70

4.4.3 Approximate Critical Crack Opening Displacements

The crack tip opening displacement (CTOD) can be measured by the DENT test, and is an indication of the extent of strain tolerance shown in an asphalt binder in the ductile state. The CTOD is a good measure of predicting the performance of asphalt binders and pavements in relation to fatigue cracking resistance [106]. The crack propagation observed in asphalt binders and pavements under ductile conditions with increased loading has been well accounted for by the CTOD [83]. This however, explains the superiority of the CTOD in comparison to the essential work of failure and plastic work of failure to give a more accurate correlation to fatigue cracking resistance in asphalt binders and pavements [57]. Figure 4.4.3 shows the crack tip opening displacement (CTOD) values for all the recovered asphalt binder samples.

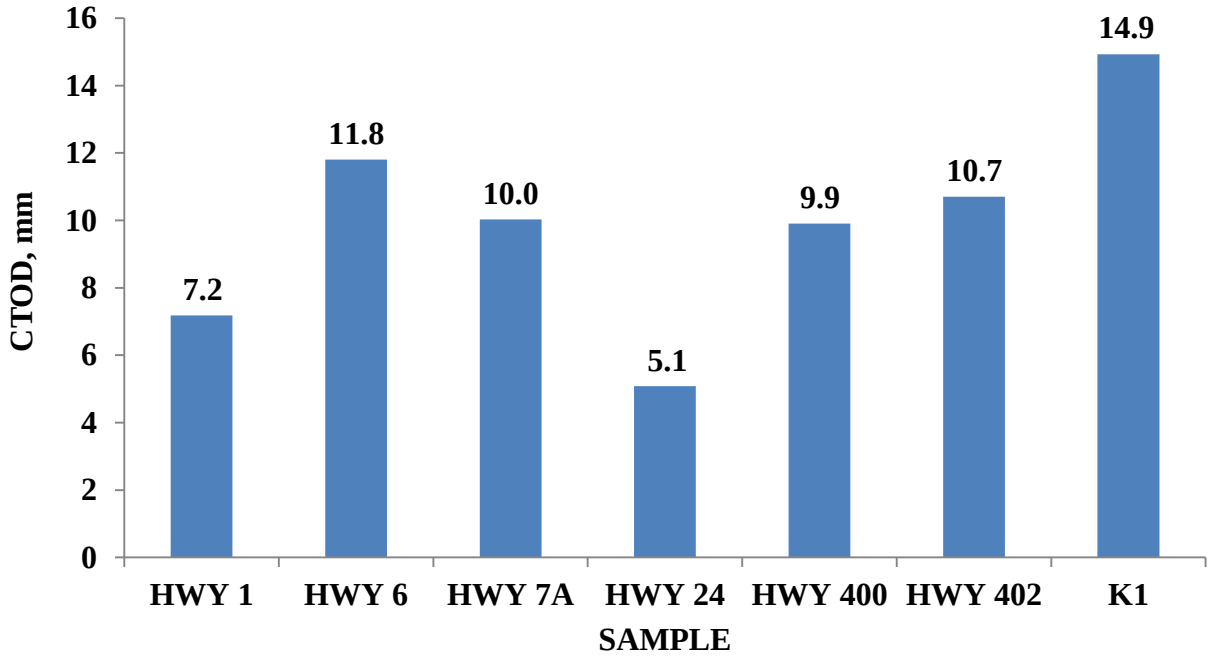

Figure 4.4.3: CTOD values for all recovered asphalt binder samples.

The CTOD values observed in figure 4.4.3 shows K1 as the sample with the highest CTOD value compared to the remaining samples. This observation suggest that K1 showed more tolerance to strain under ductile state and will be able to resist fatigue cracking much better at increased loading compared to the other samples. On the contrary, Highway 24 is observed to have shown the least CTOD value compared to the remaining sample and would be predicted to perform woefully in terms of fatigue cracking resistance.

4.5 X-Ray Fluorescence (XRF) Data Analysis

Although virgin asphalt binders contain trace amounts of heavy metals such as zinc and molybdenum, the greater amounts of these metals found in asphalt binders has been attributed to the addition of waste engine oil [102, 103]. The presence of zinc and molybdenum in asphalt binders are believed to be responsible for entrenched physical and chemical hardening [102, 103]. This may perhaps lead to the destabilization of the asphaltenes, altering its chemical properties and hence affecting its rheological performance. Additionally, the paraffinic nature of waste engine oil also enhances the precipitation of asphaltenes and thereby decreasing the adhesive strength of the asphalt binder to the aggregate, which may cause stripping and induce rutting [5]. The relative metal analyte count (%) for all the recovered asphalt binders is shown in figure 4.5. Results from figure 4.5 indicate Highway 6 to contain high amount of molybdenum and also Highway 24 with high level of zinc compared to the remaining samples. These samples will hence be likely to undergo severe physical and chemical hardening due to the high presence of these metals which is believed to originate from the addition of waste engine oil. Although Highway 24 showed the least amount of molybdenum compared to the remaining samples, it

however recorded a significant amount of zinc. K1 showed the least amount of zinc and also recorded low amounts of molybdenum. The percentage amounts of zinc and molybdenum recorded for all the samples is relative to a waste engine oil sample.

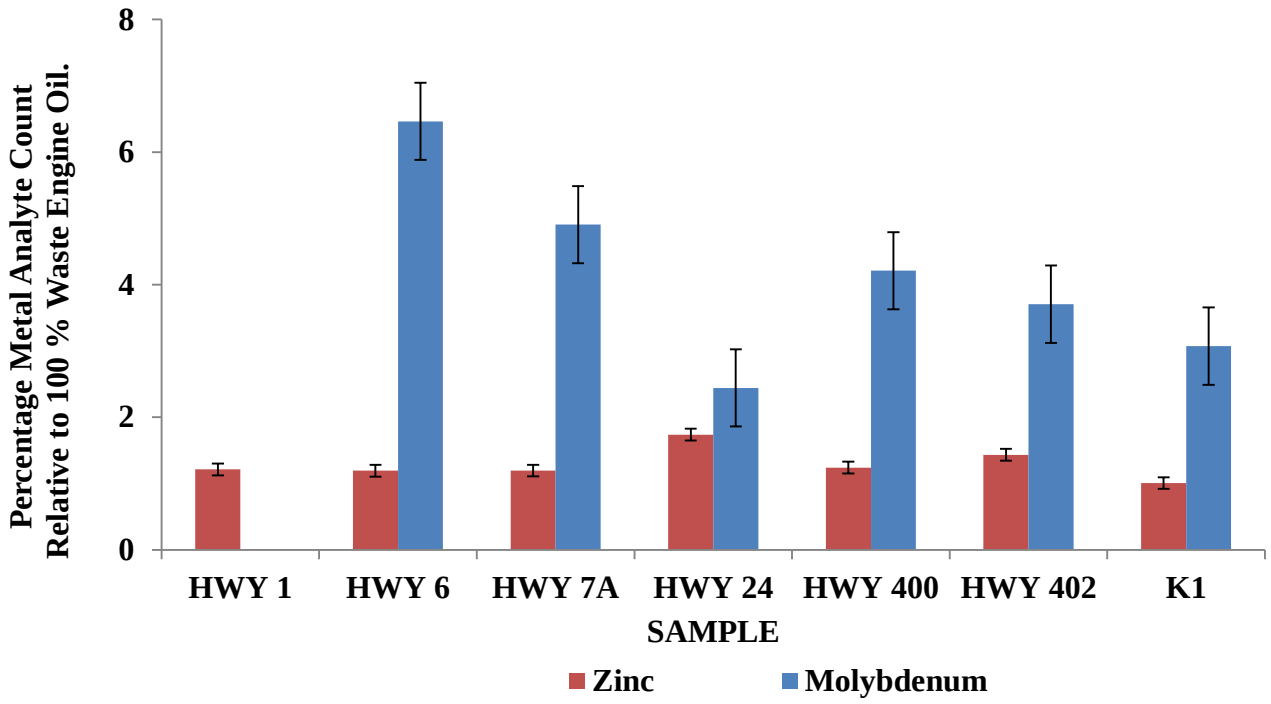

Figure 4.5: Percentage Zinc and Molybdenum amount in all recovered samples relative to a waste engine oil sample.

The percentage of waste engine oil from the levels of Zn and Mo in the respective samples was determined in relation to a 100 % waste engine oil standard.

4.6 Fourier Transform Infrared (FTIR) Data Analysis

The intake of oxygen by asphalt binders causes carbon and sulfur to be oxidised into carbonyl and sulfoxide functional groups, which leads to hardening of the asphalt binder. The hardening of the asphalt binder will eventually cause cracking to occur and result in poor performance. However, the addition of polymer modifiers such as SBS, enhances the viscoelastic property of the asphalt binder due to its elastic nature and high temperature stability. Therefore, the infrared spectroscopy analysis was performed to determine the functional groups such as carbonyl and sulfoxide present in asphalt binders. Functional groups such as styrene and butadiene, which originate from the addition of polymer modifiers such as SBS, were also determined. Figure 4.6 (a) shows an infrared (IR) spectrum of K1 asphalt binder.

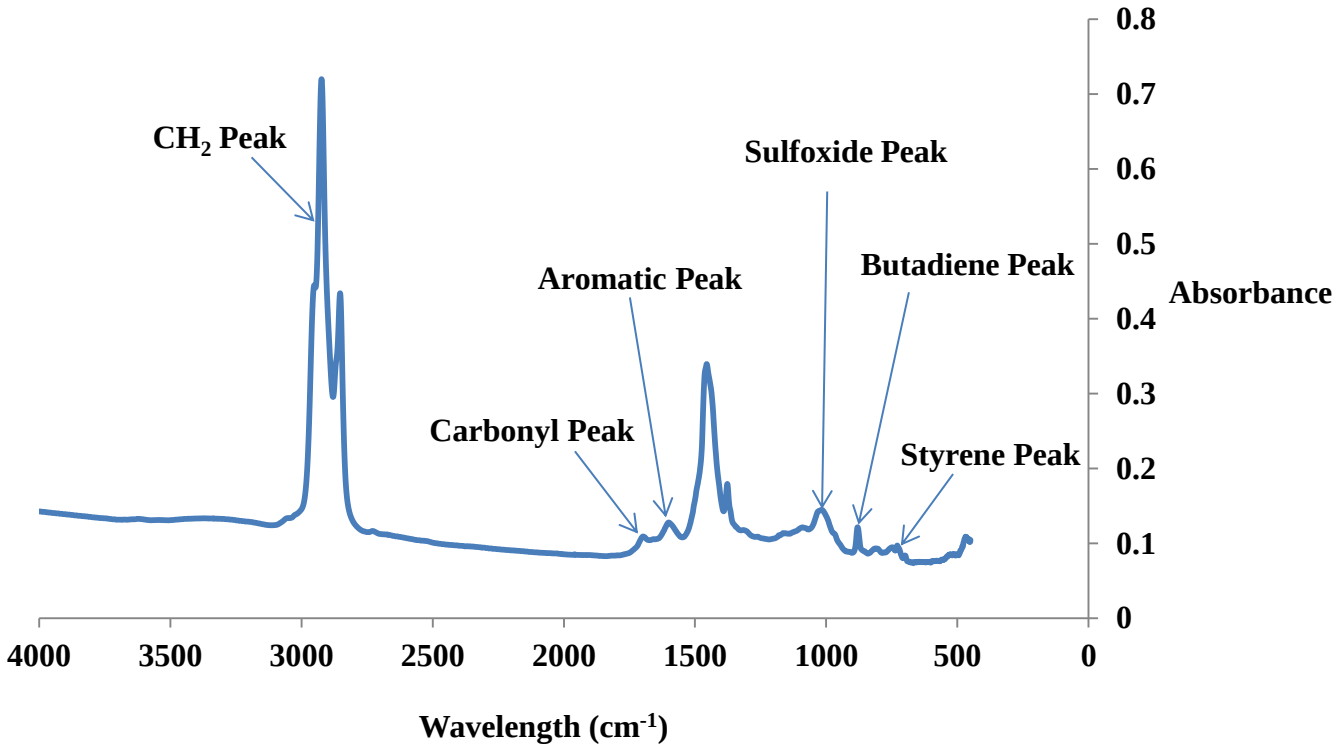

Figure 4.6: (a) Infrared (IR) spectrum of K1 asphalt binder showing peak heights of the various functional groups of interest.

Sulfoxide comes from the oxidation of sulfur in the chain CH_2-S-CH_2 .The percentage carbonyl, sulfoxide, styrene and butadiene indices for all the recovered asphalt binders are shown in the figures below.

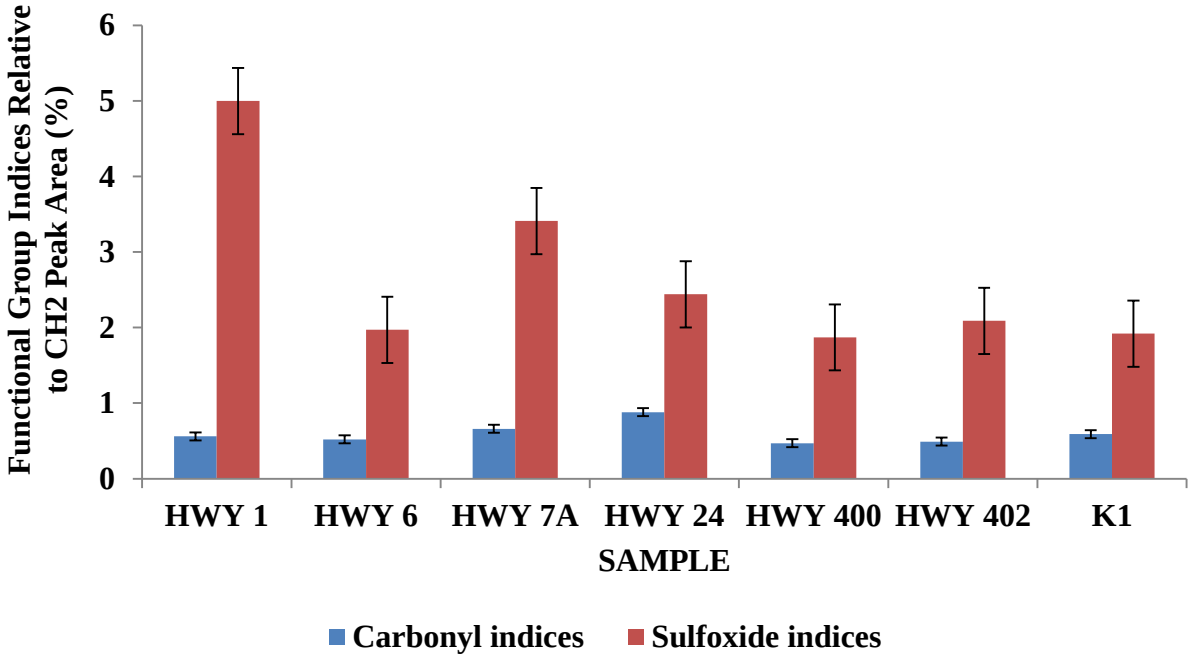

Figure 4.6: (b) Percentage Carbonyl and Sulfoxide indices relative to CH_2 peak area for all recovered asphalt binders.

Highway 24 showed the highest % carbonyl index, followed by Highway 7A compared to the remaining samples. This observation suggests a high level of oxidative hardening to occur in these samples. A high level of oxidative hardening will lead to cracking of the asphalt binder with poor in service performance. On the contrary, Highway 400 and 402 showed the least % carbonyl index and will be expected not to undergo severe oxidative hardening. However, Highway 1 showed the highest % sulfoxide index, followed by Highway 7A and 24. This observation suggests an expected severe oxidative hardening to occur in Highway 1, 7A and 24.

Highway 400, 402, 6 and K1 all showed lower % sulfoxide index and will be expected to experience minimal oxidative hardening compared to the remaining samples.

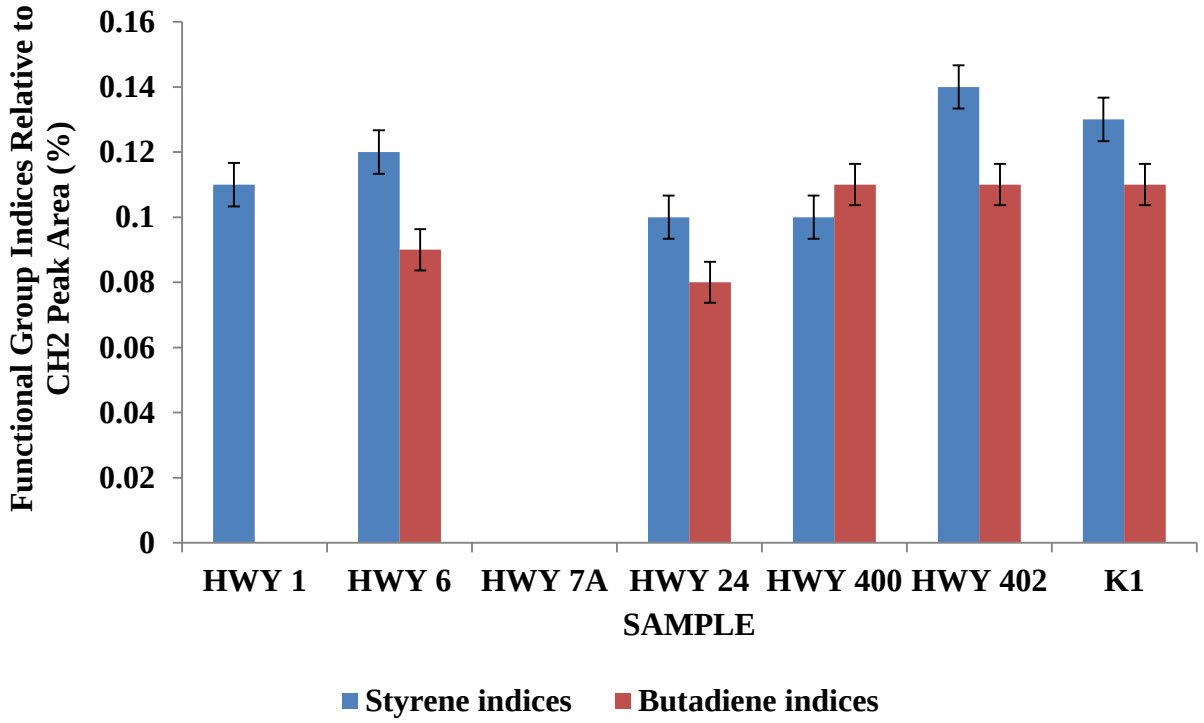

Figure 4.6: (c) Percentage Styrene and Butadiene indices relative to CH_2 peak area for all recovered asphalt binders.

K1, Highway 402, 400, and 6 all showed very high levels of % styrene and butadiene index, with Highway 402 emerging with the highest % styrene and butadiene index compared to all the samples. This observation can be attributed to some inherent or addition of SBS polymer modifier, which enhances the viscoelastic property of the asphalt binder. High amounts of % styrene and butadiene index will enhance the viscoelastic property of the asphalt binder and result in good in service performance. However, Highway 24 showed a fairly good level of % styrene and butadiene index, whiles Highway 1 only showed an appreciable level of % styrene index but recorded no amount of % butadiene index. Furthermore, Highway 7A obtained no

amount of % styrene and butadiene index, and will be said to have no trace or addition of SBS polymer modifier.

CHAPTER FIVE

SUMMARY AND CONCLUSIONS

In relation to the literature review, experimental procedures, results and the discussions made in the previous chapters, the following summary and conclusion are outlined:

- Highway 17, 631, Y1, K1, K2, Sonnewarm and Rediset WMX showed very high creep compliance, and as such, will relax thermal stresses better than the remaining Highway asphalt samples. The indirect tensile strength values were very high for 427-4, Highways 11, 17 and 402. Hence, these samples will show better resistance to fatigue and possess a great capacity to bear axle load from vehicles.
- The AASTHO Mechanistic-Empirical Pavement Design Guide (MEPDG) Software, predicted an expected pavement in service life span for K1, K2, Y1 and Highway 400 to be above 15 years. Sasobit, Rediset LQ, and Rediset WMX were also predicted to have an expected pavement in service life above 15 years.
- The various rheological tests showed K1 to be the least susceptible to low temperature cracking compared to the remaining samples whiles Highway 24 will be highly susceptible to low temperature cracking.
- The X-ray fluorescence (XRF) Analysis reveals Highway 6 to have obtained the highest molybdenum count and Highway 24 the highest zinc count. The high levels of zinc and molybdenum could be inferred to the addition of high amounts of waste engine oil which brings about physical and chemical hardening.
- The Fourier transform infrared (FTIR) analysis reveals Highway 1 to have obtained the highest % sulfoxide index and Highway 24 the highest % carbonyl index. The high levels of carbonyl and sulfoxide shows the high magnitude of oxidative hardening occurring in

these samples. However, Highway 6, 400, 402 and K1 all showed high levels of % styrene and butadiene index and will be suspected to contain some amount of SBS polymer modifier which improves the viscoelastic property of the asphalt binder.

REFERENCES

1. Ksaibati, K., Erickson, R.; Evaluation of Low Temperature Cracking In Asphalt Pavement Mixes, **1998.**
2. Jung, D.H., Vinson, T.S.; Low-Temperature Cracking: Test Selection. Strategic Highway Research Program, National Research Council Washington, DC, pp. 14-18, **1994.**
3. Hesp, S.A.M., Iliuta, S., Shirokoff, J.W.; "Reversible Aging in Asphalt Binder". Energy & Fuels, pp.1112-1121, **2007.**
4. Sugarawa, T., Kubo, H., Moriyoshi, A.; Low Temperature Cracking of Asphalt Pavements. Proceedings, Workshop in Paving in Cold Areas, Vancouver, B.C., Vol. 1, pp. 1-42, **1982.**
5. Agbovi, K.H.; Effect Of Low Temperatures, Repetitive Stresses And Chemical Aging on Thermal and Fatigue Cracking in Asphalt Cement Pavement on High 417, M.Sc. Thesis, Department of Chemistry, Queen's University, Kingston, Canada, **2012.**
6. Apeagyei, A.K., Dave, E.V., Buttlar, W.G.; Effect of Cooling Rate on Thermal Cracking of Asphalt Concrete Pavements. Journal of the Association of Paving Technologists, Vol.77, pp. 709-731, **2008.**
7. Kriz, P., Stastna, J., Zanzotto, L.; Physical Aging in Semi-Crystalline Asphalt Binders. Journal of the Association of Paving Technologists, Vol.77, pp. 795-820, **2008.**
8. Brule, B.; Polymer-Modified Asphalt Cement Used In The Road Construction Industry: Basic Principles In Asphalt Science And Technology; Usmani, A. M., Ed; New York, Basel, Hong Kong, **1997.**
9. John, R., David, W.; The Shell Bitumen Hand Book. Thomas Telford Services Limited, **2010.**

10. Abraham, H.; Asphalts and Allied Substances, Their Occurrence, Modes of Production, Uses In The Arts and Methods of Testing, Van Nostrand, New York. 5th Edition, Volume 1, **1945.**
11. Mathew, T. V., Krishna Rao, K. V.; Introduction to Pavement Design. NPTEL. Introduction to Transportation Engineering, pp. 19.1-19.6, May **2006.**
12. Gonzalez, A.; An Experimental Study on Deformational Characteristics and Performance of Foam Bitumen Pavements. Ph. D. Thesis, Dept. of Civil And Environmental Engineering, University of Caterbury, Christchurch, New Zealand, pp. 1-8, **2009.**
13. Glover, I. C.; Wet And Dry Aging of Polymer-Asphalt Blends: Chemistry and Performance: Department Of Chemistry, Lousisiana Sstate University, Phd Thesis, **2007.**
14. Harvey, J.; Concrete Pavements. University of California, Davis. Website: http://www.ce.berkeley.edu/~paulmont/165/pavement.pdf. Accessed: **August 2014**.
15. Geotechnical Aspects of Pavements Reference Manual, U.S. Department of Transportation Publication No. FHWA NHI-05-037**,** Federal Highway Administration**, May 2006**.
16. "Differences between Concrete and Asphalt Pavement" presented in American PavementConcrete Association www.pavement.com / Concrete Pavement /Technical/ Fundamentals/Differences_Between_Concrete_and_Asphalt.asp. Accessed: September **2014.**
17. Statistics Canada, "Local Government Financial Management Statistics - Capital Expenditures," Statistics Canada, **2003**.
18. Seal Master Pavement Products and Equipment; http://www.pavemanpro.com/article/ deterioration_asphalt_causes/, Accessed: August, **2014.**
19. http://www.pavementinteractive.org/article/general-guidancepavement-distress, Accessed: August **2014.**

20. Orr, D. P.; Pavement Maintenance, *Cornell Local Roads Program*. 416 Riley-Robb Hall Ithaca, New York, pp. 1-27, **2006**.
21. Kanabar, N.; Comparison of Ethylene Terpolymer, Styrene Butadiene, and Polyphosphoric Acid Type Modifiers for Asphalt Cement, Queen's University Kingston, Ontario, Canada, **2010.**
22. http://www.pavementinteractive.org/wp-content/uploads/2008/05/Mvc-037s.jpg, Accessed: **September 2014.**
23. Senthil, K.P.; Effects of Warm Mix Additives and Dispersants on Rheological, Aging and Failure Properties of Asphalt Cements. M.Sc. Thesis, Department of Chemistry, Queen's University, Kingston, Ontario, Canada, **2013.**
24. http://www.drivingtests.co.nz/blog/wp-content/uploads/2013/12/tarmac-fatigue-cracking-300x171.jpg, Accessed: **September 2014.**
25. Brown ER, Kandhal PS, and Zhang J.; Performance Testing for Hot Mix Asphalt. National Center for Asphalt Technology Report, pp. 01-05, **2001.**
26. "Let It Drain – Protecting Roads from Moisture Damage" 29 April 2013. http://www.pavementinteractive.org Accessed: **September 2014.**
27. Williams R. C.; Evaluation of HMA Moisture Sensitivity Using the Nottingham Asphalt Test Equipment. Iowa State University, Institute for Transportation, **2010**.
28. Anderson, D.A., Cristensen, D.W., Bahia, H.U., Dongre, R., Sharma, M.G., Antle, C.E., Button, J.; "Binder Charactericzation and Evaluation, Volume 3." SHRP-A-369, Strategic Highway Research Program, National Research Council, Washington, D.C. **1994**.

29. Petersen, J.C., Robertson, R.E., Branthaver, J.F., Harnsberger, P.M., Duvall, J.J., Kim, S.S., Anderson, D.A., Christiansen, D.W., and Bahia, H.U.; "Binder Charactericzation and Evaluation, Volume 1." SHRP-A-367, Strategic Highway Research Program, National Research Council, Washington, D.C. **1994.**
30. Jones, D.R.; "SHRP ASPHALT RESEARCH PROGRAM TECHNICAL MEMORANDUM #4, AN ASPKALT PRIMER: "Understanding How the Origin and Composition of Paving-Grade Asphalt Cements Affect Their Performance", Strategic Highway Research Program, The University of Texas, Austin, Texas, **1992.**
31. Lerfald, B.O.; Ageing and Degradation of Asphalt pavement on Low Volume Roads, Thesis submitted to the Faculty of Civil and Environmental Engineering, The Norwegian University of Science and Technology, in partial fulfilment of the requirements for the Dr.ing. Degree, **2000.**
32. Johansson, L.S.; "Bitumen Ageing and Hydrated Lime", Kungliga Tekniska Høgskolan, Royal Institute of Technology, Stockholm, Sweden, **1998.**
33. Dukatz, Jr., E.L, Anderson and D.A., Rosenberger, J.L.; "Relationship between Asphalt Flow Properties and Asphalt Composition". Asphalt Paving Technology, **1984.**
34. Lu, Xiaohu.; "Fundamental Studies on Styrene-Butadiene-Styrene Polymer Modified Road Bitumens". Licentiate Thesis. Kungl Tekniska Høgskolan, Stockholm. TRITA-IP FR 96-17.
35. The Shell Bitumen Handbook, **1990.**
36. Smith, B. J.; Low-Temperature and Dynamic Fatigue Toughing Mechanisms in Asphalt Mastics and Mixture, MSc. Thesis, Department of Chemistry, Queen's University, Kingston, Ontario, Canada, **2000.**

37. Barnes, H.A., Hutton, J.F. and Walters, K.; "An Introduction to Rheology". ELSEVIER, **1989.**

38. Superpave Performance Grading. http://www.pavementinteractive.org/article/superpave-performance-grading/#sthash.n6eZdwnD.dpuf, Accessed: **October 2014.**

39. www.dot.ca.gov/hq/construc/CPDirectives/CPD06-11attach2.pdf, Accessed: **October 2014.**

40. Anderson, D. A., Kennedy, T. W.; Journal of the Association of Asphalt Paving Technologists, pp. 62- 481, **1993.**

41. Anderson, D.A; Dongre, R.; The SHRP Direct Tension Specification Test- Its Development and Use. In: Physical Properties of Asphalt Cement Binders, John C. Hardin (Ed), ASTM STP 1241, American Society for Testing and Material, Philadelphia, pp.51- 66, **1995.**

42. Roberts, F.L.; Kandhal, P.S.; Brown, E.R.; Lee, D.Y. and Kennedy, T.W. (1996). Hot Mix Asphalt Materials, Mix Design and Construction. National Asphalt Pavement Association Education Foundation. Lanham, MD.

43. Becker Y.; Méndez, M. P. and Rodríguez, R. Y. Vision Tecnologica, pp.39, **2001.**

44. Read, J. and Whiteoak, D.; The Shell Bitumen Handbook, Fifth Edition; Hunter, R. N. Ed.; Thomas Telford: London, **2003.**

45. The Asphalt Handbook; 7th Edition, Ed.; Asphalt Institute: USA, **2007.**

46. Kodrat, I.; Sohn, D.; Hesp, S. A. M.; J. Transportation Res. Board, Transportation Res. Rec., pp.47, **2007.**

47. Jean-Martin C., Bernard T.; Warm Mix Asphalt Paving Technologies: a Road Builder's Perspective. Annual Conference of the Transportation Association of Canada, **2008.**

48. Zhang, J.; Effects of warm-mix asphalt additives on asphalt mixture characteristics and pavement performance, M.Sc. Thesis, Department of Civil Engineering, University of Nebraska-Lincoln, Lincoln, USA, **2010.**
49. Rashwan, M.H.; Characterization of Warm Mix Asphalt (WMA) performance in different asphalt applications, PhD Thesis, Department of Civil Engineering, Iowa State University, Ames, Iowa, USA, **2010.**
50. Hussain UB, Andrew H, Pouya T.; Effect of WMA Additives on Binders Workability and Performance. 2nd International Warm Mix Asphalt Conference, St.Louis, Missori, October 12, **2011.**
51. Anderson, R. M., Baumgardner, G., May, R., and Reinke, G.; "NCHRP 9-47: Interim Report: Engineering Properties, Emissions, and Field Performance of Warm Mix Asphalt Technologies." TRB, National Highway Research Council, Washington, D.C., **2008.**
52. D'Angelo, J., Harm, E., Bartoszek, J., Baumgardner, G., Corrigan, M., Cowsert, J., Harman, T., Jamshidi, M., Jones, W., Newcomb, D., Prowell, B., Sines, R., and Yeaton, B.; "Warm-Mix Asphalt: European Practice." FHWA Report No. FHWA-PL-08-007, American Trade Initiatives, Alexandria, Virginia, **2008.**
53. Jenkins, K.; Mix Design Considerations for Cold and Half-Warm Bituminous Mixes with Emphasis on Foamed Bitumen. Doctoral Dissertation, Stellenbosch University, **2000.**
54. European Asphalt Pavement Association (EAPA); The Use of Warm Mix Asphalt. January **2010.**
55. Eurovia Services, Website: http://www.eurovia.com/en/produit/135.aspx, Accessed: November, **2014.**
56. Chen, J. S; Tsai, C. J.; Journal of Materials Engineering and Performance, pp. 443, **1999.**

57. Subramani, SK.; Validation of New Asphalt Cement Specification Test Methods using Eastern Northeastern Ontario Contracts and Trial Sections, MSc. Thesis, Department of Chemistry, Queen's University, Kingston, Ontario, Canada, **2009.**

58. Mang T.; Bituminous Material, University of Florida, Website: http://nersp.nerdc.ufl.edu/~tia/Bituminous-Materials.pdf, Accessed: **November, 2014.**

59. American Society for Testing and Materials 2004. Annual Book of ASTM Standard, ASTM, Philadelphia, Pennsylvania.

60. Laboratory-Pavement Materials; Penetration of Bituminous Materials, School of Civil and Structural Engineering, Nanyang Technological University, **2002.**

61. American Society for Testing and Materials; Standard Test Method for Softening Point of Bitumen (Ring And Ball Apparatus), D36-95, **2002.**

62. Universal Penetrometer; Penetration of Bituminous Material, Website: www.hoskin.ca, Accessed: **November, 2014.**

63. K80000 Softening Point Apparatus, Website: http://www.koehlerinstrument.com, Accessed: **November, 2014.**

64. Pavement Tools Consortium; Pavement Interactive guide, http://training.ce.washington.edu/PGI/, Accessed: **November, 2014.**

65. Benzene International, Website: http://www.benzeneinternational.com/ viscosity_grade_bitumen.html, Accessed: **November, 2014.**

66. West Test LLC, Website: http://www.westest.net, Accessed: **November, 2014.**

67. Asphalt Institute, Performance Graded Asphalt Binder Specification and Testing, Superpave Series No. 1 (SP-1), pp. 22-28, **2003.**

68. US Department of Transportation: Federal Highway Administration; Background of Superpave Asphalt Binder Test Methods, Publication No. FHWA-SA-94-069, **1994.**

69. Superpave: Performance Graded Asphalt Specification and Testing New York, Asphalt Institute, **2003.**

70. Washington.edu/wsdot/modules/03_materials/03-3_body.htm

71. Harman, T.P., G* Complex Shear Modulus A Detailed Review, Federal Highway Administration, Office of Technology Application, Demonstration Projects Program HTA-21, August **1993.**

72. AASHTO M320; Standard Specification for Performance-Graded Asphalt Binder American Association of State Highway and Transportation Officials, **2002.**

73. Bending Beam Rheometer, website: http://www.pavementinteractive.org/article/bending-beam-rheometer/ Accessed: **November, 2014.**

74. Bending Beam Schematic diagram, website: http://classes.engr.oregonstate.edu/cce/spring2014/ce492/Modules/03_materials/Images/3_figures_thumb/real.htm, Accessed: **November, 2014.**

75. Struik, L. C. E.; Physical Aging in Amorphous Polymers and other Material, Elsevier Scientific Publishing Co. Amsterdam, **1978.**

76. Traxler, R. N.; Schweyer, H. E. Proceedings of the Thirty-Ninth Annual Meeting, American Society for Testing Materials, Atlantic City, NJ, 36(II), 544, **1936.**

77. Traxler, R. N.; Coombs, C. E. Proceedings of the Fortieth Annual Meeting, American Society for Testing Materials, New York City, NY, 37(II), 549, **1937.**

78. Traxler, R. N.; Asphalt – Its Composition, Properties and Uses. Reinhold Publishing, New York, **1961.**

79. Ministry of Transportation of Ontario; LS-308 – Determination of Performance Grade of Physically Aged Asphalt Cement Using Extended Bending Beam Rheometer (BBR) Method, Revision 24 to Laboratory Testing Manual, **2007.**
80. Ministry of Transportation of Ontario; LS-299 – Determination of Asphalt Cement's Resistance to Ductile Failure Using Double-Edge-Notched Tension Test (DENT), Revision 24 to Laboratory Testing Manual, **2007.**
81. Cotterell, B.; Reddel, J. K. International Journal of Fracture, 13(3), 267, **1977.**
82. Togunde, O. P.; Low Temperature Investigations On Asphalt Binder Performance – A Case Study on Highway 417 Trial Sections, MSc Thesis, Department of Chemistry, Queen's University, Kingston, Canada, **2008.**
83. Andriescu A, Gibson N, Hesp SAM, Qi X, and Youtcheff, JS. Validation of The Essential Work of Fracture Approach to Fatigue Grading of Asphalt Binders. Journal of the Association of Asphalt Paving Technologists, Vol. 75E, pp. 1-37, **2006.**
84. Soleimani, A.; Use of Dynamic Phase Angle and Complex Modulus for the Low Temperature Performance Grading of Asphalt Cements, MSc. Thesis, Department of Chemistry, Queen's University, Kingston, Canada, **2009.**
85. Instro Tek Inc, Pine Gyratory Compacted, website: http://fyegraphics.com/instrotek/services/pine-gyratory-compactor/ Accessed: **December, 2014.**
86. Struers, Exoton -150 cut-off machine, website: http://www.struers.com/default.asp?doc_id=244, Accessed: **December, 2014.**

87. Bulk Specific Gravity of Compacted Hot Mix Asphalt Using Saturated Surface Dry Specimens, in AASHTO T 166-07, American Association of State Highway and Transportation Officials, Washington, D.C, **2007.**

88. American Association of State Highway and Transportation Officials, "Determining the Creep Compliance and Strength of Hot Mix Asphalt (HMA) Using the Indirect Tensile Test Device," AASHTO T-322, **2007.**

89. Thomas Scientific, R-215 Rotary Evaporator, website: http://www.thomassci.com/Equipment/Evaporators/_/Rotavapor-R-215-Rotary-Evaporator, Accessed: **December, 2014.**

90. Yee, P., Aida, B., Hesp, S.A.M., Marks, P., Tam, K.K.; Analysis of Three Premature Low Temperature Pavement Failures. Transportation Research Record: Journal of the Transportation Research Board, Number 1962, pp. 44-51, **2006.**

91. NHCRP Report 530; Evaluation of Indirect Tensile Test (IDT) Procedures for low-temperature performance of Hot-Mix Asphalt, **2004.**

92. Richardson, D.N., Lusher, M.S.; Determination of Creep Compliance and Tensile Strength of Hot Mix Asphalt for wearing courses in Missouri. Missouri University of Science and Technology, **April 2008.**

93. Marasteanu, M., Buttlar, W., Bahia, H., Williams, C.; "Investigation of Low Temperature Cracking in Asphalt Pavements National Pooled Fund Study 776 Final Report," Minnesota Department of Transportation, Minnesota, **October, 2007.**

94. Fromm, H.J. and Phang, W.A.; "A Study of Transverse Cracking of Bituminous Pavements", Proceedings, the Association of Asphalt Paving Technologists,Vol. 41, pp. 383-423, **1972.**

95. Haas, R., Meyer, F., Assaf, G. and Lee, H.; "A Comprehensive Study of Cold Climate Airport Pavement Cracking", Proceedings of the Association of Asphalt Paving Technologists, Vol. 56, pp. 198-245, **1987.**

96. NHCRP Synthesis 457; "Implementation of the AASTHO Mechanistic-Empirical Pavement Design and Software", Transportation Research Board, Washington, D.C. **2014.**

97. Pavement Interactive; "What Is Mechanistic-Empirical Design? – The MEPDG and You", website:http://www.pavementinteractive.org/2012/10/02/what-is-mechanistic-empirical design-the-mepdg-and-you/, Accessed: **December, 2014.**

98. ARA, Inc., ERES Consultants Division, "Guide for Mechanistic Empirical Design of New and Rehabilitated Pavement Structures," National Cooperative Highway Research Program, Champaign, **2004.**

99. Maurer, P.; "Asphalt Performance Testing, ENCH 417 Thesis Project", Queens University, Kingston, Canada, **2014.**

100. Pavement Interactive; Pouring asphalt into a DSR Sam" website: https://www.youtube.com/watch?v=aFveDItDl_w, Accessed: **December, 2014.**

101. KHMER ELITE; "Pouring a BBR Sample" website: http://khmertube.khmerelite.ws/index.php/view/aCCIESWaoVI&searchsub=Pouring%20a%20BBR%20sample#.VJm8wf8wDA, Accessed: **December, 2014.**

102. Hesp, S. A. M., Shurvell, H. F.; "X-ray fluorescence detection of waste engine oil residue in asphalt and its effect on cracking in service" International Journal of Pavement Engineering, pp. 541, **2010.**

103. Rubab, S., Burke, K., Wright, L., Hesp, S.A.M., Marks, P., and Raymond, C.; "Effects of Engine Oil Residues on Asphalt Cement Quality" Proceedings, Canadian Technical Asphalt

Association, Quebec City, Quebec: 1-12.

104. Petersen J. C.; A Review of the Fundamentals of Asphalt Oxidation, Transportation Research Circular E-C140, **2009.**

105. Hesp, S.; An Improved Low Temperature Asphalt Binder Specification Method – Final Report, Queen's University, Kingston, Ontario, Canada, **2004.**

106. Bodley, T., Andriescu, A., Hesp, S. A. M., Tam, K. K.; Journal of the Association of Asphalt Paving Technologists, pp. 345, **2007.**

107. Minerals zone; website: http://www.mineralszone.com/stones/granite.html, Accessed: **January, 2015.**

108. Asphalt Sand - Gernatt Asphalt Products, Inc; website: www.gernatt.com/Tools/Portfolio/frontend/item.asp?type, Accessed: **January, 2015.**

109. Kennedy, T. w., Tam, W. O., Solaimanian, M.; Effects of Reclaimed Asphalt Pavement on Binder Properties Using the Superpave System, Research Report 1250-1, Texas Department of Transportation, **June, 1998.**